TESTING AND ANALYSIS OF A NOVEL SPUR GEAR DESIGN USING DOUBLE INTEGRAL BEARING RACEWAYS

by

Astrid Richter-Allen

B.S., Mechanical Engineering
Massachusetts Institute of Technology

Submitted to the Department of Mechanical Engineering
in Partial Fulfillment of the Requirements for the Degree of

Master of Science

at the

Massachusetts Institute of Technology

June 1996

© 1996 Astrid Richter-Allen
All rights reserved

Signature of Author . . . .
Department of Mechanical Engineering
May 10, 1996

Certified by . . . .
David M. Parks
Professor of Mechanical Engineering
Thesis Supervisor

Accepted by . . . .
Ain A. Sonin
Eng. Chairman, Department Committee on Graduate Students

TESTING AND ANALYSIS OF A NOVEL SPUR GEAR DESIGN USING DOUBLE INTEGRAL BEARING RACEWAYS

by

Astrid Richter-Allen

Submitted to the Department of Mechanical Engineering on May 10, 1996
in Partial Fulfillment of the Requirements for the Degree of Master of Science in
Mechanical Engineering

ABSTRACT

In the 1950's, the American Gear Manufacturer's Association (AGMA) set a standard for rim thicknesses of gears which is still used in gear design today. In designing a new product in which the bore of the gear also acts as the outer raceway for two tapered roller bearings, the AGMA standard was re-examined. On the assumption that material properties had become more robust over the past decades and because the AGMA standard did not address the use of a double tapered bore in gears, the effects of this change in gear geometry were analyzed.

The research was based entirely on a case study of an actual customer application. A finite element analysis (FEA) was conducted on a gear design employing a double tapered bore, as well as on the existing gear design used in the application. Furthermore, a relatively inexpensive and simple testing method was designed and implemented to compare and correlate the results of the finite element analysis to actual test data. Prototypes of gears with double tapered bores and straight bores were tested to establish this correlation.

The results of the experiment indicated that there was indeed correlation between the finite element and test results, although it was recommended that additional experimental data be gathered. The data indicated similar test results for the tapered and straight-bore versions of the prototypes. It was also found that the tapered bore prototypes failed in a way which could be less detrimental to the surrounding machinery. The results also serve as a proof of concept for the testing method developed which has several advantages over existing test designs.

Thesis Supervisor: David M. Parks
Title: Professor of Mechanical Engineering

ACKNOWLEDGEMENTS

TABLE OF CONTENTS

CHAPTER 1

INTRODUCTION

Current manufacturing trends appear to be moving from the 'bigger is better' attitude to one of energy conservation wherein 'bigger' may actually be worse. Though manufacturers are still concerned with increasing the power output of machines, it would be preferable if this increase in power output were accomplished with increasingly smaller and fewer parts. This drive for "power density" and the reduction of the total part count has caused companies to rethink every aspect of manufacture and design. Gears and bearings are among the products which are in the process of being reexamined. In the theoretical ideal, the gear is mounted on a shaft which in turn is supported by a bearing on either side of the gear. With the decrease of space those bearings have not only been brought closer to the gear but have gone so far as to be placed *inside* the gear.

In 1950's, the American Gear Manufacturer's Association (AGMA) set a standard[1] for *rim* thicknesses[2] which is still used as a rule of thumb in gear design. According to the AGMA standard "Any external or internal gear. . . should have a minimum thickness under the tooth root (rim thickness) equal to the whole depth of the tooth".

---

[1] ANSI/AGMA 6002 - B93. February 5, 1993, p.5

[2] All lettering in *italics* will indicate that the definition can be found in the Glossary.

As the issue of *integral gears* is contemplated, it becomes obvious that one of the limiting factors in power density is the thickness of the rim. If the size of the bearing placed in the bore of the gear is increased, the rim thickness must be decreased accordingly. Thus the initial AGMA standard for rim thicknesses must be revisited under the assumption that over the past 40+ years, research has led to stronger and tougher materials which would be able to withstand higher strains and stresses than materials existent in the 1950's. With the desire to use *tapered roller bearings*[3], the gear requires a *tapered-bore* rather than the straight one referred to in the AGMA standard, so it is unclear at which point along the *gear rim* the standard should be applied.

This research will examine this fundamental 'rule of thumb' and establish how the rim thickness standard relates to tapered-bores. To keep the study focused on the effects of rim thickness alone, no design changes will be made to either fundamental gear or bearing designs. Instead, design changes will concentrate on varying rim thickness by incorporating different bearings of standard design into a gear of standard design. An analytical tool via finite element analysis will be applied for investigation of future designs using gears with integral tapered-bores. Also, a new method for testing gears will be designed which will employ a simpler and more cost-effective scheme than has ever been attempted before. Finally, the test results will be correlated with the analytical study.

---

[3] For their ability to support combined radial and thrust loading conditions.

Motivation

As the industrial market moves toward greater power density, every component in industrial equipment is in the process of being re-examined and redesigned for greater load-bearing capacity while maintaining the same geometrical envelope. In 1994, The Timken Company conducted a market analysis for *GearSpexx*™ [4] and concluded that there was market potential for this new product. Moreover, it was established that there were two distinct applications for GearSpexx™. Planetary torque hub reduction units, used in heavy machinery such as earth moving equipment, use spur gears[5]. Split idlers employing helical gears with integral *raceways* are predominantly used in trucks. The company established that the split idler manufacture, a low volume, high precision operation, was considered a core competence by potential customers and thus not likely to be an outsourced product. However, companies manufacturing planetary torque hub reduction units were far more likely to outsource this high volume, lower precision product. The Timken Company chose to concentrate on spur gears with integral raceways such as the ones used in planetary torque hub reduction units.

Product development methodologies call for direct customer interaction throughout the design of new products. For this reason a gear and planetary torque hub reduction unit manufacturer was intimately involved in every aspect of this research. The work which was conducted, was based entirely on an actual case study of this customer's

---

[4] A spur gear with double integral raceways will be referred to as GearSpexx™ throughout the remainder of this document.

[5] In an effort to increase power output and decrease the number of parts, some customers already use gears with integral raceways.

product[6]. Moreover, customer interaction was maintained throughout the project to ensure that development remained in line with the customer's values and interests. Quality of the analysis, prototypes and test design were confirmed with the customer to guarantee that the research conducted would meet their standards as well as The Timken Company's.

Outline

The document will follow actual steps taken in completion of the research to facilitate comprehension of the issues discussed. Also, a brief outline is included at the beginning of each chapter, to aid in navigation through this thesis.

Chapter 2 is a description of the nomenclature which will be utilized throughout the remainder of the document. Since the terminology in this document draws on three different fields - finite element analysis, tapered roller bearings and gears - the chapter is also divided in three distinct sections dealing with each field in turn.

Chapter 3 is a description of the Finite Element Analyses conducted on GearSpexx™. First, the basic premises of gear operations, on which the finite element analysis was based, are discussed. Another section gives a step-by-step description of the steps necessary to model GearSpexx ™ accurately. Finally the results of the finite element analysis are described and discussed in the conclusion.

Chapter 4 is a discussion of the particular design issues which were addressed in creating GearSpexx™ prototypes. Customer data is presented and followed by a description of manufacturing options and issues. Then, design issues - such as bearing

---

[6] See Chapter 4 for further discussion of the product used as a case study.

selection and raceway profiling - are discussed. The chapter concludes with a quality analysis of the finished prototypes.

Chapter 5 begins by describing the goals and options of gear test designs. General and detailed assumptions are addressed and quantified. Next, test designs are described and compared to the actual application with the customer. Issues relating to the final test design are followed by results and conclusions of the testing.

Chapter 6 discusses conclusions drawn from the finite element analysis and testing results. Then, recommendations are made with regards to future work.

A Glossary and three Appendices follow Chapter 6.

CHAPTER 2

NOMENCLATURE

This document will employ terminology from three different fields: finite element analysis, bearing design and gear design. Each of these businesses employs a vocabulary which may not be familiar to all. Therefore, this chapter will focus on describing some of the terms used in finite element analysis, bearings and gears. Additional definitions will be found in a glossary at the end of the document

Finite Element Analysis (FEA)

Figure 2.1 is an example of a typical two-dimensional finite element model which is ultimately used for analysis. For this project two programs were employed: the basic geometry was developed on the commercially available FAM[7] software package while the analysis was conducted using the finite element software program - ABAQUS[8]. In FAM, the geometry is created by establishing the coordinates for number a of **points** (i.e. P1 in Fig. 2.1). The points are connected into the final shape via straight lines or arcs. The

---

[7] FAM Reference Manual, Version 3.5. FEGS Ltd., Cambridge, Great Britain, 1993.

[8] ABAQUS User's Manual, Version 4.8. Hibbitt, Karlsson & Sorensen, Inc., Pawtucket, Rhode Island, 1989.

geometry can also be copied, mirrored and translated. Once the contour is complete, a

mesh is created across the surface as illustrated on the figure. The mesh is composed of

quadrilateral shapes - *elements* - which are the building blocks of the model. The program

also establishes *nodes* at the corners of the elements. Together, nodes and elements are

the core building blocks of all models in two or three dimensions. ABAQUS uses the list

of nodes and elements in the analysis to calculate stresses and strains on an element-by-

element basis. The details of the ABAQUS program will be discussed in greater detail in

Chapter 3.
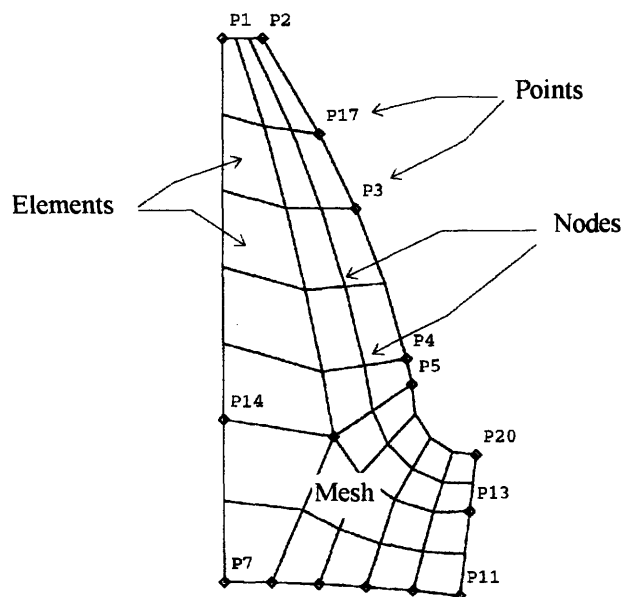
Figure 2.1: Illustration of finite element nomenclature.

Tapered Roller Bearing Geometry

A tapered roller bearing is composed of four major components which work

together to create true rolling motion[9]. Shown in Fig. 2.2 are the *cup* (or outer ring), a

tapered *roller* and the *cone* or (inner ring). These parts are designed to carry the load

[9] The Timken Company, Bearing Selection Handbook Revised - 1986, The Timken Company, 1986, p. 13.

while the fourth component, the *cage*, spaces and retains the rollers. The cone assembly is

separable from the cup and consists of the cone, rollers and cage. Generally the cone

assemblies are shipped in a pre-assembled and unseparable form. The rollers roll between

the **cone race** (inner raceway) and the **cup race** (outer raceway). The *large end* and

small end cup diameters will be critical in establishing the geometry of the bore in

GearSpexx™.
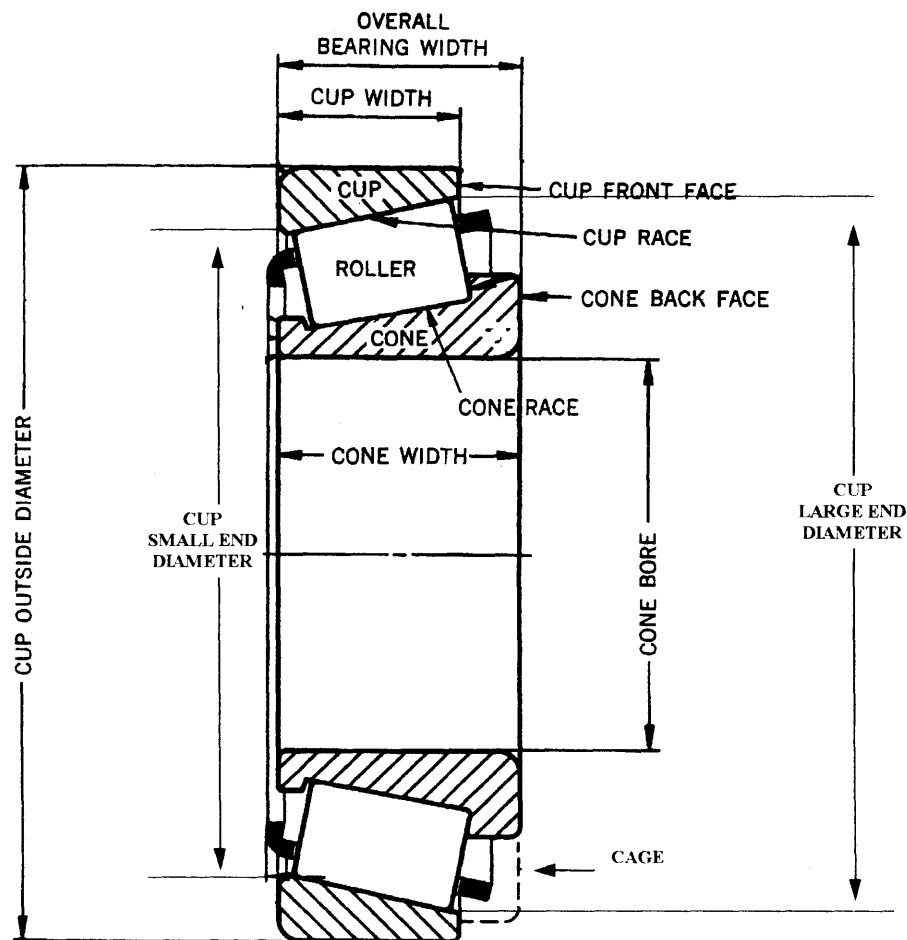
Figure 2.2: Bearing nomenclature.

Manufacturing Summary

The following manufacturing summary is intended to aid in gaining an understanding of the basics of tapered roller bearings.

- Green Machining - creates a near net shape via material removal from steel tubing or bars. Alternatively, near net shapes can be attained through forging.

- *Heat Treatment* - is critical in creating the proper material properties for the bearing. The heat treatment used in steel gears and bearings results in parts which have a relatively soft but tough inner *core* with a strong (or hard) outer shell.

- *Grinding* - is a surface-finishing and fine-shaping technique wherein small amounts of material are removed at a time. Surfaces with tight tolerances and/or stringent surface finish requirements will be ground. Examples of these critical surfaces are the cone bores (which are press fit onto shafts) and the inner and outer races (where the rollers will make contact with them).

- *Honing* - is a super-fine finishing process which produces a better surface finish than grinding but does not alter geometry. This technique, which removes almost no material, is used on those surfaces which are extremely sensitive to surface finishing. Depending on operating criteria, inner and outer races as well as rollers are honed to create products with longer fatigue lives.

Spur Gear Geometry[10]

The terminology of spur gears is illustrated in Figures 1.3 and 1.4. The **base circle**

---

[10] Joseph Edward Shigley and Charles R. Mischke, <u>Mechanical Engineering Design</u>. McGraw-Hill Book Co. New York, 1989, pp. 527 - 610.

represented in Fig. 1.3 is the circle from which the **involute** shapes of the gear teeth are

shaped. However, the *pitch* **circle** is the theoretical circle upon which most calculations

are based. The **addendum circle** is the outer diameter of the gear. The **rim** is the

material between the **dedendum circle** (also referred to as the root diameter) and the **gear**

bore. The *pressure* **angle** represents the direction in which the resultant force acts

between two gears, and is the common tangent between two gear pitch circles.
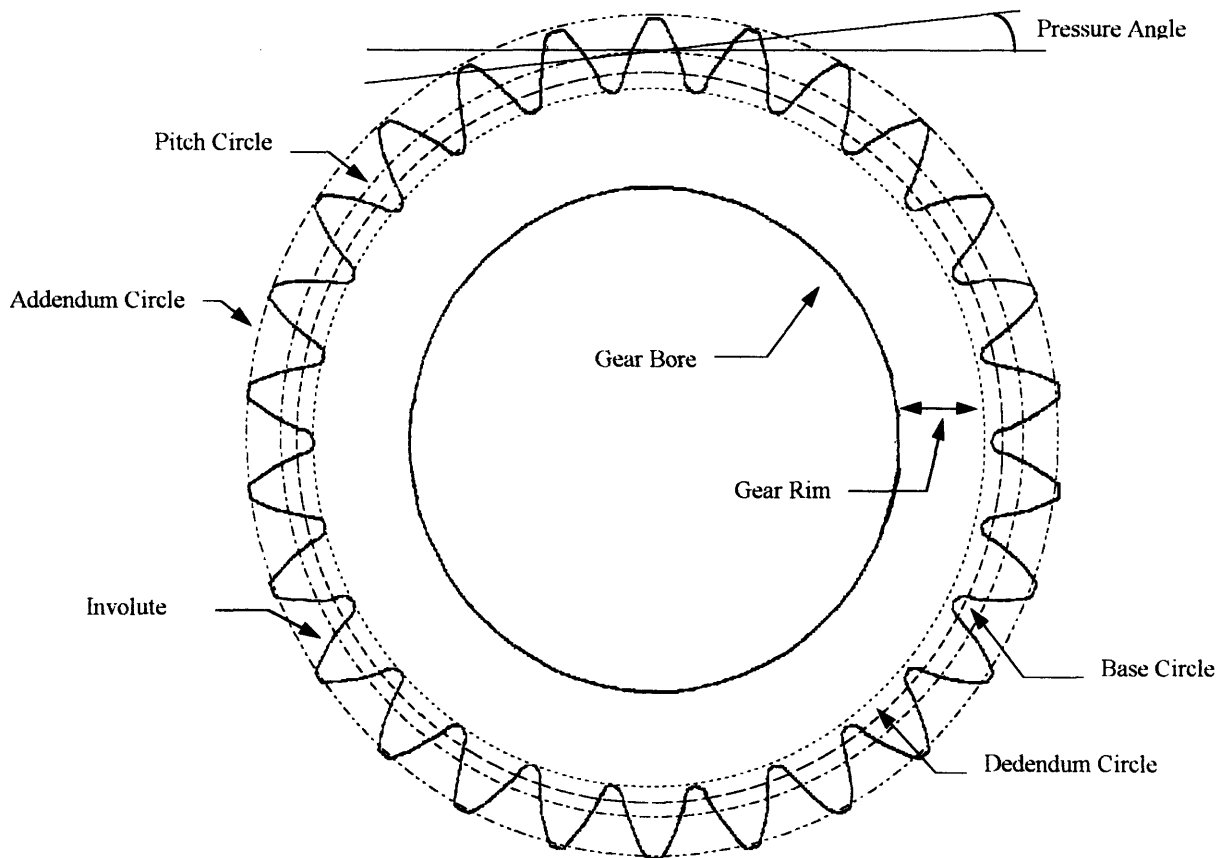
Figure 2.3: Gear Terminology.

Tooth terminology is illustrated in Fig. 2.4. The **tooth thickness** is measured at

the pitch circle. The **addendum** is the radial distance between the **top land** and the pitch

circle and the **dedendum** is the radial distance between the **bottom land** and the pitch

circle. The *whole tooth depth* is the sum of the addendum and the dedendum.
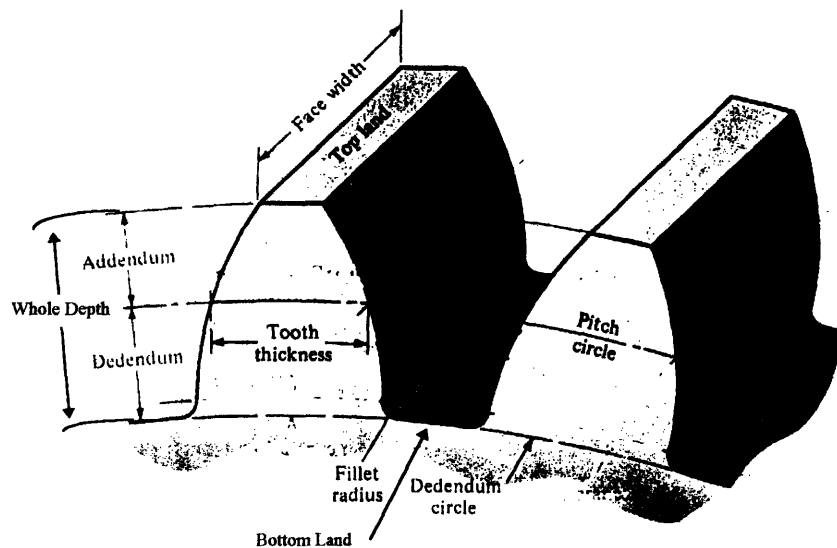
Figure 2.4: Gear tooth nomenclature.

Manufacturing Summary

This manufacturing summary is intended to aid in understanding some of the basic

manufacturing options available to gear manufacturers.

- Tooth Cutting - as in bearing manufacture, a near net shape of the gear teeth is usually

  created by material removal from *gear blanks* - a 'donut' of steel cut from steel tubing

  or bars. The options for tooth cutting are quite varied - however, the most common

  method is called *hobbing* - a versatile and accurate method of gear tooth cutting.

- Heat Treatment - is very similar in scope to heat treatment of bearing components.

- Tooth Finishing - since the results of tooth cutting are sufficient for most applications,

  tooth finishing is not always utilized. As in tooth cutting, there are several methods of

tooth finishing which vary in speed and accuracy. Among the options are *shaving*, finish-hobbing, and grinding.

- Honing - although it is extremely rare, honing is sometimes conducted using wheels similar to the grinding wheels used in tooth finishing.

CHAPTER 3

FINITE ELEMENT ANALYSIS

This chapter will examine the finite element models which were created to analyze a gear with a double tapered-bore. The first section, titled "Basic Model", will examine every aspect of creating a realistic representation of a gear, with a tapered-bore and two bearings, which is mounted on a pin. The geometry of the gear and ensuing model will be discussed in detail, followed by explanations of the forces and boundary conditions applied to the model. The section will continue with a discussion of the modeling techniques for bearing roller reactions and the actual analysis input code. The section will conclude with the results gained. The next section, titled "Tapered-Bore Model", will describe the way in which the basic model was altered to be more sophisticated and accurate with respect to the relatively simple geometry and loading considerations of the basic model. The section will conclude with the results of the altered model. The final finite element model will be described in the section titled "Straight-Bore Model". This section will not only describe the geometrical changes in the model but will also explain the premises behind creating such a different model. The chapter will close with a conclusion based on finite element results.

Basic Model

In conducting a Finite Element Analysis (FEA) of GearSpexx™, it was necessary

to observe some of the basic principles of gear operation. Figure 3.1 is a schematic of the

forces involved during the operation of a planetary gear arrangement. When the machinery

first starts moving, the sun gear attempts to rotate, exerting a force on the planet gears

through the tooth mesh between them. The force on the planets is transmitted to the ring

gear through the meshing of the planet and ring gear teeth. Since GearSpexx™ would

substitute the traditional, straight-bore planet gear, the finite element analysis focused on

the loads which the planet gear experiences. The analysis modeled a point in time when

the sun gear had exerted a force on the planet gear tooth but the ring gear had not yet

begun to move. The theoretical finite element model is illustrated in Fig. 3.2. As

illustrated, the model was chosen to consist of a line load on one tooth to signify the force

exerted by the sun gear while the tooth 180° away from the load consisted of a fixed

boundary to model the ring gear. The worst case would occur during single tooth contact

between the sun and planet gears. Presumably, the maximum load would be experienced at

the pitch diameter.
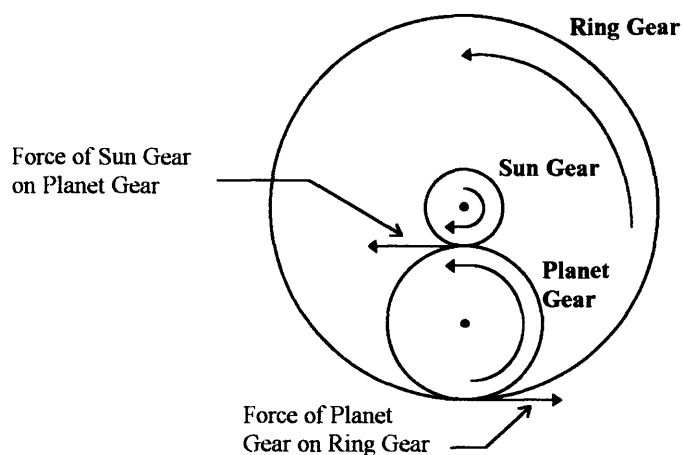
Figure 3.1: Schematic of loads applied to the planet gear.
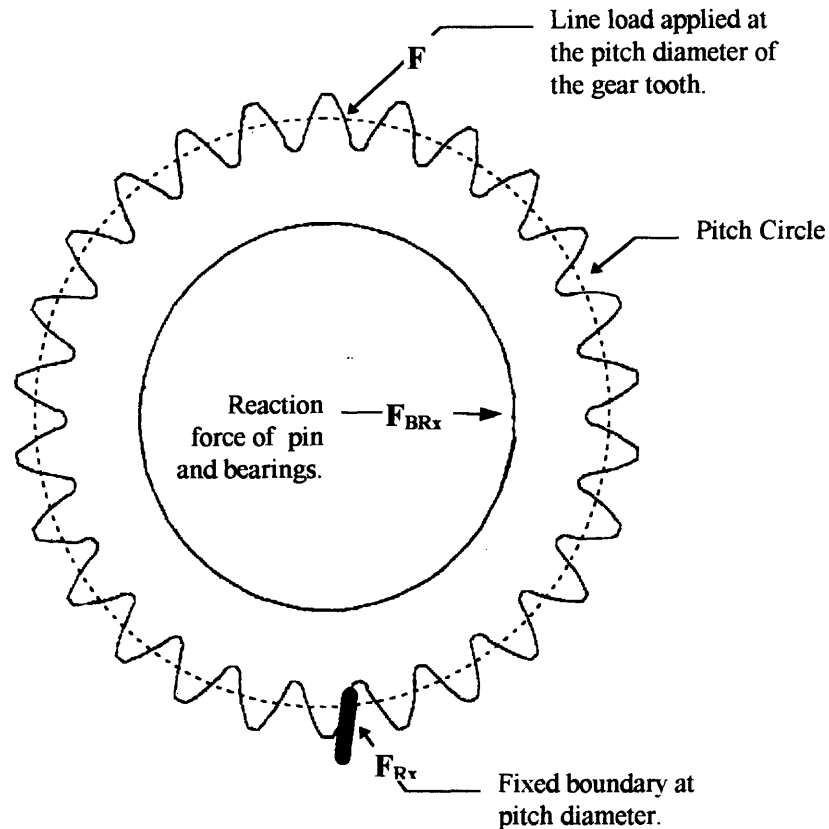
Figure 3.2: Free body diagram of applied loads and boundaries

Geometry

Figure 3.3 is a two-dimensional representation of the planet gear which was

created using the finite element modeler 'FAM'. Although the depiction of the gear was

as true to customer-supplied designs as possible, a few changes were made. For example,

the gear teeth were not modeled as involute shapes but as straight lines. This decision was

based on the assumption that at this stage, the effort required to create the involute shape

would not justify the additional accuracy gained in the analysis. However, it was

necessary to model the entire 360° of the gear rather than assuming symmetry about an

axis. This was so because loading and reactions were not necessarily expected to be

symmetric. Figure 3.4 is a cross sectional view of the three-dimensional model used in the

analysis. This viewpoint allows for better inspection of the tooth depth and rim thickness,
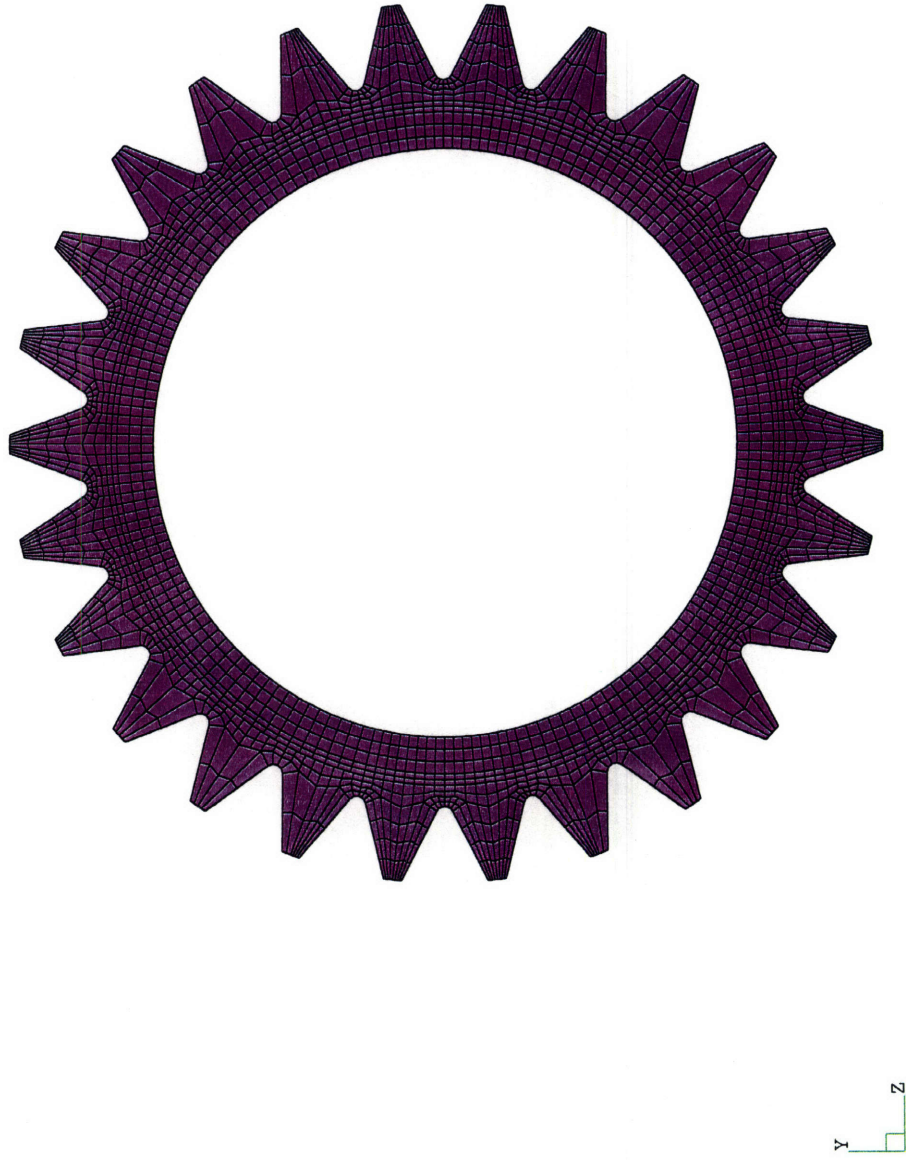
Figure 3.3: Two dimensional representation of the planet gear for the FEA - Basic model.
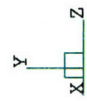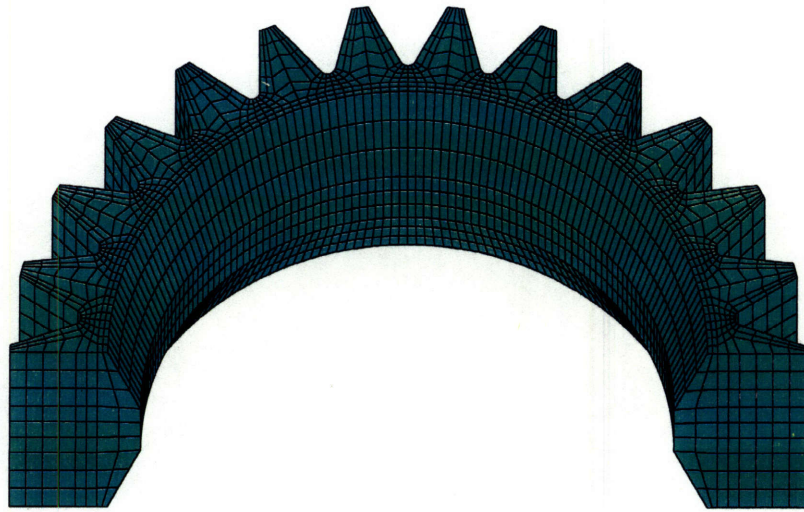
Figure 3.4: Cross Sectional view of the three dimensional model used for the FEA - Basic model.

as well as the shape and number of elements used in the design. The gear rim, which acts

as the outer bearing raceway, was designed using existing Timken Company bearing cup

dimensions (see Chapter 4 for a detailed discussion). As will be discussed, only one

tapered rim geometry was analyzed and tested; thus only one tapered rim design was

analyzed with the finite element tools. Since the gear used in the case study was mounted

on a short cantilevered pin, the full thickness of the gear was modeled to ensure that

asymmetric deflection of the cantilever would be taken into account in the analysis. The

completed three-dimensional model is depicted in Fig. 3.5.

Applied Loads

Because The Timken Company had already conducted an engineering analysis for

the application in which GearSpexx™ would ultimately exist, it was established that the

bearings in the planet gear would have a maximum radial load of 11,400 lb (50,500 N)

(see Fig. 3.6). The force on the two bearings was a result of the force applied by the sun

gear. However, since force from the sun gear was always transmitted normal to the

involute surface of the gear teeth, that force had to be resolved into its radial (Y) and

tangential (Z) components. Therefore, the bearing load of 11,400 lb (50,500 N) was a

reaction to the sum of the tangential force applied by the sun gear and the reaction load of

the ring gear (modeled as a displacement boundary condition in the FE model). The

tangential force was equal: 5,700 lb (25,300N). The radial force of 2,650 lb (11,800 N)

was then calculated using the knowledge that the pressure angle for the planet teeth

was 25°.
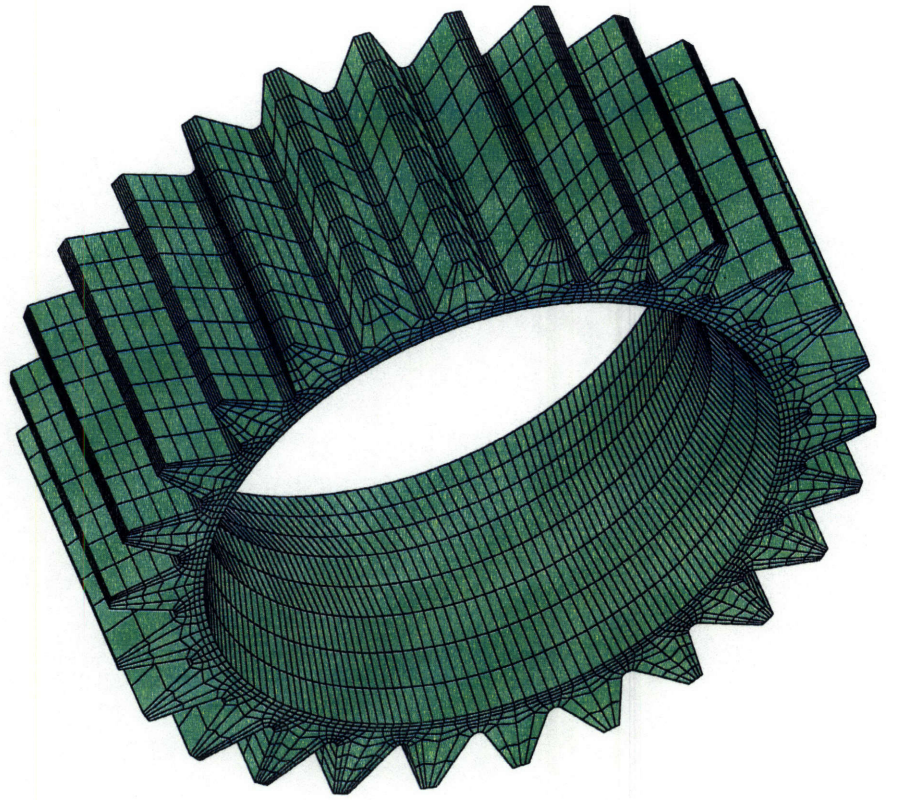
Figure 3.5: Three dimensional model used in the FEA - Basic model.
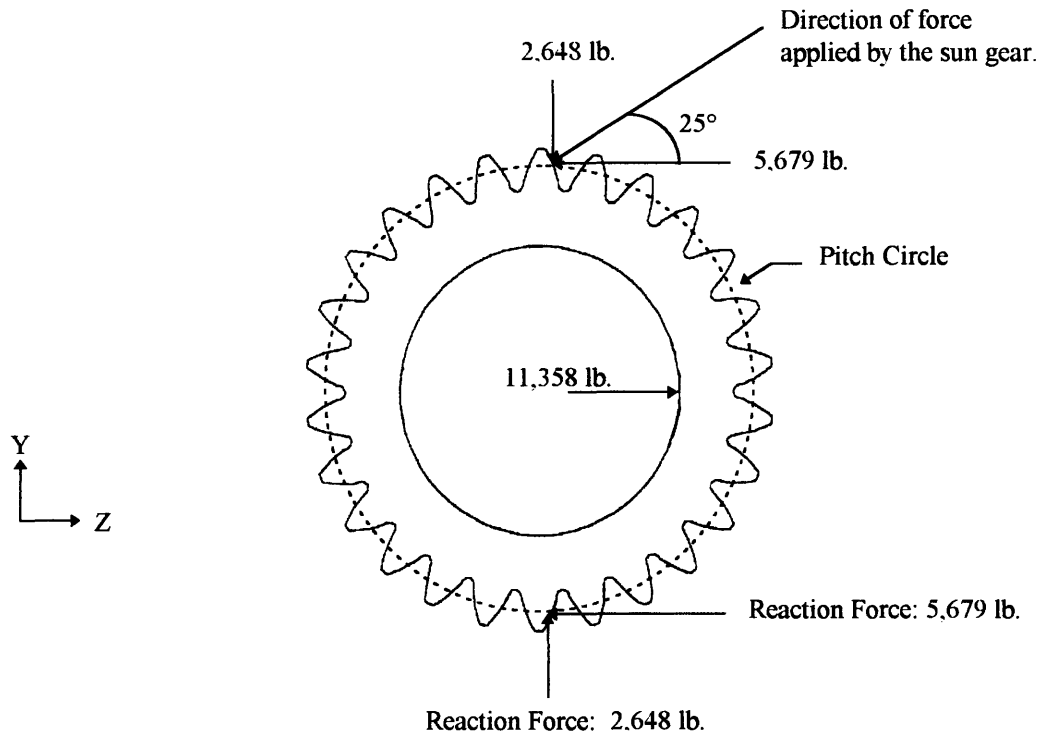
Figure 3.6: Calculation of applied loads.

Although it was desirable to apply a uniform load across the face of the gear tooth at the pitch diameter, the nature of the modeling program allowed only discrete point loads. Because of this, great care was taken in considering the magnitude of the point loads which were applied. Since the model of the tooth may be composed of elements of unequal size, it was important to apply the correct force to each node. The best way to accomplish this was to apply graduated forces. Figure 3.7 is an example of a tooth to which point loads will be applied. The variables $d_{1...4}$ depict the lengths of each of the elements which make up the tooth width. Force per unit length (f) can be calculated by dividing the total load applied to the tooth by the total width of the tooth face. The point loads, which must be applied to the nodes labeled A through E in the finite element model, are designated by $F_{A...E}$. The point load forces can be calculated as in the following example: in reality the load on the pitch diameter between nodes A and B (designated by

AB) signifies some portion of the total force along the tooth which is proportional to the

total length (fd_1). Since, the finite element modeling program is limited to applying point

loads at each node, the total force (fd_1) must be evenly divided between nodes A and B.

As a result of the force on AB , the load on A is $F_A = \frac{1}{2}fd_1$. However, node B

experienced a load not only from AB but a load from BC as well. Thus the total force on

B is $F_B = \frac{1}{2}fd_1 + \frac{1}{2}fd_2$.
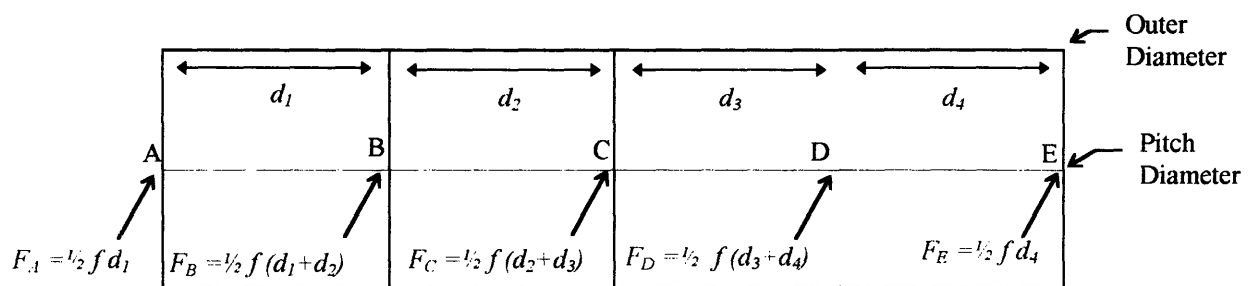
Figure 3.7: Example of point load calculations.

Roller Data

Once the three-dimensional geometry of the gear had been established, the bearing

roller properties had to be included in the emerging model of the gear. The Timken

Company had developed an algorithm[11] which was based on Hertzian contact equations

and took roller dimensions, raceway specifications and applied loads into account to

establish the properties of the non-linear spring elements which would ultimately model

the bearing rollers. A second program[12] utilized user-defined geometrical information,

bearing design data and the three-dimensional gear model to attach the 'roller' springs to

the appropriate locations along the outer raceway (i.e. the tapered-bore of the gear). The

rollers were modeled at a moment in time when one of the rollers was located directly

[11] R.E. Southam and R.G. Lang. Internal Timken Research project report, October 1985.

under the tooth on which forces were applied. The program also built an appropriately-dimensioned 'beam' to support the gear and 'rollers'. As a result of these two programs, model pre-processing was complete. The gear geometry had been designed and the bearing rollers had been located and modeled as a row of springs. The pin, on which the gear rotated during actual operation, had been given the appropriate material and geometrical properties.

Analysis

When the geometrical issues had been resolved, it was possible to import the data into the analysis tool, ABAQUS. However, before the analysis could be conducted, the ABAQUS input deck had to be verified to ensure that geometrical and load data was correct. The model of the gear had been sufficiently complicated that its sheer size was difficult for the computer to negotiate. For this reason the model was broken into two separate programs. In the first, the 'Super Element', only geometrical considerations were addressed. In the 'Main Model', the results from the Super Element were combined with force and boundary conditions. In this way, ABAQUS could calculate the geometrical and force issues separately, keeping the matrices of the analyses to a relatively manageable size. Appendix A is an example of the Super Element and Main Models which were used as input decks to the ABAQUS analysis engine[13]. The following will be a step-by-step description of each of the header cards (marked by a ✷ in the input decks).

---

[12] John D. Dougherty, Internal Timken Research Software.

[13] Because of the great similarity among them, not all of the ABAQUS models have been included in Appendix A. Instead, only one set is included as an example.

Super Element

As mentioned before, the geometry of the gear was too complex to be easily

analyzed in a single model. Therefore the model was broken up into two programs:

'Super Element' and 'Main Model' which focused only on geometry and force issues,

respectively. The following is a tour of the Super Element program:

*HEADING - in this section resides the information which identifies the file to the user.

  This section is not considered by ABAQUS in the analysis.

*SUPER, ID=Z0001 - this section names the super element.

*NODE, NSET=CUP - each of the nodes in this set establish the gear through the use of

  Cartesian coordinates. In this example, the model had a total of 10,800 nodes! The

  NSET (node set) name "CUP" is a user-defined variable.

*NSET, NSET=ROLLT & NSET=ROLL - this set of nodes establish the Cartesian

  coordinate locations of the rollers.

*NSET, NSET=FIXED - the set "FIXED" was used to define the set of nodes which

  would be fixed against displacement on the gear geometry. An example of fixed nodes is

  the boundary indicated in Fig. 3.2.

*NSET, NSET=FORCEN - this set of nodes identified those nodes to which forces would

  be applied.

*ELEMENT, ELSET=CUP, TYPE=C3D8R - once the nodes had been given names (1,

  2, 3, . . . 10,800) and located in three-dimensional space, they can be used to create

  three-dimensional 'bricks' named "elements". This element set establishes and names the

  7,040 elements which make up the three-dimensional geometry seen in Fig. 3.5.

* SOLID SECTION, ELSET=CUP, MATERIAL=CUP - this and the next two commands

give ABAQUS the information it needed to establish the material of the gear.

* MATERIAL, NAME=CUP - see description for "SOLID SECTION" above.

* ELASTIC,TYPE=ISO - here the isotropic, linear elastic material properties of steel are

given as Young's Modulus of $E = 30 \times 10^6$ psi. and a Poisson's ratio of $v = 0.3$.

* RETAINED DOFS - this set identifies all the nodes which will be needed in the Main

Model. For example, the 'roller' springs will need to be attached to the nodes in ROLLT

and ROLL, whereas forces will be applied to the nodes in FORCEN.

* BOUNDARY, OP=NEW - this command identifies the nodes which will be subject to

newly applied boundary conditions in the Main model.

* END SUPER - informs ABAQUS that it has completed the analysis.

Main Model

Once the geometrical analysis was complete, the result could be used in the Main

Model to apply the appropriate forces. The following is a tour only of the * Header cards

which were not discussed in the previous section but which appear in the Main Model, as

shown in Appendix A:

* NODE, NSET=BEAM - this set of nodes establishes the location of the 'beam' or pin,

on which the gear is mounted, via Cartesian coordinates. These points were established

by the second computer algorithm described in the section titled "Roller Data".

* ELEMENT, TYPE=Z0001,ELSET=SUPER,FILE=INVOLSE96 - this operation causes

ABAQUS to return to the previously created super element (recall the naming of the

supplement as 'Z0001' in the previous section). The list of element names refers to all of

the element nodes which were retained in the previous section under the *RETAINED

DOFS header card.

*ELEMENT,ELSET=BEAM,TYPE=B31 - this set of elements define the 'beam' using

the previously established nodes (NSET=BEAM).

*ELEMENT,ELSET=ROLLF1. . . ROLLF4, TYPE=SPRINGA - this section establishes

spring elements modeling the rollers which connect between the tapered-bore of the gear

and the beam as discussed in the previous section titled "Roller Data". The spring

characteristics will be defined later in the model.

*ELEMENT, ELSET=EXTRA1. . .EXTRA3, TYPE=SPRING1 - these springs are weak

springs (compared to the bearing springs) designed to 'ground' the structure in three-

dimensional space.

*BEAM SECTION,ELSET=BEAM, SECTION=CIRC,MATERIAL = BEAM - this

section primarily establishes the diameter of the beam.

*SPRING - all of the commands beginning with the word "spring" will define the

properties of the springs which ABAQUS will use. The non-linear springs were defined

by the Hertzian contact stress program referred to in the section titled "Roller Data".

The remaining three springs are the linear springs which will keep the model from

'floating' in three-dimensional space.

*BOUNDARY,OP=NEW - this section includes a number of new nodes which will act as

boundaries. For example, node number 10,806 is the point where the beam is mounted

into a wall and thus is fixed in all directions (translational and rotational)

*EL PRINT . . .The commands in this section establish what results ABAQUS should

return in a file as well as the format of the results.

* CLOAD,OP=NEW - this section defines magnitude and direction of the loads which will be applied to the model (these loads will be applied as concentrated nodal forces in the way described in conjunction with Fig. 3.7 above).

* END STEP - alerts ABAQUS that it has come to the end of the program.

Results

Figures 3.8 through 3.10 are the results of the ABAQUS analysis conducted. As can be seen in Fig. 3.8, the maximum Mises equivalent tensile stress is located at the root of the tooth and has a magnitude of 96.1 ksi (663 MPa) (Since the yield strength of the material used is approximately 210 ksi (1,470 MPa). The stress induced in the gear would result in elastic deformation of the gear-thus a long life would be expected. The gear model is rotated such that the stresses along the inner raceway can also be seen. From the stress patterns created around the areas where the roller springs were attached, it is apparent that the bearings had a *load zone* of approximately 180°. The remaining rollers are not loaded at all[14].

Figure 3.9 is a closer view of the loaded tooth. As can be seen, Mises stresses along the pitch diameter where the load was applied are of the order of 45 ksi (315 MPa). As expected, the high stress occurred at the interface of the tooth face and tooth root. Moreover, both sides of the tooth displayed high stresses, signifying that the respective compressive and tensile loads where of approximately the same magnitude. The raceway under the tooth also illustrates higher Mises stresses relative to the remainder of the raceway. The explanation for this stress is closely related to the fact that the finite element

---

[14] In fact, the rollers on this side may not even make contact with the raceway due to formation of open gaps.
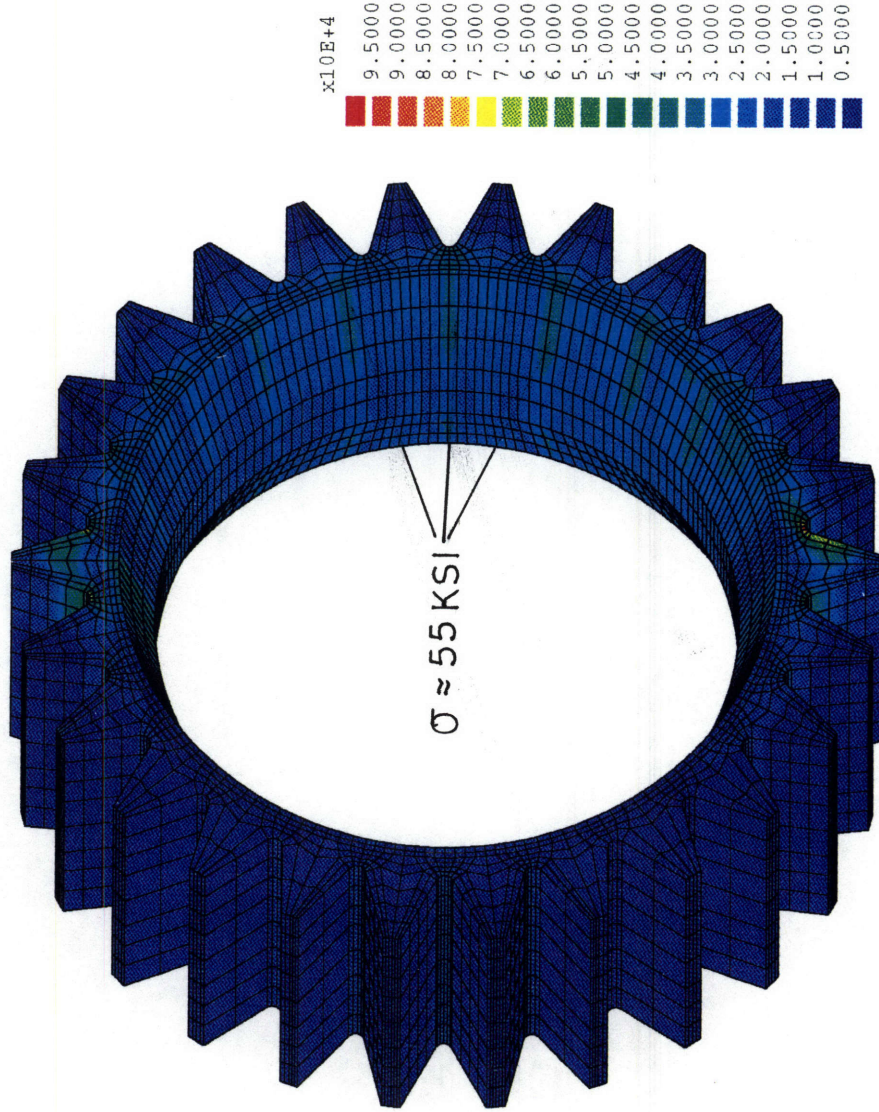
Figure 3.8: Results of the FEA for the basic model - view of the loaded raceway.

FAMresult : 3.50 /277   Date: 23 Aug 1995   Model: cdata

LOAD/PITCH LINE ≈ 45 KSI
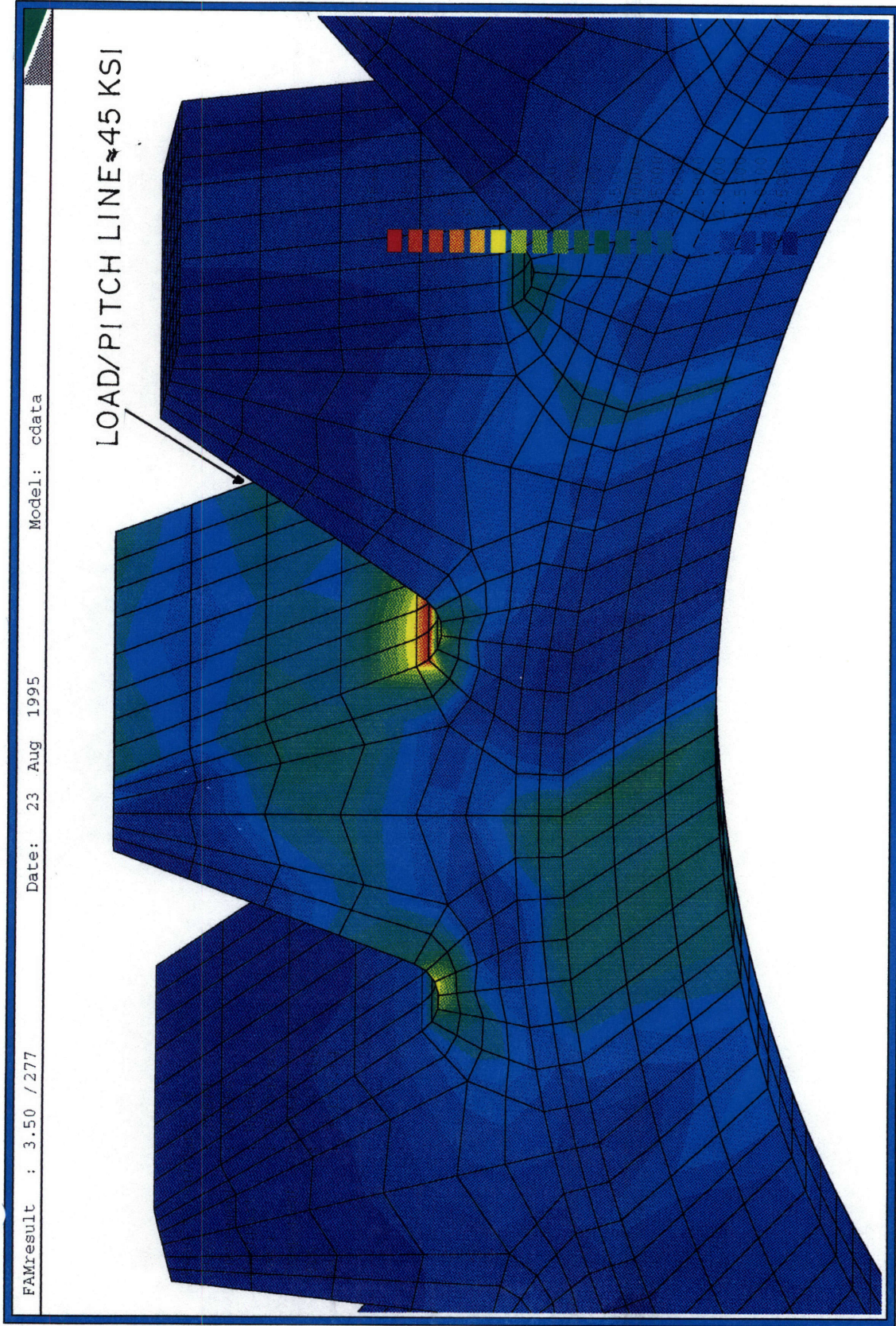
Figure 3.9: Results of the FEA for the basic model - close view of the loaded tooth.

model was of a moment in time when one bearing roller was exactly underneath the loaded tooth. The forces applied to the tooth cause a reaction from the roller resulting in a higher stress on the raceway at that point.

Figure 3.10 is a closer view of the raceway under load. Again, it is possible to see the increased stresses where the bearing rollers apply the reactive forces. Although these stresses are not comparable to the tooth root stresses, it is of interest to note that the stress in the gear increases while the rim thickness decreases (i.e. more stress near gear face than at the flat inner diameter of the bore).

In conclusion, it is apparent that the stresses in GearSpexx™ are acceptably small for testing purposes because maximum stresses calculated (~97 ksi, 679 MPa) are substantially smaller than the yield strength of SAE 8620 case carburized alloy steel is ~190 ksi (1,330 MPa). The prototypes which will be tested are expected to exhibit the fatigue life of a system with elastic deformation.

Tapered-Bore Model

Once the gear design had passed the preliminary model, a second, more accurate Finite Element model was created for several reasons. First, the basic model had not utilized involute gear teeth. Since the stresses calculated in the previous model were higher than the endurance limit of SAE 8620 case carburized alloy steel[15], it was important to have an accurate model of the gear to establish the 'exact' stresses. Also, during operation the highest load on a gear tooth does not occur at the pitch diameter but at a larger diameter. The Highest Point of Single Tooth Contact (*HPSTC*) on the planet gear

---

[15] See "Conclusion" section for details.

Figure 3.10: Results of the FEA for the basic model - close view of the loaded raceway.

occurs just after the preceding tooth pair releases. Whereas the Pitch diameter was 3.071 in. (78 mm), the HPSTC diameter was 3.222 in. (81.8 mm). This difference in radial location of load, along with the change in tooth geometry (from straight-sided to involute) had the potential of changing the results substantially. Moreover, the method of loading the tooth in the basic FE model did not concentrate on the planet gear only. The insertion of a boundary condition at the bottom tooth forced the program to evaluate reaction forces. In the tapered-bore model, the reaction forces were simply added to the analysis in lieu of the boundary condition. Another reason for choosing to model the gear without a displacement boundary condition was that the machine to be used in testing would not be a design which incorporated a boundary condition of the type included in the Basic finite element model[16]. As a result, a test design loading two teeth separated by 180° was created, enforcing the need to load the gear in a new way for the finite element model. Again, due to test design limitations, the gear had to be mounted on a shaft supported on either side, rather than on the cantilevered pin used in the case study application. A resulting benefit of this design change was that the finite element model of the gear could use symmetry along the radial plane. Since any deflection which would occur due to the shaft would be symmetrical about the radial axis (Y), it was possible to model only half the thickness of the gear and thus only one bearing raceway. Since the resulting model would be half - size, it was possible to include a finer mesh on the gear teeth themselves, again resulting in a more accurate model. In conclusion, the tapered-bore model was expected to be a very accurate representation of the gear as it would be tested.

---

[16] See Chapter 5 for a detailed discussion.

Since the bearings and other geometrical issues remained unchanged, the techniques for calculating applied loads, establishing roller spring characteristics and locations as well as the completion of the analysis input files were identical to the techniques used in the basic model. Thus these issues will not be discussed again.

Results

Figures 3.11 through 3.14 represent the ABAQUS results from the tapered-bore model. Figure 3.11 gives a very good view of the involute shape of the gear teeth. From the information on this figure, it is apparent that the maximum stress of the gear at 96.7 ksi (666.7 MPa), has increased only by ~0.6 ksi (6.1 MPa) above the stress calculated in the basic model. The reason for such a slight change lies primarily in the different shape of the gear teeth. Although the moment arm of the application increased because loading occurred at the HPSTC rather than at the pitch line, the thickness of the tooth also increased. This change in tooth geometry was enough to balance the added stresses induced by the increased moment arm.

Figure 3.12 is a closer view of the tooth at the top of the gear. The result is somewhat surprising at first because only the root in compression exhibits the maximum stress. On second consideration, it becomes apparent that since the load is applied at a larger diameter (as indicated in the figure), the tooth has a greater tendency toward counter-clockwise bending. The root experiencing a tensile stress is free to move in an upward direction. However, the root experiencing a compressive stress encounters stiff resistance from the bearing roller spring below, as can be seen by the increased stress on the raceway underneath the root in compression. In other words, the root in tension is 'free' to move radially outward, whereas the root in compression experiences two
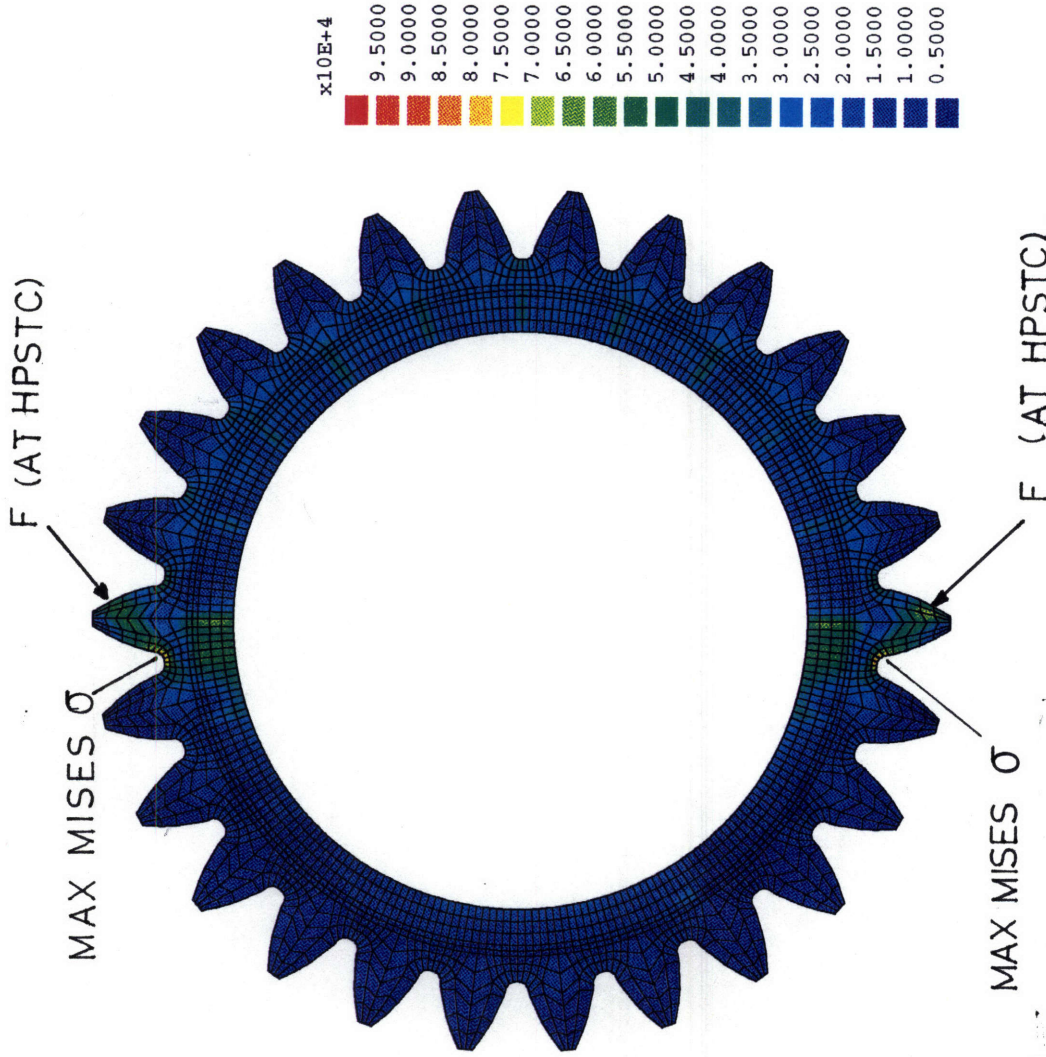
Figure 3.11: Two dimensional representation of the planet gear for the Finite Element Analysis - Tapered bore model.
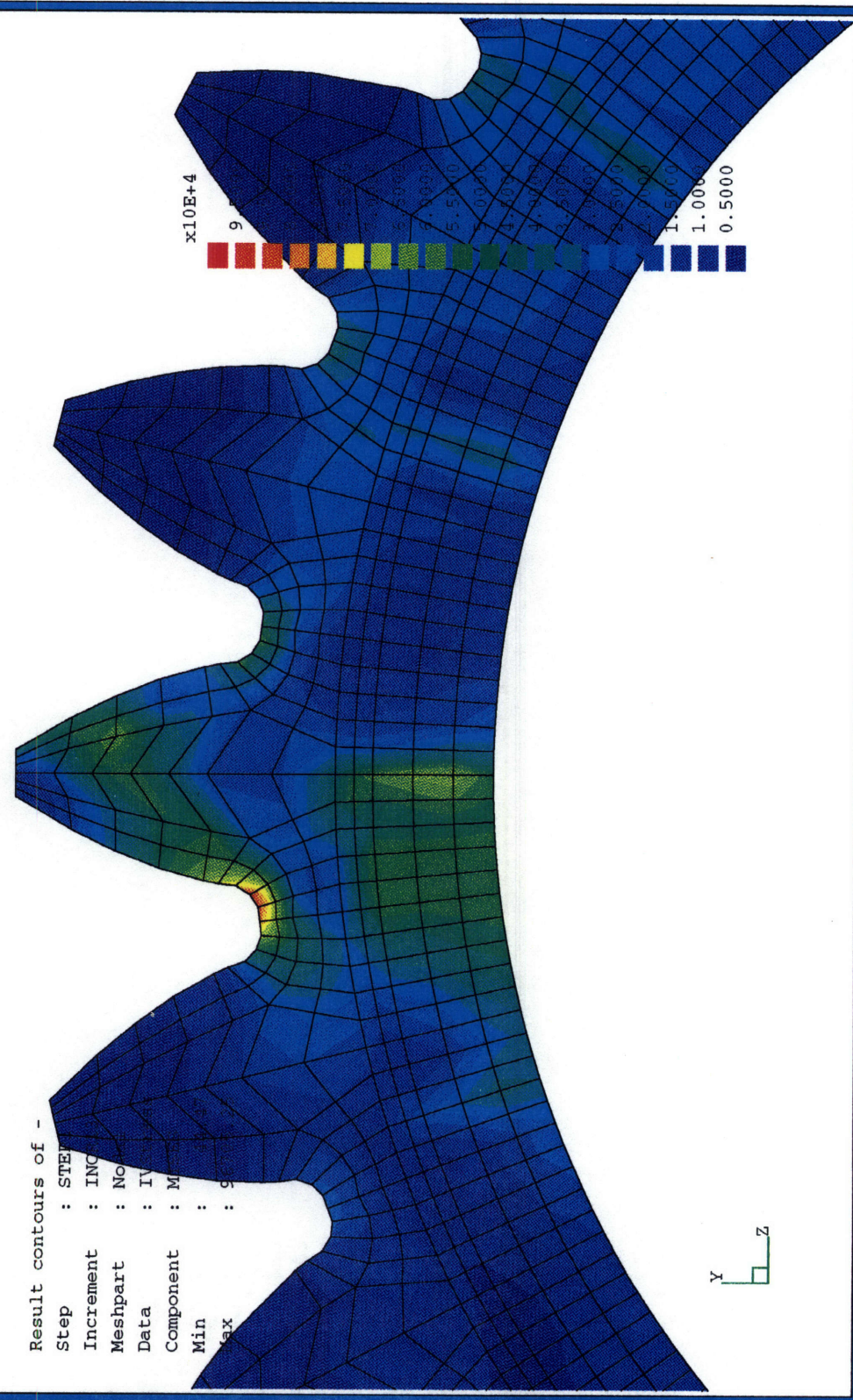
Figure 3.12: Results of the FEA for the tapered bore model - close view of the loaded tooth.

compressive forces; one along the direction of loading and another as the reaction force from the roller spring, radially outward. As in the basic model, the maximum stress occurs at the interface of the tooth root and tooth face.

Figure 3.13 shows the gear from a slightly different view. In this view it is possible to note that, as expected, the stress along the tooth root is uniform. Moreover, the tooth at the bottom has stress patterns along the raceway which are identical to the patterns along the raceway at the top tooth. This was expected, confirming that the two teeth had been properly loaded. In Figure 3.14 the stress patterns created by the roller springs are apparent again. As in the basic model, the load zone is approximately 180° and the stress along the raceway increases as the rim thickness decreases. Once again, the stress in the root of the tooth is substantially greater than the stresses along the bearing raceway.

Straight-Bore Model

A final element analysis was conducted to evaluate the stress of the straight-bore gear which was successfully used in the case study application. The customer of the case study had already adopted the integral gear method and had already designed the bore of the gear to act as the outer raceway for two cylindrical roller bearings, as will be discussed in greater detail in Chapter 4. It was especially important to analyze this gear because the straight-bore gear, used in the case study, would also be tested. This would act as a control in both the FEA and the testing because it had already proven successful in the application targeted for GearSpexx™. As in the previous model, the gear geometry was as close to the actual gear design as possible. Moreover, the only difference between the tapered-bore model and the straight-bore model was the rim geometry - in the straight

Figure 3.13: Results of the FEA for the tapered bore model - view of the tooth root and raceway of loaded teeth.

FAMresult : 3.80/260   Date: 29 Mar 1996   Model: involmmmarch

Result contours of -

Step   : STEP1
Increment   : INCR13
Meshpart   : Nodal
Data   : IVStress
Component   : MISES
Min   : 44.47
Max   : 96705.25

x10E+4

9.5000
9.0000
8.5000
8.0000
7.5000
7.0000
6.5000
6.0000
5.5000
5.0000
4.5000
4.0000
3.5000
3.0000
2.5000
2.0000
1.5000
1.0000
0.5000

Figure 3.14: Results of the FEA for the tapered bore model - view of the loaded raceway.

model, rim thickness remained constant throughout the entire gear. The programs which modeled the tapered rollers were used to model the straight rollers as well because it was possible to indicate the angle of taper for the roller (=zero in the case of the straight roller) and the number of rollers (20 in the tapered roller bearing, 24 in the straight roller bearing). All other variables were identical to the tapered-bore model.

Results

Figures 3.15 through 3.18 are the results of the analysis conducted. Figure 3.15 is a front view of the straight-bore gear and displays the difference in rim thickness as compared to the tapered-bore model. The maximum stress, calculated to be 87.2 ksi (601 MPa), is approximately 10% lower than the stress in the tapered-bore model. Moreover it is apparent that although the maximum stress in the model is still quite high, the overall stress in the gear is lower than that of the tapered-bore model.

Figure 3.16 is a close up of the top tooth to which a force is applied. As in the tapered-bore model, the high stresses occur in the compressed root. This root still has the compressive force induced by the line force applied at the HPSTC. However, due to the increased rim thickness, the stress from the rollers is less than in the tapered-bore model.

Figure 3.17 allows a better view of the stresses in the tooth root at the top tooth and the raceway along the bottom of the tooth. The high stress area is uniform along the length of the tooth root at the top tooth but is smaller in 'width' than the high stress area of the tapered-bore model (as seen in Fig. 3.13). Moreover, the stress along the bottom raceway, as seen in the figure, is more uniform and lower in magnitude than the similarly-located stress in the tapered-bore model. In Fig. 3.18, the bearing reactions can be very

Figure 3.15: Two dimensional representation of the planet gear for the Finite Element Analysis - Straight bore model.

Figure 3.16: Results of the FEA for the straight bore model - close view of the loaded tooth.

FAMresult : 3.80 /260

Date: 29 Mar 1996

Model: custmm1

Result contours of -

Step   : STEP1
Increment : INCR6
Meshpart : Nodal
Data   : IVStress
Component : MISES
          : 119.84
          : 87250.60

FAMresult : 3.80/260   Date: 29 Mar 1996   Model: custmm1

Result contours of -

Step   : STEP1
Increment : INCR6
Meshpart : Nodal
Data   : IVStres
Component : MISES
Min   : 0
Max   : 87

x10E+4
8.5000
8.0000
7.5000
7.0000
6.5000
6.0000
5.5000
5.0000
4.5000
4.0000
3.5000
3.0000
2.5000
2.0000
1.5000
1.0000
0.5000

MAX σ ≈ 87 KSI

MAX σ ON RACE
≈ 40 KSI
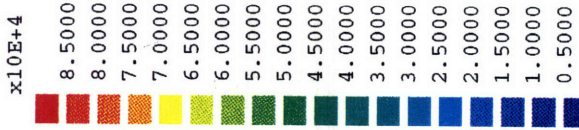
Figure 3.17: Results of the FEA for the straight bore model - view of the tooth root and raceway of loaded teeth.

Figure 3.18: Results of the FEA for the straight bore model - view of the loaded raceway.

FAMresult : 3.80 /260   Date: 29 Mar 1996   Model: custmm1

Result contours of -

Step   : STEP1
Increment : INCR6
Meshpart   : Nodal
Data   : IVStress
Component : MISES
Min   : 119.84
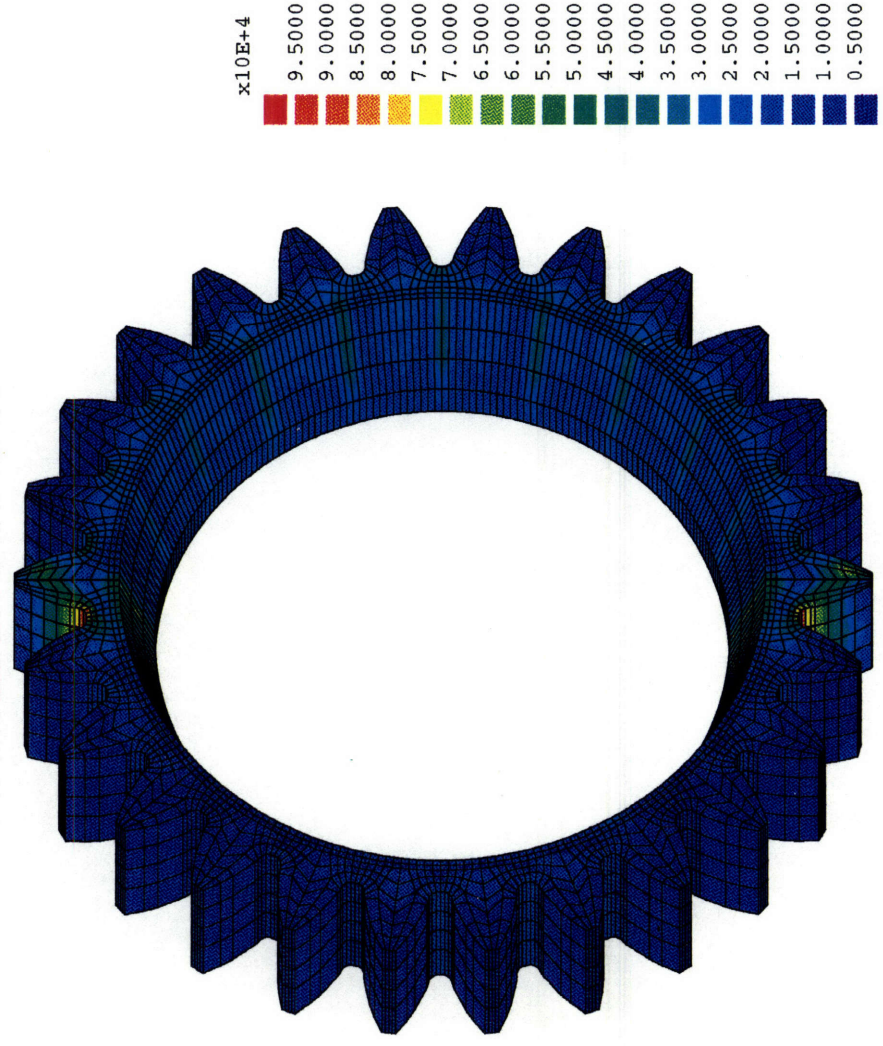Max   : 87250.60

x10E+4

8.5000
8.0000
7.5000
7.0000
6.5000
6.0000
5.5000
5.0000
4.5000
4.0000
3.5000
3.0000
2.5000
2.0000
1.5000
1.0000
0.5000

clearly seen. As in the tapered model, the load zone is ~ 180° although the individual

spring-induced stresses are lower. This lower stress is in part explained by the fact that

the bearing which is actually used in the case study has two sets of 24 cylindrical rollers, as

opposed to the double set of 20 tapered rollers of the actual tapered bearing to be used in

the tapered-bore gear. The higher number of rollers over which the load can be distributed

explain the lower 'per roller' stress observed in the figure. As anticipated, the stress for

each 'roller' along the width of the raceway is constant because the rim thickness has

remained unaltered.

Conclusion

Although the stresses calculated in the tapered-bore model are not substantially

different from the basic model, this set of results are more accurate and representative of

the real application. Using this data, the expected life can be calculated. As the yield

strength of ASE 8620 case carburized, alloy steel is ~190 ksi (1,330 MPa) and the

calculated stresses for the straight-bore gear (87.3 ksi, 611 MPa) and for the tapered bore

gear (96.7 ksi, 677 MPa) indicate that the prototypes will experience primarily elastic

strain. For primarily elastic strain, fully-reversed fatigue life can be calculated using

Basquin's equation:

$$\sigma_a = (\sigma_f')(2N_f)^b$$

where σ_a is the cyclic stress amplitude, σ_f' is the cyclic fatigue strength, $2N_f$ are the number

of reversals to failure and b is the fatigue strength exponent. Although the value for the

fatigue life exponent is known (b = -0.1), the cyclic fatigue strength (σ_f') must be determined. It is known that the endurance limit (σ_e) is approximately one third of the ultimate tensile strength of SAE 8620 case carburized alloy steel (σ_{UTS}). In other words:

$$\sigma_e \approx (0.33)\ \sigma_{UTS}$$

where

$$\sigma_{UTS} \approx 210\ ksi\ (1,470\ MPa)$$

for this material, σ_e = 69.3 ksi (485.1 MPa)[17]. Using this knowledge, it is possible to calculate the cyclic fatigue strength (σ_f') from Basquin's equation, assuming an estimate of achieving 10^6 reversals if the cyclic stress amplitude is equal to the endurance limit. Rearranging Basquin's equation:

$$\sigma_f' = \frac{\sigma_e}{\left(2N_f\right)^b} = \frac{69.3ksi}{\left(10^6\right)^{-0.1}} = 275.8ksi$$

This value for the cyclic fatigue strength can be used in connection with Basquin's equation again to calculate the expected life expectancies for the straight-bore and tapered-bore designs:

$$\sigma_a = (275.8)(2N_f)^{-0.1}$$

where σ_a is the value for cyclic stress as calculated in the finite element analysis and N_f are the cycles to failure. Completing the above calculations, the life expectancy of GearSpexx™ is 35,600 reversals and the fatigue life of the straight-bore gear is expected to be approximately 99,000 reversals. However, these life calculations are based on the peak surface stress calculated by the finite element analysis. Since the stress in the region

---

[17] See also: J.M. Waraniak and D.F. Socie, "Cyclic Deformation and Fatigue Behavior of Carburized Steel", American Society for Metals, Metals Park OH, 1981, p. 249.

of the root is not homogeneously equal to the peak stresses calculated in the FEA, the

stress gradient must be taken into consideration when determining the fully-reversed

fatigue life of the gears. According to Peterson, the peak surface stress must be modified

using an effective load factor of $\left(K_f \middle/ K_t \right)$ which can be calculated using Peterson's

empirical expression:

$$K_f - 1 = \frac{K_t - 1}{1 + \frac{\rho^*}{\rho}}$$

where K_f is the notch fatigue factor, K_t is the stress concentration factor, ρ is the notch

root radius, and ρ^* is the material grain size. Evaluating the above equation establishes

the relationship needed:

$$\left(K_f \middle/ K_t \right) \cong 0.9$$

Thus, modifying Basquin's equation for the effective stresses would result in the

following equation:

$$\sigma_a \left(K_f \middle/ K_t \right) = (0.9)\sigma_a = (\sigma_f')(2N_f)^b$$

evaluating the equation using the results from the finite element analysis for GearSpexx™

and the gear with the straight bore, the fatigue life expected for GearSpexx™ is 103,000

reversals and 283,000 reversals for the gear with the straight bore.

Also based on the analyses, the straight-bore gear appears to be much less likely to

fail through the rim than the tapered-bore gear. This conclusion may be understood best

by comparing Figures 3.13 and 3.17. The stress in the tapered-bore rim has an average

stress of 60 ksi (420 MPa) through the entire rim. On the other hand, the straight-bore

rim has an average stress of 35 ksi (245 MPa) on the raceway and only an average stress

of 20 ksi (140 MPa) through the remainder of the rim. Therefore, it is expected that the

tapered-bore gear will be more likely to fail through the rim than the straight roller gear.

CHAPTER 4

PROTOTYPES

GearSpexx™ is an interesting combination of gear and bearing with an interface at the bore of the gear. As the goal of this research was to examine only the interaction of the two components, some basic control factors were incorporated. The gear and bearing designs were maintained to their standard designs as much as possible, with the only alterations occurring at the gear bore. Thus, variations in GearSpexx™ performance would be a result of rim alteration not due to any deviation from standard bearing and gear design practices. To accomplish this, a case study was used as the basis for all design. The teeth and overall geometry of the gear were maintained, while the bore of the gear was designed to be the outer raceway for the bearing. The bearing cones and rollers were also chosen in strict adherence to standard practice at The Timken Company. Through every stage of design of the prototype gear, bearings and the test, previous data from the application was utilized as much as possible.

The following chapter will discuss the issues which were addressed in creating the prototypes. First, the application which was used as the case study for this research is described in as much detail as would be necessary to understand the role which GearSpexx™ would play. Then a section will describe some of options available for

53

manufacture of the prototypes. Next, the design decisions which ensured that bearing

design practices had adhered to the quality standards required by The Timken company

will be discussed. The final section of the chapter will examine the results of the prototype

manufacture by conducting a quality analysis of the final products.

Customer Data

Like many companies, the customer who supplied the case study, was redesigning

product families to take advantage of technological advances and lower cost

opportunities. In improving the torque hub reduction unit product line, the customer chose

product X as the prototype for the remainder of the customer's 'X' line. In this

application, GearSpexx™ could be relevant for use in the third stage reduction of the

torque hub reduction unit as indicated on Fig. 4.1.

The customer supplied drawings and dimensions of product X, as well as the

existing gear design. The customer had already applied the integral gear concept to their

design. However, the previous gear employed a straight-bore and a double row of

cylindrical bearings - each bearing had a total of 24 rollers. Both the existing gear and a

double-tapered-bore gear were used in the design of prototypes and the analytical

analyses.

Other information available about the application included the following:

• the bearings would encounter average speeds of 57 rpm with a maximum speed as high

as 228 rpm.
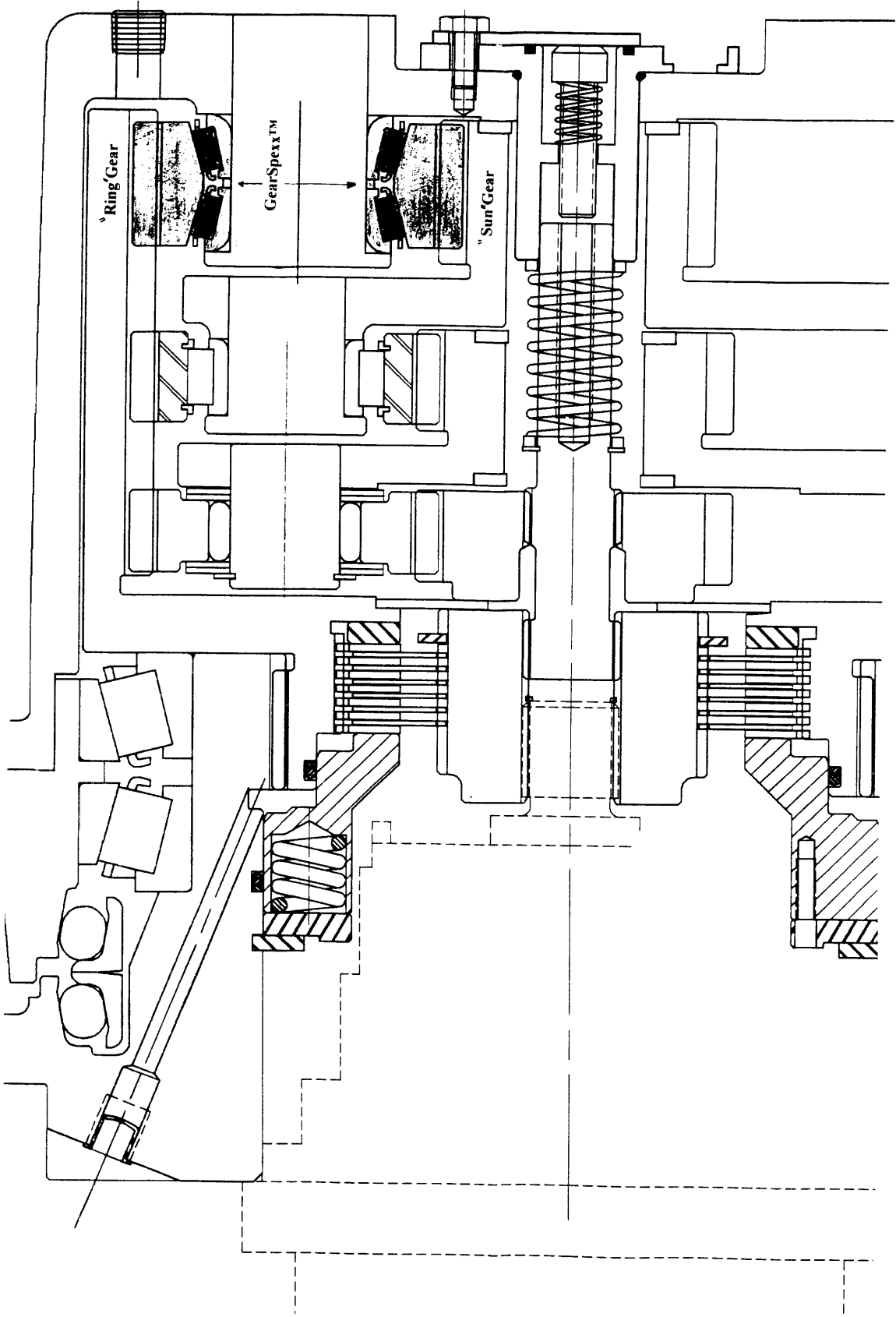
Figure 4.1: Illustration of the case study torque hub reduction unit. Proposed GearSpexx™ is shaded.

- the bearings would be expected to operate under combined loads of 11,400 lb[18]

  (78,300 N).

- the bearings would not be sealed and be lubricated by the oil in the torque hub, an oil of

  viscosity of SAE90

- the average operating temperature of the unit would be 150° F (65.6 ° C)

The customer also supplied a design envelope in which to operate. Although the company

was willing to change the diameter of the pin, it was essential that the new design include

the same outer gear envelope as was already in product X.

Prototype Manufacture

Prototype manufacture was a joint venture combining the core competencies of the

bearing and gear manufacturers. GearSpexx™ is composed of two major types of parts:

- the gear with double integral tapered-bores and

- two bearing cones.

As mentioned before, it was not within the scope of the project to redesign the bearings

which would be used in GearSpexx™. Therefore, the appropriate bearings were selected

from an existing base of standard Timken parts.

Since GearSpexx™ employed a double tapered-bore, the gear portion of

GearSpexx™ had to be specially manufactured for this project. The procedural options

for manufacturing the gear portion of GearSpexx™ are illustrated in Fig. 4.2. Tooth

---

[18] "Combined Loads" refers to the fact that two tapered roller bearings would support the same load such that each
bearing would theoretically only experience loads of 5,680 lb (25,300 N).

cutting is the core competence of the gear manufacturer, while raceway finishing is the core competence of the bearing manufacturer. Either of the manufacturers would have been able to cut the gear blank and heat treat the formed gear. After discussion with the customer it became apparent that, due to high demand on their facilities, they would be unable to produce the gear prototypes for a timely completion of this research. Therefore, the gear manufacture was outsourced to a local supplier. The supplier agreed to manufacture and heat treat double tapered-bore gear prototypes. Since the gears in the case study were not finished in any way, the prototype gears would also not be shaved or ground but merely finish-hobbed. The Timken Company would then conduct the final steps of finishing the raceways according to company standards.
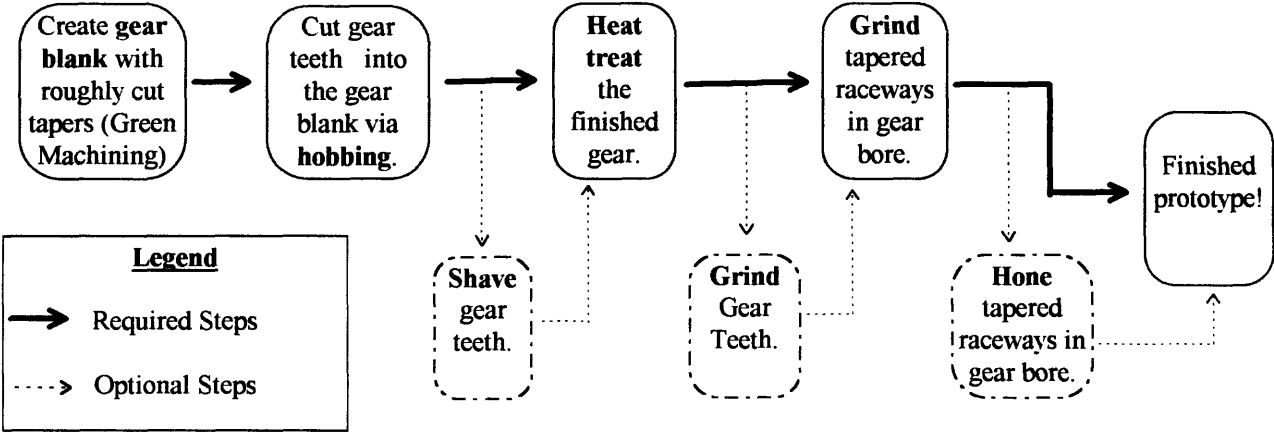
Figure 4.2: Manufacturing flow chart for GearSpexx™.

Prototype Categories

The prototypes were divided into four categories as illustrated in Table 4.1.

Table 4.1 Prototype categories, number ordered and bore style.		
Category Name	Number of Prototypes	Bore Style
Test	40	Tapered
VF	20	Tapered
Control	10	Straight
Supplier	10	Straight

The **Test** category was a group of prototypes of the design modeled in the finite element

analysis (Tapered-Bore Model, Chapter 3). The design of the prototypes in the **VF**

category was identical to design of the prototypes in the Test category. However, these

gears were given an additional finishing operation - *Vibratory Finishing*. Vibratory

Finishing is a process which creates a very fine surface texture on all surfaces using a

Vibratory process[19]. The purpose of this set of prototypes was to compare the effects of

surface texture on otherwise identical products. The **Control** category consisted of gears

of the existing design, and were supplied by the customer. These prototypes, employing

straight-bores as described previously, were intended to act as the 'control' group to

ensure that any failure of a gear in testing was a result of the design change (tapered-bore)

rather than a result of testing procedure. This gear design was also analyzed analytically

using the finite element tools (Straight-Bore Model, Chapter 3) which created a strong

information base for the group. Finally, the gear manufacturer which supplied all of the

tapered-bore prototypes, produced an additional set of prototypes using the customer's

design of a straight-bore gear (**Supplier** category). The Supplier category was

established to ensure that any failure of a gear in testing was a result of gear design

changes rather than a difference in manufacturing technique. Thus if the manufacture and

---

[19]Vibratory finishing is a proprietary process of The Timken Company.

quality of the supplier was similar to that of the customer, then both straight-bore gear sets should fail at the same rate.

Design Decisions

Bearing Selection

Since it was not the scope of this research to redesign the tapered roller bearings used in GearSpexx™, the bearings which were used in the prototype were merely selected from an existing catalogue of Timken bearings. Using data provided by the customer, a number of bearings which would be suitable, given the geometrical and load constraints, were selected. Table 4.2 illustrates the critical dimensions of the cups for these bearings. The rim thicknesses indicated in this table would result if existing cups had been fit inside the bore of the gear and the effective rim had been measured across the actual gear rim and bearing cup. From the point of view of bearing performance, the largest bearing to fit into the gear would result in the best life. However since the outer diameter of the gear was fixed, as the bearing increased in size (diameter), rim thickness necessarily had to be reduced. This caused the gear rim to be more vulnerable to fatigue damage. The whole depth of the gear tooth of the case study was 0.278 in (7.061 mm). Thus, according to the AGMA standard, the rim thickness which was of equivalent size would be the most desirable. However, since the standard does not refer to tapered-bores, this simple selection process could not be utilized. The most conservative design of the gear rim would include part number E because it is the largest bearing which would still maintain the AGMA standard for the minimum rim thickness across the entire cross section (see Fig. 4.3 for an illustration). However, the most aggressive design from the point of view

of the gear, would use the bearing indicated by number A. Using this large bearing, would

mean that only the maximum rim thickness of the part would come close to satisfying ᴜᴜᴇ

AGMA standard.

Table 4.2 The Timken Company Cups Arranged in Ascending Rim Thickness				
Timken Bearing Number	Small End Diameter (in)	Large End Diameter (in)	Maximum Rim Thickness[20] (in)	Minimum Rim Thickness[21] (in)
A	2.236	2.513	0.272	0.133
B	2.043	2.338	0.368	0.221
C	2.155	2.328	0.313	0.226
D	1.974	2.291	0.403	0.244
E	1.937	2.224	0.422	0.278
F	1.921	2.181	0.430	0.299
G	1.887	2.143	0.446	0.319
H	1.863	2.130	0.458	0.325
I	1.810	2.056	0.485	0.362
J	1.643	1.850	0.568	0.465

The primary scope of this research - to 'push the design envelope' and create

analytical tools for future designs - caused somewhat of a leave from the case study

application. If this product were intended for immediate use, a margin of safety would be

imperative, so a bearing which would allow for a larger rim thickness would undoubtedly

be selected. However, since the scope of this research is an attempt to create a correlation

between analytical and test results, a more aggressive design would yield the more

valuable information. For this reason, a design using part number A was created. Figure

4.4 is the design chosen for the tapered-bore prototypes. Figure 4.5 is the design used to

create the straight-bore prototypes used in the Supplier category[22].

---

[20] Small end diameter subtracted from the root diameter.

[21] Large end diameter subtracted from the root diameter.

[22] Note: Although this design was based on the actual customer design, it is not a design drawing created by the customer.
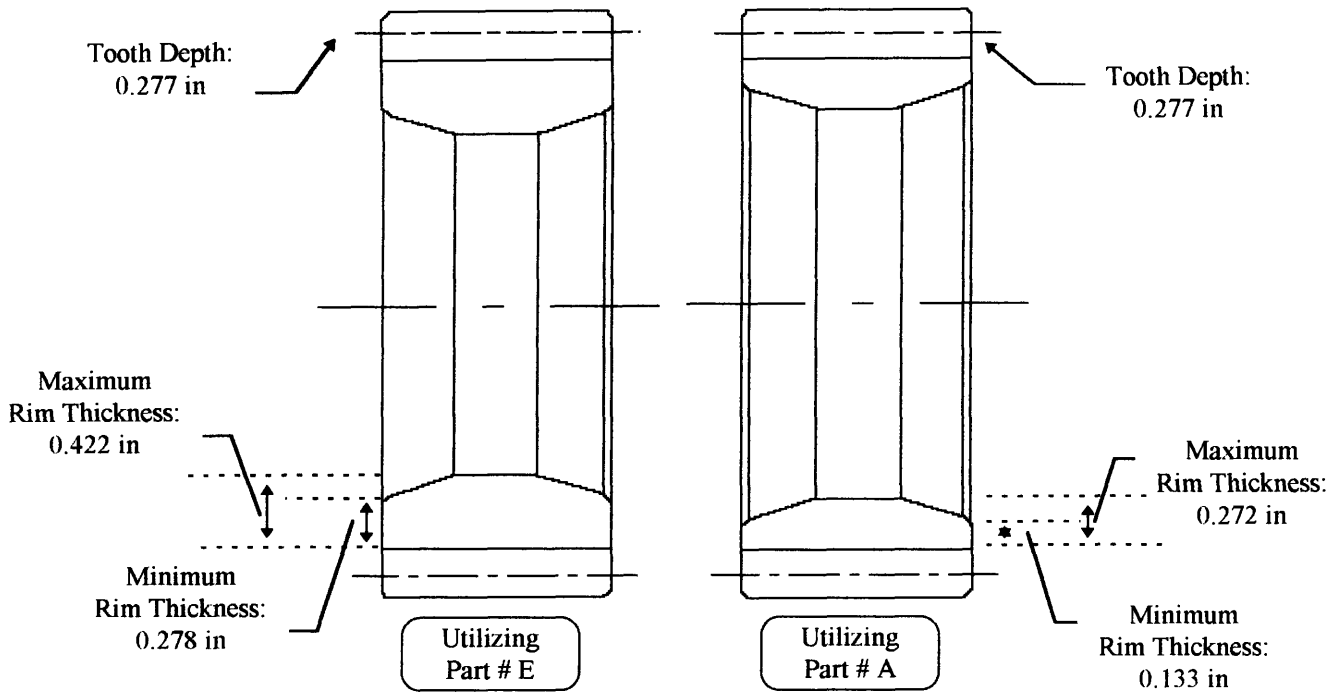
Figure 4.3: Comparison of rim thicknesses using different bearing cones.

Preload

Since the combined width of the cones for use in GearSpexx™ was smaller than the width

of the gear, a spacer was designed to fit between the cones and maintain the proper

preload during assembly. Preload is the amount of axial force on the bearing when it is

mounted and is in a 'no (transverse) load' state. The cone is seated in the cup with a

given force, which induces a certain number of rollers to be in contact with the cup. As

was seen in the finite element model (Chapter 3), the more rollers over which a load can

be distributed, the less stress is induced by each individual roller on the raceway. It is

critical that the proper amount of preload be applied to ensure the longest life. Preload is

measured in negative length, and is on the order of thousandths of inches (tens of mm). If

the bearing is allowed to move freely along the axial direction on the shaft, the bearing is

said to have *endplay*, which is measured in positive length.

NOTE: 33° 0', TAPERED BORES TO BE FINISH GROUND BY THE TIMKEN CO.

33° 0'
BOTH ENDS

REF FACE DIM FOR ANGULAR BORE

2.480

.414 REF

√GRIND

√GRIND

1.275

√GRIND

.030 X 45° CHAM BOTH ENDS

BOTH ENDS 45°

.049 CHAM DEPTH BOTH ENDS

3.327

2.236

MATERIAL   SAE 8617 H

GEAR DATA

NUMBER OF TEETH	26
NORMAL DIAMETRAL PITCH	8.466
NORMAL PRESS ANGLE	25° 0'
PITCH DIAMETER	3.070
BASE CIRCLE DIAMETER	2.783
SAP DIA 2.892 SAP ANGLE	16° 21'
ADDENDUM	0.133
DEDENDUM	0.144
WHOLE DEPTH	0.277
PIN DIAMETER	0.216.

MEASUREMENT OVER PINS	3.412
	3.406
CIRCULAR TOOTH THICKNESS	0.196
	0.193.
TOTAL BACKLASH	.012'/.006
AGMA QUALITY	9

Figure 4.4: Illustration of the tapered-bore design for the prototypes used the FEA and testing.
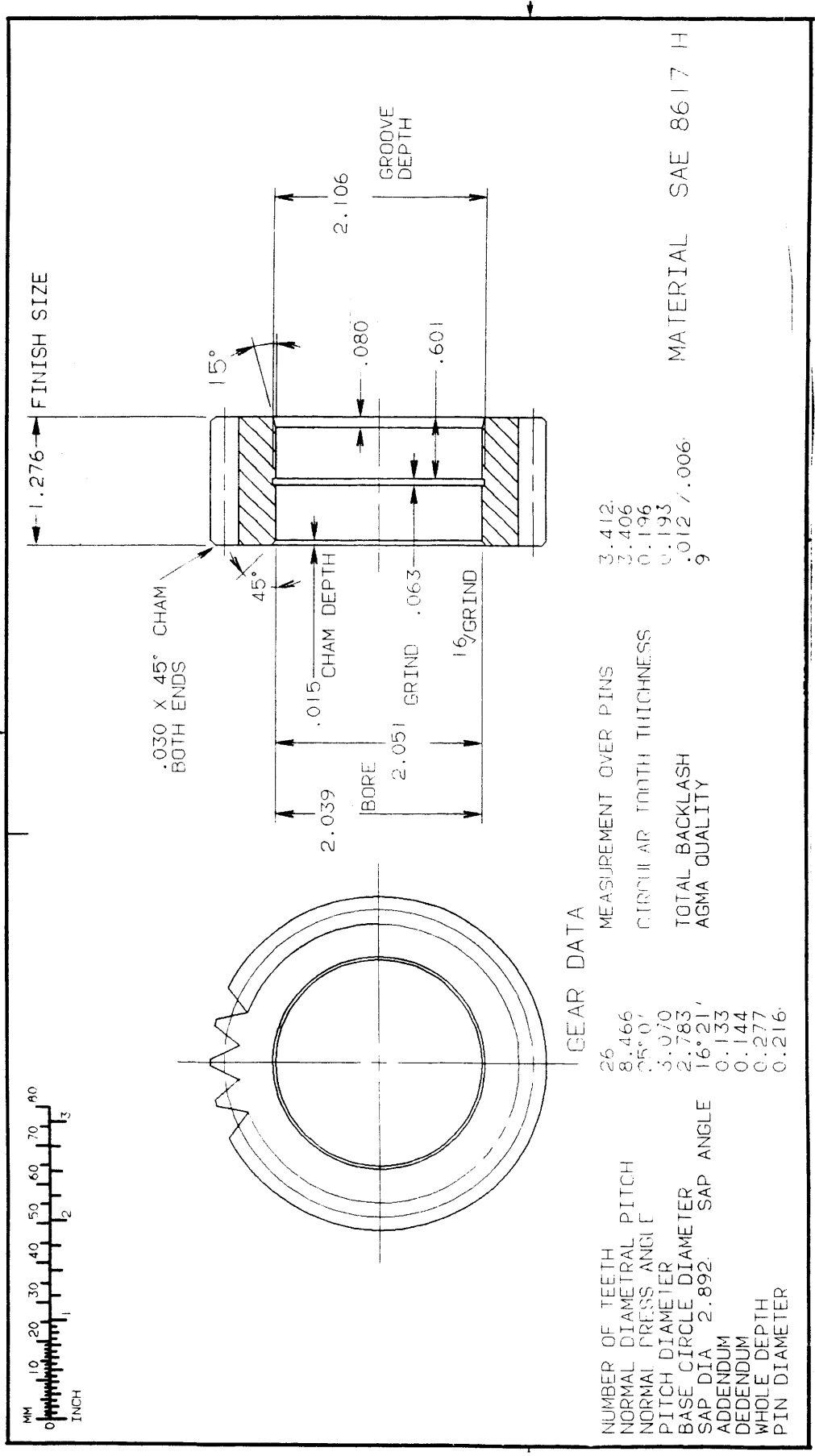
Figure 4.5: Illustration of the straight-bore design which was used as a control in the FEA and testing.

Another computer algorithm created by The Timken Company was applied to calculate the necessary preload. Traditionally, bearing life equations have been calculated as follows[23]:

$$L_{10} = \left(\frac{C_{90}}{P}\right)^{10/3} \left(\frac{1.5 \times 10^6}{S}\right) \quad hours$$

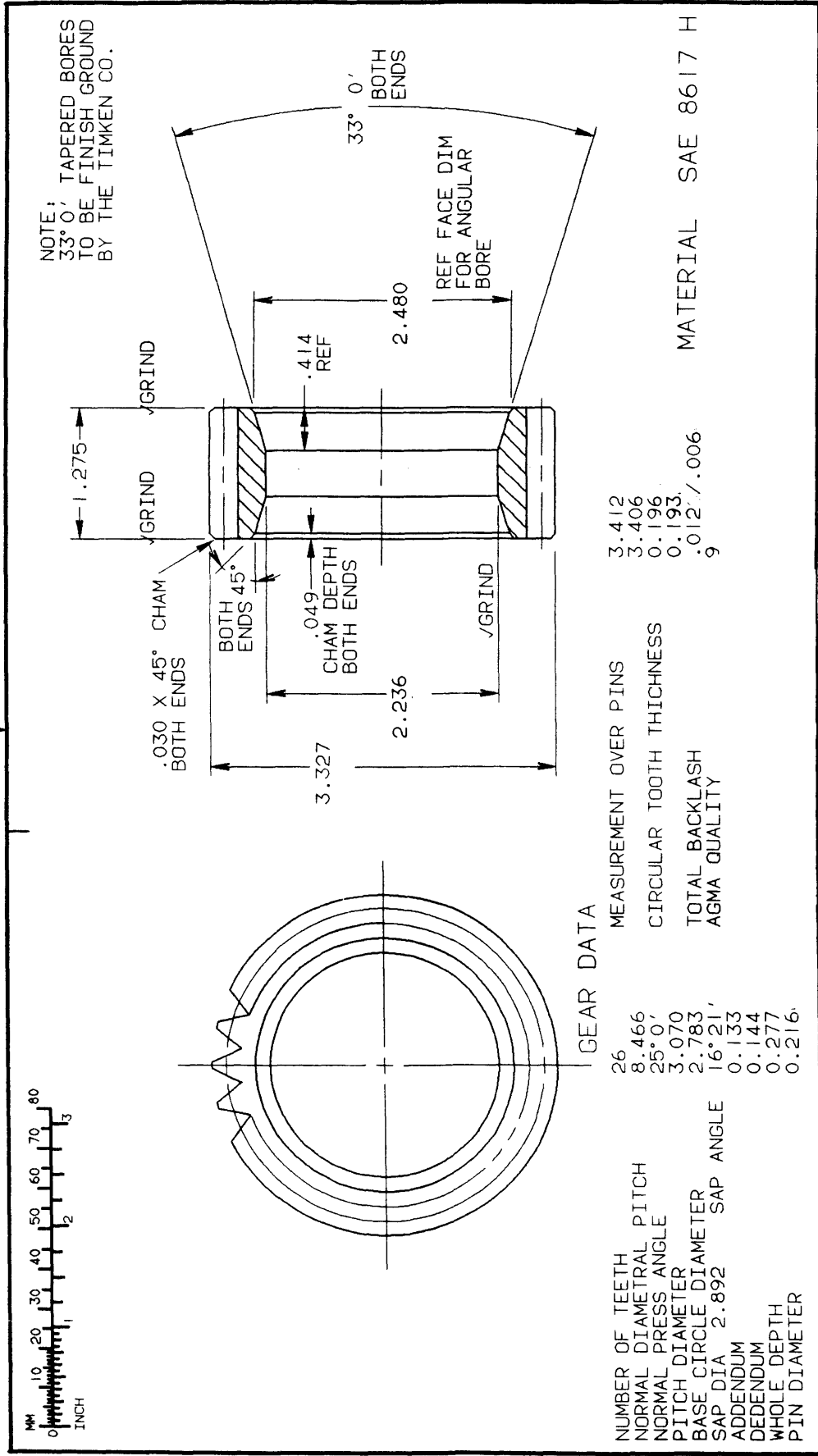where L_{10} (hours), the standard rating life at Timken, ensures that at least 90% of all bearings will reach or exceed the calculated life. C_{90} (lb, N) is the basic dynamic radial load rating and S is the speed of the bearing in rotation per minute (rpm). P (lb, N) is the dynamic equivalent radial load which is applied to the bearings. Over the years, this calculation has been refined to take other factors into consideration such as bearing material, load zone, lubrication and misalignment. These additional variables have been experimentally established and are used as modifying multipliers to the above equation. The computer algorithm which The Timken Company developed radically speeds up the calculation process by taking into account all variables and offering a number of appropriate bearing selections within minutes. Using this program, the previously-selected bearing was examined under several different preload and temperature conditions. The results are illustrated in Fig. 4.6[24].

[23] The Timken Company, Bearing Selection Handbook Revised - 1986, The Timken Company, 1986, pp. 21-26.

[24] Note that Figure 4.6 does not attempt to give absolute values, but is merely intended as a relative comparison of life under varying conditions.
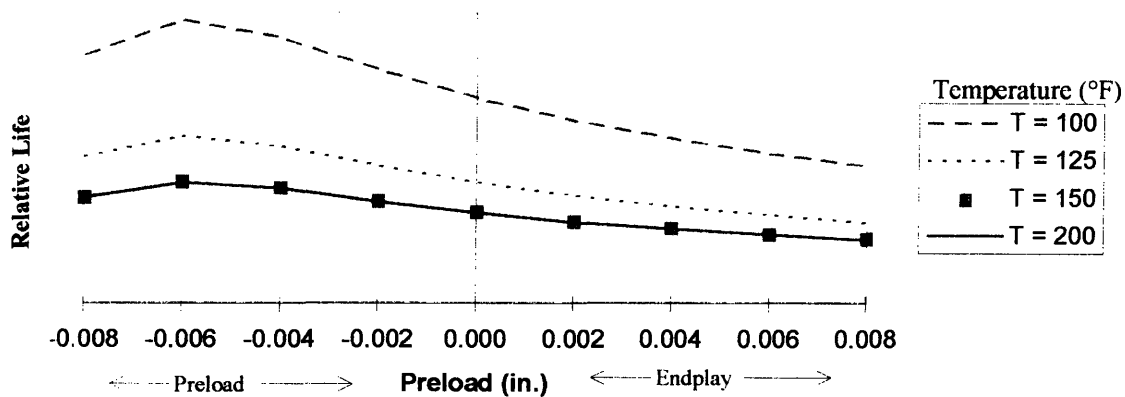
Figure 4.6: Analysis of temperature effects on relative bearing life using selected bearing.

It appears that under any temperature condition, the ideal preload is 0.006 in.

(0.152 mm). However, it is important to consider that the bearing is mounted at room

temperature and expands while reaching operating temperature. It is also important to

note that as preload increases past the optimum of 0.006 in. (0.152 mm), life expectancy

decreases very rapidly. Experience has established that a bearing under such conditions

should be mounted with 0.002 in. (0.051 mm) preload to accommodate for the expansion

due to heat and to avoid overloading the bearing.

Raceway Profile

The profile of a bearing raceway is at least as important to bearing life as surface

finishes. During bearing operation, there are extremely high Hertzian contact stresses

between the rollers and the raceways. If the raceway were perfectly flat, high stress

concentrations would occur at the points where the corners of the roller made contact

with the raceways. For this reason most raceways and rollers have a 'crown' - a convex

surface to avoid the edge stresses which would normally occur. Timken has developed a

highly sophisticated computer algorithm to calculate a *multi*-radius surface which

equalizes Hertzian contact stresses as much as possible. This proprietary program was

very instrumental in designing the raceways for GearSpexx™. A raceway profile was created which strictly adhered to the company standards for a cup in a similar application. In this case, including the profile resulted in an increase of calculated bearing life from 6.5 x 10^6 cycles to a total of 26.2 x 10^6 cycles. The mere inclusion of a profile increased life expectancy of the bearings by ~400%.

Honing

The decision regarding the honing of GearSpexx™ raceways was an important one because of the required quality of Timken bearing raceways. However, honing the raceways in a gear would have proven very cumbersome, so calculations were conducted to establish whether honing was truly necessary. The average lubricant film thickness can be calculated using an equation developed at The Timken Company[25] (based on the Grubin Equation):

$$h = 0.039(\mu V a)^{0.728} \left(P/_L \right)^{-0.091} \left(\Sigma \left(1/_R \right) \right)^{0.364}$$

where h is the lubricant film thickness (μin, μm), μ is the viscosity of the lubricant (mm^2/s, in^2/s), V is the surface viscosity (mm^2/s, in^2/s), a is the lubricant pressure viscosity coefficient, P is the load between the raceway and rollers (lb, N), L is the effective length of contact between the rollers and raceway (in, mm), and $\Sigma(1/R)$ is the sum of the inverses of the contact radii (in^{-1}, mm^{-1}). Under the established operating conditions, the

---

[25] British Timken Division of The Timken Company, The Tapered Roller Bearing Guide, Douriez-Bataille, 1994, pp. 107 - 108.

film thickness (h) of SAE90 oil was calculated to be 0.4μin. (0.01 μm) using the equation described above.

Another equation developed by The Timken Company was used to establish whether the gear had to be honed, or if surface finishes gained by grinding the raceways would be sufficient. The equation for the *Lambda Ratio*, λ, is[26]:

$$\lambda = \frac{Film\ Thickness}{Combined\ Surface\ Finishes}$$

where:

$$Combined\ Surface\ Finishes = \begin{cases} Cone\ Surface\ Finish + Roller\ Surface\ Finish \\ Cup\ Surface\ Finish + Roller\ Surface\ Finish \end{cases}$$

Standard Timken ground finishes were found adequate and honing was not truly necessary. The standard Timken finish for roller bodies, cone and cup raceways result in lambda ratio values of λ=0.03 for the cup/roller interface and λ= 0.04 for the cone/roller interface. As the lambda ratio decreases, bearing life will also decrease. However, the values of λ=0.03 and λ= 0.04, are within the tolerances for standard Timken bearings. Thus, as with all other aspects of the design, normal standards of The Timken Company for bearings were strictly adhered to in the design process.

Quality Analysis

To establish the soundness of the prototypes, detailed reports on the chemical makeup of the steel, heat treatment procedure and the Vibratory Finishing process which was conducted on 20 prototypes were requested and received. Correct hardness was

---

[26] C.A. Moyer, "1986 - Lube-Life Adjustment Factor", The Timken Company, April 1988.

confirmed by Timken Company metallurgists. They used microscopic Rockwell hardness tests at a cross-sectional point where the rim had a minimum thickness as well as at a location where the rim had a maximum thickness. Likewise, Ms^{27} tests for 0.5%, 0.7% and 0.8% carbon content were conducted and approved at these cross sectional locations (see Fig. 4.7 for an example). Furthermore, the customer examined one prototype for geometrical and metallurgical soundness. In all instances, the prototypes were confirmed to be within tolerance.

As surface finish can have a substantial effect on life, surface mapping tools were employed to compare the surface finish of the customer-supplied gear to the gear manufactured by the supplier[28]. Figure 4.8a and Fig. 4.8b are the surfaces of a tooth root from the customer gear and supplier gear, respectively. As can be seen, although neither gear root had been ground, the supplier gear root surface quality is substantially worse than the customer gear. Given these variables, the value for cyclic fatigue strength (σ_f) can be adjusted to reflect the discrepancy through the surface factor multiplier[29]

$$(C_s = \sigma_{fb} \cdot \sigma_{fx})$$

where σ_{fb} is the cyclic fatigue strength established for a baseline and σ_{fx} is the cyclic fatigue strength for a specimen with a given surface quality. If a specimen, which has been mirror polished is used as a baseline, the surface factor for the customer's gear would be approximately $C_s \approx 0.62$ while the surface factor for the supplier's gear is approximately

---

[27] F.S. Rowland and S.R. Lyle. "The Application of Ms Points to Case Depth Measurement", The Timken Company, Canton. OH, June 1945. Martensite start temperature establishes the carbon content profile of a cross section. This method was developed at the Timken company to ensure that the case depth profile is optimal for bearing raceways

[28] MapVue ZSCAN - Surface Mapping Software, Version 3.10. Phase Shift Technology, Inc. 1995.

[29] A. Buch, Fatigue Strength Calculation, Trans Tech SA, Switzerland, 1988, p52.

$C_s \approx 0.60$. If the customer's gear is used as a baseline, the cyclic fatigue strength for

GearSpexx ($\sigma_{ft}^{'}$) is:

$$\sigma_{ft}^{'} = 0.97\, \sigma_{fs}^{'} = 0.97(275.8\ ksi) = 267.5\ ksi$$

where $\sigma_{fs}^{'}$ is the baseline cyclic fatigue strength calculated in Chapter 3. Thus, the cyclic

fatigue life calculated for the gears in Chapter 3 must be altered to reflect surface quality

differences as illustrated in Table 4.3[30].

Table 4.3: Cyclic fatigue life adjustments with respect to surface quality factors		
Description	Adjusted Cyclic Fatigue Strength ($\sigma_F^{'}$)	Expected Cyclic Fatigue Life (No. of reversals)
Control Category - Customer's Prototype	275.8 ksi	283,000
Supplier Category - Supplier's Prototype	267.5 ksi	209,000
Test Category - Supplier's Prototype	267.5 ksi	75,500
VF Category - Vibratory Finishing	372.3 ksi	1,030,000

---

[30] Although no surface maps were conducted on the specimens which had undergone Vibratory Finishing, the surface finish factor as compared to a mirror polished specimen was expected to be $C_s \approx 0.78$ so the corresponding cyclic fatigue strength would be $\sigma_f^{'} \approx 347.5$ ksi.
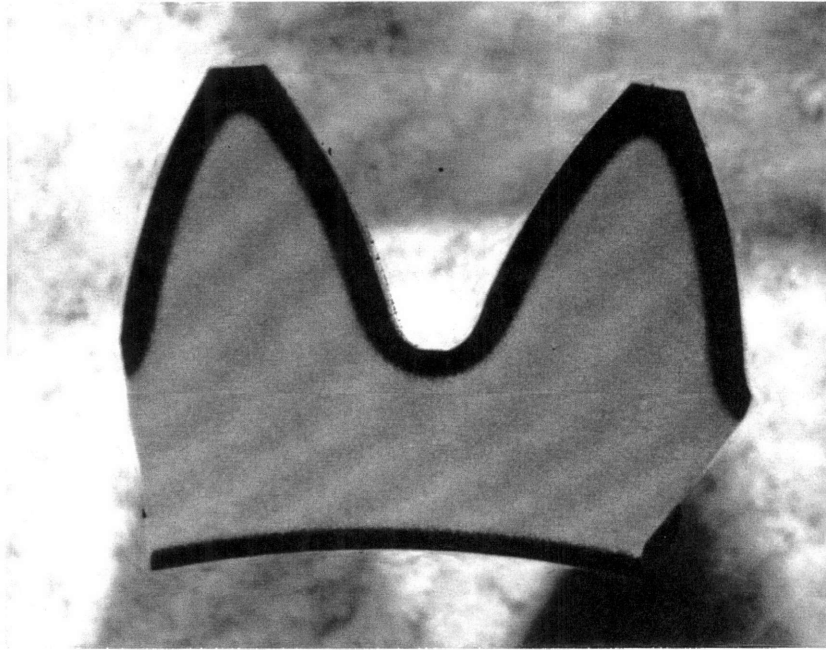
Figure 4.7a: Example of specimen with an Ms 50 procedure completed - darker material indicates 0.5% carbon content
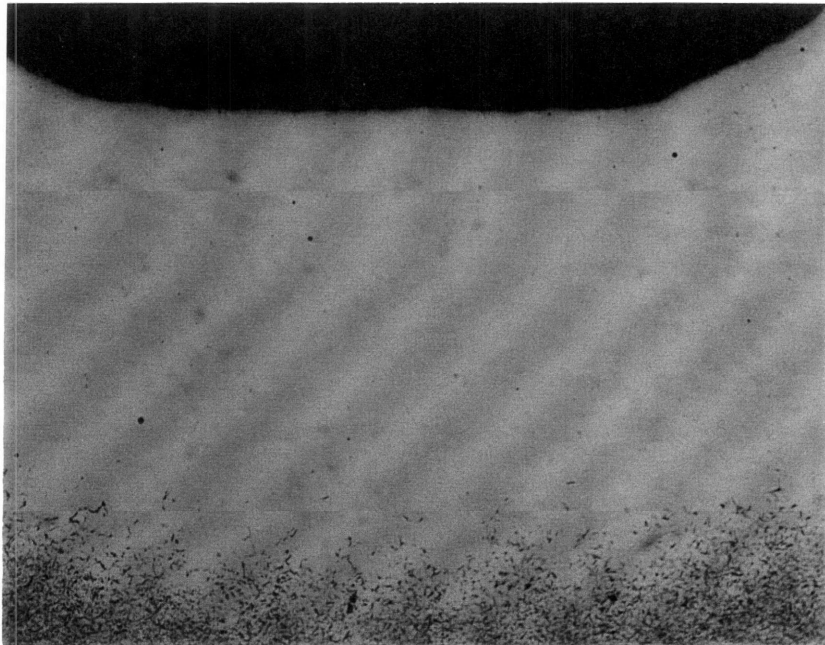
Figure 4.7b: Example of specimen with an Ms 50 procedure completed - close-up of gear root.

Solid Surface

Z2

Y2

Z1

0

X2   0

X2: 557.7um   Z2: 23.1um*
Y2: 613.8um   Z1:-23.1um*
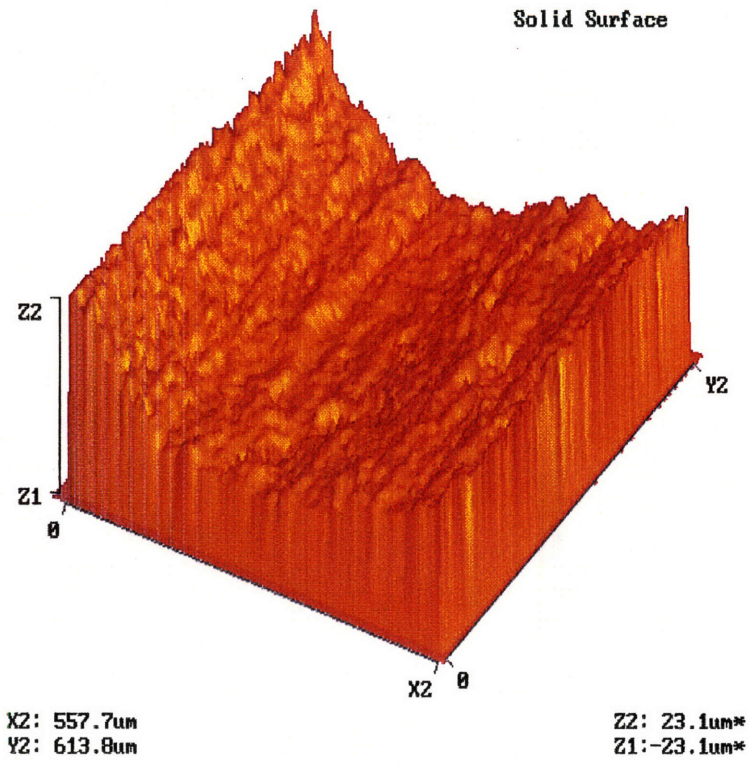
Figure 4.8a: Surface map of the gear root from the customer-supplied gear.

Solid Surface

Z2

Y2

Z1

0

X2   0

X2: 557.7um   Z2: 23.1um*
Y2: 613.8um   Z1:-23.1um*
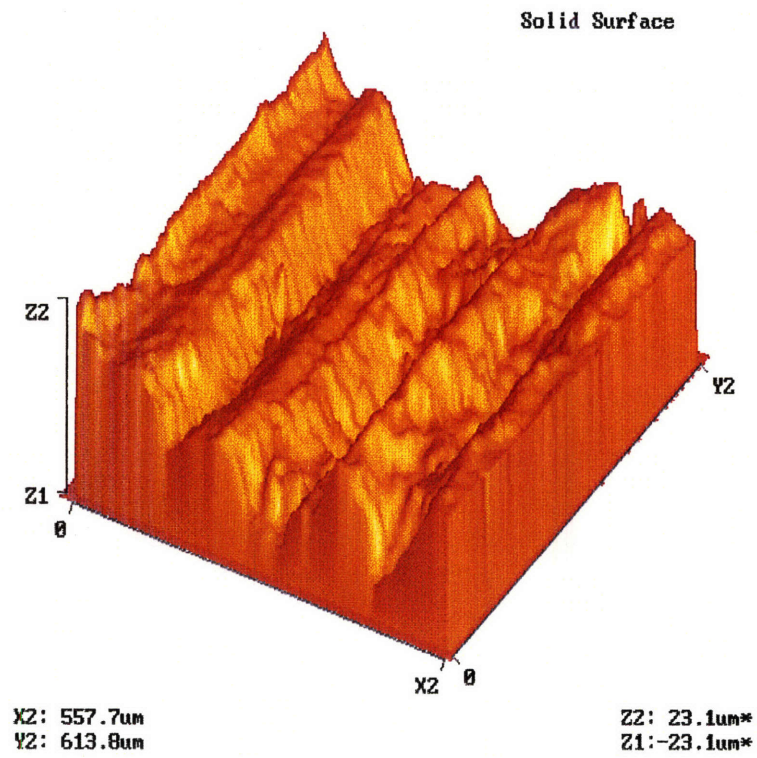
Figure 4.8: Surface map of the gear root from the supplier manufactured gear.

CHAPTER 5

TESTING

Once the prototypes had been manufactured, the analytical results described in Chapter 3 remained to be compared with actual test results. This chapter will describe how the final test design and procedure were established. First, the goals on which the ultimate test design was based will be discussed. Before test-designing could begin, a number of assumptions about planet gear operation had to be made. This section will discuss the assumptions and their relevance to the test scheme. The following section will continue the pre-design discussion with a number of 'proof-of-concept' calculations. Next, several design ideas will be analyzed to illustrate important issues addressed before the final design was completed. The following section will compare the test with the case study application, and another will examine the quality analysis conducted on the physical test. The chapter will conclude with the results of the tests.

Goals

The objective in designing and conducting tests on prototype gears was twofold: to correlate finite element results with actual test results and to establish fatigue life as an aid in the evaluation of the integral gear design.

Different levels of testing can be conducted to evaluate new designs. The tests vary in complexity and require proportionally-sized time and capital investments. As the test procedure moves from simple to complex, there may be an increase in the amount of knowledge gained. However, a complex test may provide much more data than is required, whereas a simple test may not provide enough. Moreover, the information received from some tests is closely coupled and complex, making it difficult to examine only one particular aspect of gear operation. A common testing procedure, where four meshing gears are tested at once, is an example of a relatively complex and expensive experiment. The 'four square' method gives a great deal of valuable data about the gears in operation, but this information is also dependent on speeds, temperatures and lubrication used. Since one of the primary goals of experimentation was to correlate FEA results to test results, it was concluded that a testing technique which did not include such issues as lubrication would be more appropriate. A test was designed to apply loads to the prototype gear in the same way that the loads were applied in the case study (and in the finite element model). The resulting test was relatively uncomplicated and addressed only the information relevant for this research. Although this test design would offer many answers without the great time and money investment needed for a full-scale life test, it is important to recognize that this experiment was not designed as a replacement to life testing which manufacturers currently use. Instead, this test design could serve as a

preliminary step toward establishing the optimal gear and tapered roller bearing combination with a relatively low time and capital investment. GearSpexx™ would still need to be subjected to full-scale life testing before it moved from the prototype stage to customer use.

General Assumptions

Forces

At any instant in time, two teeth of a planet gear separated by 180°, experience identical tangential loads as seen in Fig. 5.1. Each gear tooth would undergo fully-reversed bending because forces from the sun gear acted on the opposite side of the tooth from the reaction forces applied by the ring gear. Thus each gear tooth would undergo fully reversed bending during one complete rotation. It was established that by loading only one pair of teeth during testing, the test could be simplified while maintaining the general purpose of the test: to examine the effects of an altered rim geometry on overall gear life. The gear would still experience all of the forces as a whole even if not every individual gear tooth was subjected to the loading. As mentioned before, the gear and bearings in this case study were mounted on a pin and rotated about a mutual axis. Therefore, at any instantaneous moment the gear teeth experienced bending due to applied loads while the rim stiffness varied depending on the location (or absence) of nearby bearing rollers.

Testing Apparatus

Since only two teeth would be loaded, a tensile testing machine (MTS) was chosen to simulate the stresses that GearSpexx™ would experience during a cycle. This machine

was capable of applying cyclical axial and torsional loads in the vertical direction, as

displayed in Fig. 5.2, but had an important and critical limitation. Any motion beyond a

few thousandths of an inch, either axial or torsional, about the X and Z axes could have

been extremely detrimental to the hydraulic actuator of the MTS machine. At a maximum,

the MTS was capable of applying 50,000 lb (222,000 N) of force at a rate of 12 Hz. It

was also capable of applying the cyclical loads in a square, sine or haver-sine wave form.

Given these capabilities, it was established that the MTS would adequately satisfy any

requirements the test design would ultimately call for.

Tooth Side A:
Force applied to
planet gear by
sun gear

Tooth Side B

Reaction force from
shaft and bearings

Bearing cones
and rollers

Support Shaft

Tooth Side A`

Tooth Side B':
Reaction force
from ring gear
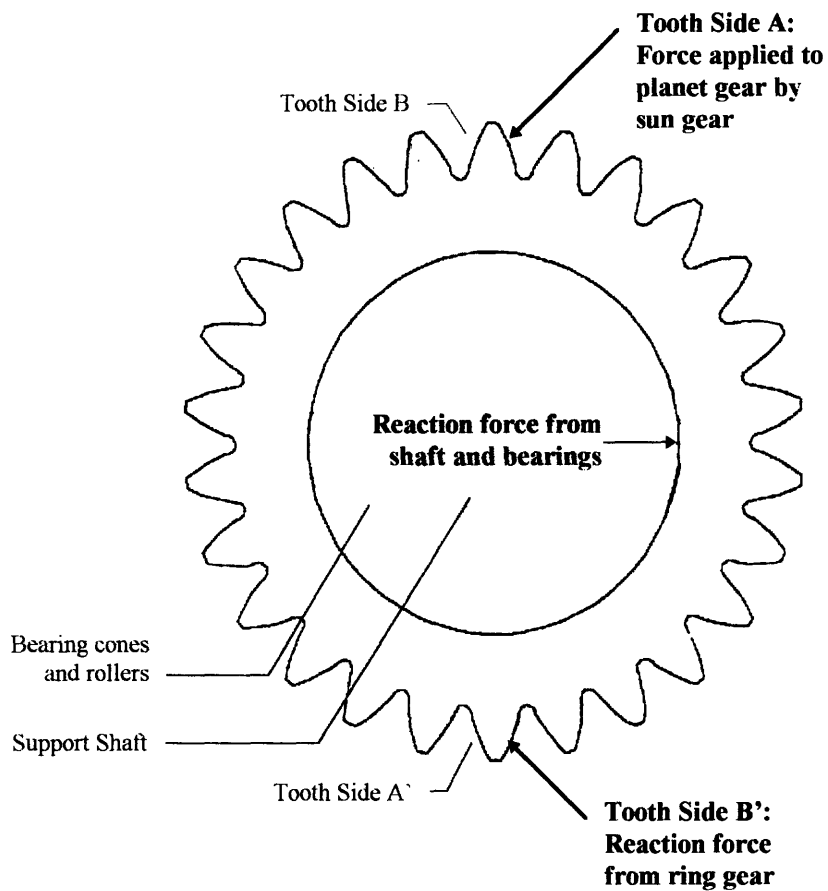
Figure 5.1: Free body diagram of forces acting on the gear. The teeth are labeled A/B and A`/B` for easier tracking.
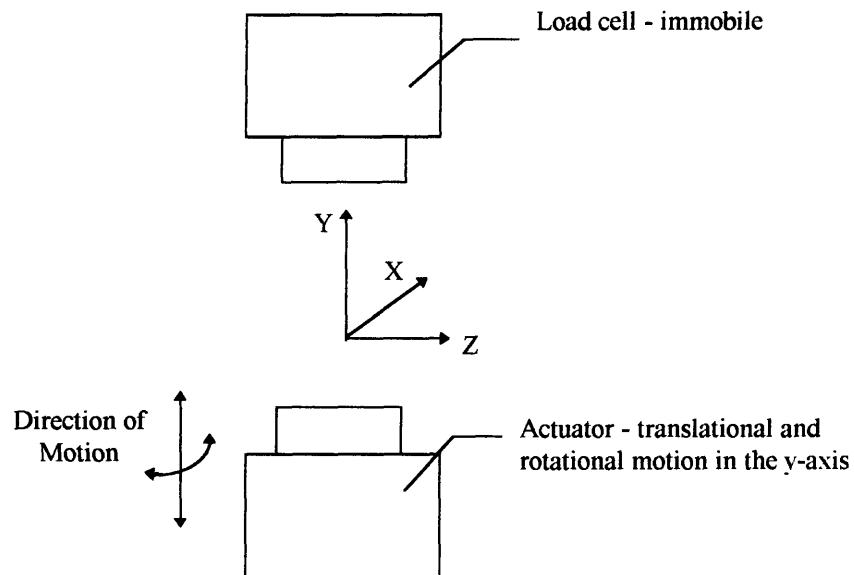
Figure 5.2: MTS: Basic geometry and motion.

V-block Loading

It was established that the actuator would apply a cyclical, tension-compression force to the gear teeth via a V-block as illustrated in Fig. 5.3. The involute surface of the gear would allow the block to be designed and manufactured in such a way as to ensure that the straight surface of the V-block would be tangent to the gear tooth at the HPSTC. Thus, as seen in Fig. 5.3, the force induced by the MTS on the V-blocks would be transmitted normal to the surface of the gear tooth, mimicking the real application. Most importantly, the V-block configuration would ensure that it would make contact with the gear tooth at the same radial location every time.

Force applied
by MTS

Force applied by
V-block tangent
to tooth surface.
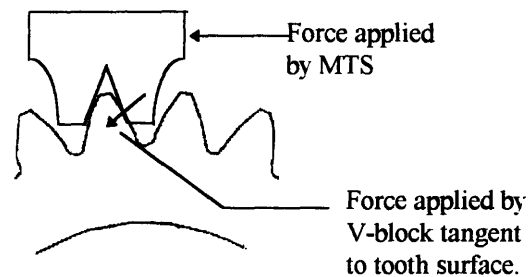
Figure 5.3: Schematic illustration of V-block loading of gear tooth.

Bearing Rotation

As has been discussed previously, the bearings inside the gear bore provided

additional stiffness to the gear, depending on roller location. Each point on the gear rim is

and more compliant when the space between the rollers moves under that point on the rim.

This variable, dynamic stiffness through the rim, is an important factor in gear operation

and so it would be preferable if it were included in the test procedure. Although the case

study planet gear rotated about its own axis, implementing such motion on the MTS

would have proven very difficult. Instead, the design assumed that the shaft supporting

GearSpexx™ would rotate instead of the gear. This alteration would not compromise the

test, and the desired outcome of variable rim stiffness would be satisfied.

Lubrication

It was previously established that this test design would not include any aspects of

gear operation which would not be affected by a change in rim geometry. One of the

issues which was chosen to be excluded from testing was lubrication. Moreover, to

include lubrication in the design would have complicated the testing procedure substantially because in the case study application the entire torque hub operated in an SAE 90 oil bath. Though the lubrication can be omitted from gear operation, it can not be omitted from bearing operation since the bearings would be rotating while supporting a cyclical load in the experiment. It would have caused substantial complication to duplicate an oil bath in the test design; therefore the bearings would be lubricated by grease. A lubrication specialist at The Timken Company selected a grease which would have qualities most like SAE 90 oil. Though this was a reasonable solution, failures would be carefully observed to ensure that the different method of lubrication would not affect the test results.
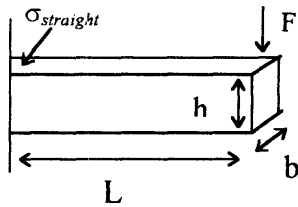
Design Details

Detailed calculations were conducted on some assumptions to ensure the validity of hypotheses before the test was designed. The important issues included in the following sections are: an analysis of the type of force wave function needed to model the case study gear, proof of concept calculation for the V-blocks and investigation of the misalignments which could be a result of deflection of the mounting pin. These issues, once addressed, established some of the critical parameters of the test design.

Applied Forces

As the MTS would be applying "artificial" forces onto the gear teeth, it was critical to understand the nature of the forces which one tooth experienced in the course of one rotation. Basic bending stress calculations gave insight on the stresses that a gear tooth

experienced when engaged. The equation for bending stress for a straight beam is

depicted as follows:
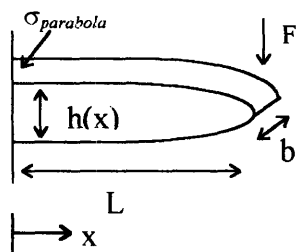
$$\sigma_{straight} = \frac{My}{I} = \frac{(FL)(^1{}_2 h)}{\left(\frac{bh^3}{12}\right)}$$

Figure 5.4: Stress equations for a cantilevered beam.

where $M(= FL)$ is the moment induced by the tangential force on the gear tooth,

$y(= \frac{1}{2}h)$ is the distance from the neutral axis of the beam to the outer surface, and

$I(= bh^3 / 12)$ is the moment area of inertia of the beam. However, a simple straight beam

did not model the geometry of a gear tooth accurately. Alternatively, the gear tooth could

be modeled as a parabola which would result in the following equation[31]:

$$\sigma_{parabola} = \frac{6FL}{bh^2}$$

$$h(x) = h\left(\frac{L-x}{L}\right)^{1}{}_2$$

Figure 5.5: Stress equation for a parabolic, cantilevered beam.

where F is the applied tangential force, L is the moment arm and b and h are the width and

height of the beam at its base, respectively. In reality, the above equation is still only the

equation for a straight beam:

$$\sigma_{straight} = \frac{My}{I} = \frac{FL\,^1{}_2 h}{\frac{bh^3}{12}} = \frac{6FL}{bh^2} = \sigma_{parabola}$$

[31] Erik Oberg, Franklin D. Jones, Holbrook L. Horton and Henry H. Ryffel, Machinery's Handbook, Industrial Press Inc. New York, 1992, p. 233.

so beam shapes are not really taken into consideration in elementary stress equations.

If only one tooth of the sun gear applied a load to a single tooth of the planet gear, the bending stress in the planet gear tooth might be illustrated by Fig. 5.6. The force applied by the sun gear would remain constant throughout the interaction between the two teeth. However, the involute profile of the sun gear tooth would make contact with the planet gear tooth near the root of the planet gear tooth. As rotation continued, the point of contact of the sun gear tooth on the planet gear tooth would move radially outward along the planet gear tooth. This interaction would continue until the sun gear tooth contact had reached the HPSTC on the planet gear tooth. Since the designed test would load the tooth at a stationary location, the force applied would need to be varied to reflect the loads encountered in the case study application. Figure 5.6 illustrates the actual calculations of the force which would need to be applied to the planet gear tooth to simulate the bending stress which the tooth would normally encounter in the case study.
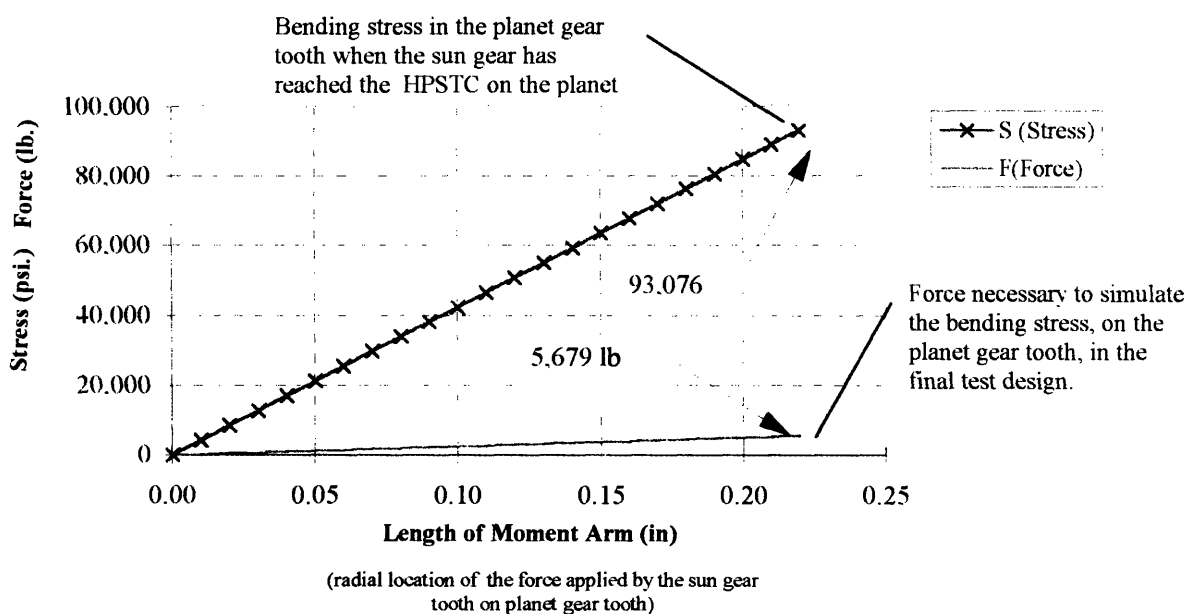
Figure 5.6: Force required to simulate bending stress in the planet gear tooth.

As a spur gear tooth goes through one complete rotation, each tooth experiences

fully-reversed loading as it first engages with the sun gear on one face of the tooth and

then with the ring gear on the opposite face of the tooth. Figure 5.7 schematically

illustrates this cycle. However, Fig. 5.7 is not an accurate picture because in an actual

application, more than one tooth is engaged some of the time. This means that the load on

the planet gear tooth is not constant as it moves radially outward along a tooth as

neighboring planet teeth are engaged and disengaged. Figure 5.8 is a more accurate

schematic representation of the load that would be needed to model a realistic gear. At

first the load increases relatively slowly because more than one tooth is engaged. The

slope becomes steeper as the cycle moves into single tooth loading. After the peak of

force in Fig. 5.8, the cycle moves into double tooth loading again where the first tooth is

still engaged but the next tooth has also started carrying load. The final part of the cycle is

the portion of the loading cycle where the tooth has disengaged and thus carries no load.

As in the previous figure, the second portion of the load cycle is a mirror image of the first

and represents the reverse loads applied to the planet gear tooth by the ring gear.
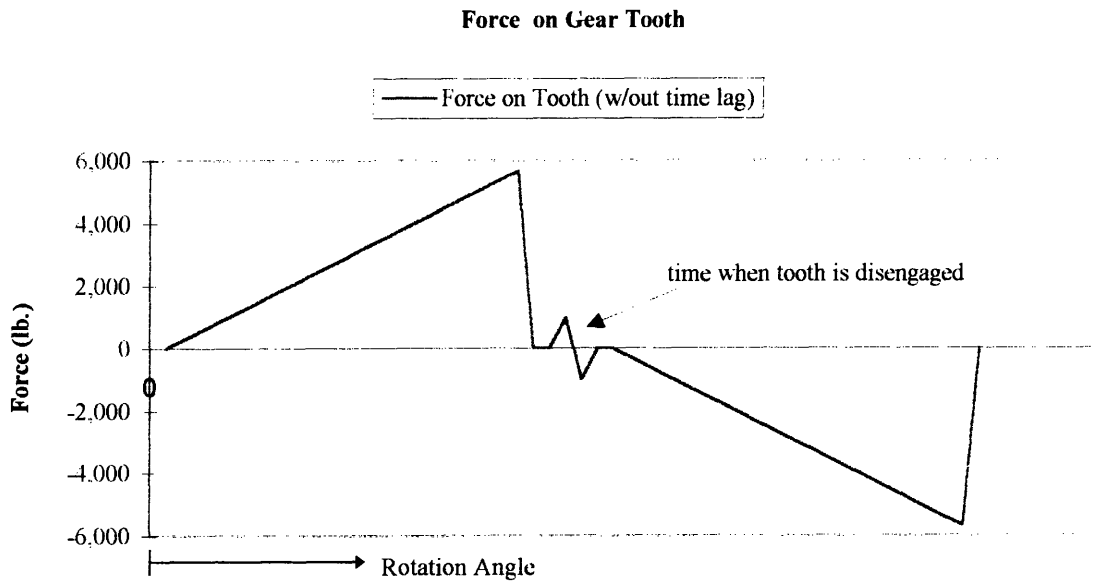
Force on Gear Tooth

Figure 5.7: Load on one gear tooth during a full planet gear rotation.
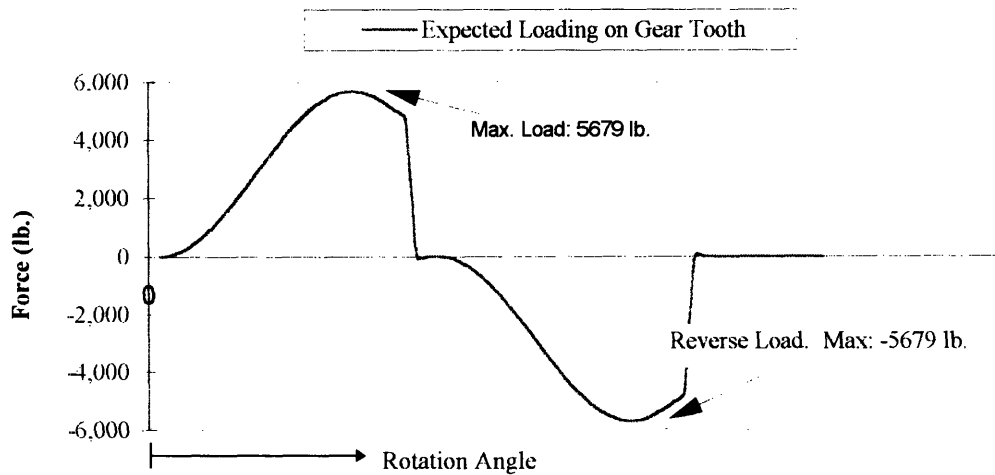
Figure 5.8: Fully reversed force approximation in a gear with multiple tooth mesh.

The actual slope of loading is even more complicated than represented here, but

the forces illustrated in Fig. 5.8 are an adequate approximation of the forces needed to

simulate the fully-reversed loading that a gear tooth sustains. However, since the MTS is

capable of creating only simple wave forms, the sine wave will be used to approximate the

forces on a gear tooth during one rotation, as shown in Fig. 5.9. Because fatigue life

results are relatively insensitive to wave form in the absence of corrosive elements, and

because high cycle fatigue depends primarily on the stress amplitude imposed, this

approximation should be adequate for gaining insight on the fatigue life performance of

GearSpexx™.
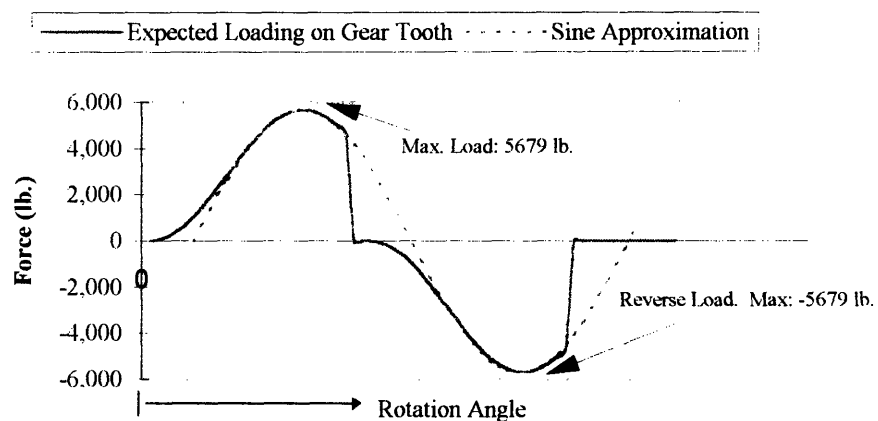
Figure 5.9: Approximation of force on gear tooth.

V-Block Calculations

One of the major concerns regarding the design of an acceptable test was

establishing how to load the teeth. Although it had already been established that the V-

block concept would load the gear teeth as desired, it became clear that spacing would be

critical. Although it is an accepted practice to completely eliminate the adjacent teeth off

the gear when testing a single gear tooth[32], such an action would have an unrealistic effect

on rim stiffness when testing an entire gear. As it was not possible to eliminate large

---

[32] To make room for testing apparatus.

enough portions of the teeth in the vicinity of the tooth being tested, the loading block dimensions were quite limited. Since the V-block would have to be small enough to fit between the gear teeth, it was a great concern that the V-block would experience more stress than the gear tooth resulting in a fatigue test on the loading block rather than the gear. Because of this, the most robust   V-block was designed and analyzed. Calculations were conducted not only to establish comparative stresses but also to establish the deflection which would result. If deflection were not taken into consideration, the combined deflections of the tooth and V-block could have resulted in a cyclical impact of t'e loading block on adjacent gear teeth.

To establish answers to these questions, the basic beam-in-bending stress analyses were conducted on both the gear tooth and the V-block. From the previous calculation, it had been established that the basic stress equation was not affected by the exact shape of the beam as long as the 'height' of the beam was measured at its base. Figure 5.10 illustrates an approximation of the gear tooth (using a parabola) and the V-block:
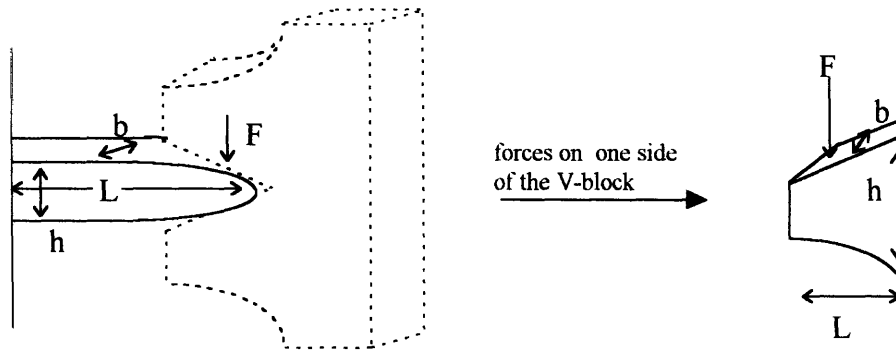
Figure 5.10: Free body diagrams of a gear tooth and the V-block.

Conducting the equation for the V-block and gear tooth in parallel:

	Gear Tooth		V-Block	
L (Length)	0.179 in.	4.55 mm	0.202 in.	5.13 mm
F (Force)	5,680 lb	25,300 N	5,680 lb	25,300 N
h (height)	0.250 in.	6.35 mm	0.284 in.	7.21 mm
b (width)	1.28 in.	32.5 mm	1.50 in.	38.1 mm
$\sigma = \dfrac{6FL}{bh^2}$	107 ksi	749 MPa	56.8 ksi	398 MPa
$\delta = \dfrac{FL^3}{3EI}$	2.26×10^{-4} in.	5.75×10^{-3} mm.	1.87×10^{-4} in	4.75×10^{-3} mm

Thus from the above calculations it was clear that the V-block would experience

less than 50% of the stress that the tooth would experience (stress concentration factors

were ignored for this proof of concept calculation). The deflection of both the tooth and

V-block are so slight that they should be insignificant. A clearance of 0.020 in

(0.508 mm) between the V-block and the adjacent teeth would ensure that there would be

no danger of impact between the V-block and adjacent gear teeth.

Pin Deflection

In the case study application, the planet gear was supported by a pin. Since the

mode of failure for this application had been pin breakage, it was of interest to incorporate

the effects of pin deflection into the test design to simulate the application more

effectively. However, it was unclear whether the movement of the gear experienced was a

result of deflection in the pin or of a deflection in the planetary torque hub unit housing.

Figure 5.11 is a representation of the gear mounted on a pin. The housing was

modeled as a rigid wall so the problem was one of a cantilevered beam. For these

calculations, the system has been simplified to a free body diagram of a cantilever with a

single point force. Using the known values, the bending stress in the pin was:

$$\sigma_b = \frac{My}{I} \Rightarrow (Fa)R\left(\frac{64}{\pi d^4}\right) \Rightarrow 46,863 \; psi$$

where (Fa) is the moment on the pin, R is the distance from the center of the beam to the

surface, and $\left(\frac{\pi d^4}{64}\right)$ is the moment of inertia. To gain high fatigue life, loads needed to

remain well within the elastic regime of stress. For ASE 8620 steel, yield stress is ~ 210

ksi (1,470 MPa), so it was concluded that the pin was not in danger of being plastically

deformed. In fact, to reach the yield strength of the pin, the force applied would have to

be at least 3.5 times greater (41,000 lb, 183,000 N).

Known Variables
F = 11,359 lb.
R = 0.75 in.
L = 2.13 in.
a = 1.367 in.
b = 0.763 in.
E=29x10^6 psi.

Free Body Diagram

Figure 5.11: Pin in bending calculations.
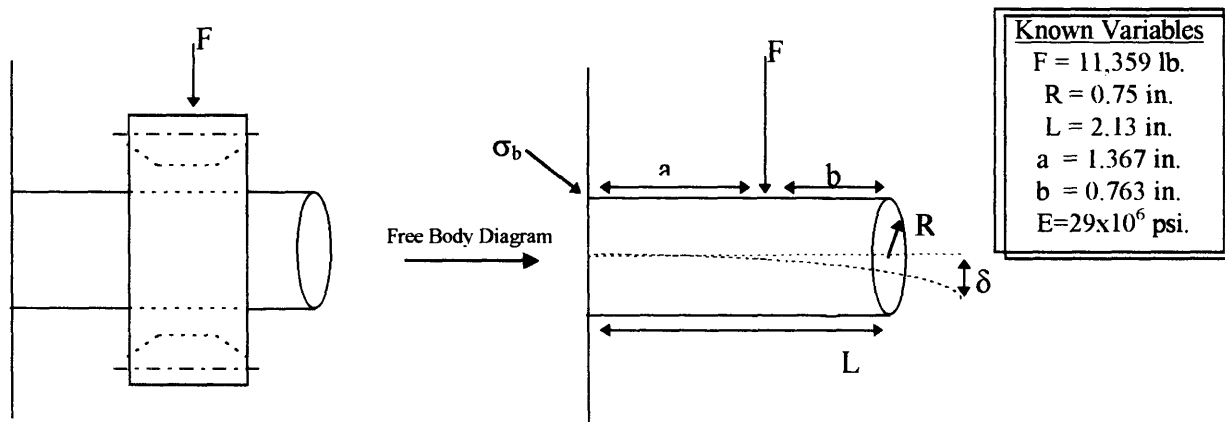
As illustrated in Fig. 5.11, the non-axial motion of the pin, due to the loads applied

to it, were also evaluated both at the load and at the free end of the pin. The results are

shown below:

$$\delta_{load} = \frac{Fa^3}{3EI}$$

$$\delta_{end} = \frac{Fa}{6EI}(2a + 3b)$$

$$\delta_{load} = 0.0013 \, in \quad (0.033 \, mm)$$

$$\delta_{end} = 0.0025 \, in \quad (0.064 \, mm)$$

where F is the radial load on the gear teeth, E is Young's Modulus, I is the moment of inertia and a and b are the beam lengths relative to the effective location of the radial load as shown in the figure. From the calculations it is clear that the deflection of the pin was not expected to be greater than 0.003 in (0.076 mm) in the vicinity of the gear. This amount of misalignment was approximately the amount expected in bearing alignment, so the deflection of the pin was not expected to substantially affect the stresses in the gear or its fatigue life.

Test Designs

As is usually the case, the test design experienced several alterations before achieving its final form. Some of the unused designs are presented here in addition to the final design to better illustrate some issues which had to be considered.

Cantilevered Design

Figure 5.12 represents the initial design in which GearSpexx™ would have been mounted on a cantilevered shaft. The length of the cantilevered portion coincided exactly with the length of the pin in the case study (see Chapter 4 for an illustration). The actuator would simulate the sun gear tooth by applying a load to GearSpexx™ via the V-block, as indicated. The ring gear would be modeled by the immobile load cell. The reaction force applied to the gear tooth would also be transmitted normal to the gear tooth via the V-block on the left. The shaft would be rotated by the variable speed motor and supported by a Timken Unipac Plus™ bearing.

On discussion with MTS experts, it became clear that it would not be possible to mount or load the gear as planned. Though desirable because of the closeness to the case study application, mounting the gear on a cantilevered pin could cause damage to the actuating piston. If the pin experienced a deflection, the MTS actuator could be damaged due to the applied torque around the Z axis. The desire to apply a load to only one side of the gear, though true to the case study application, was also potentially problematic. As a load was applied to the gear, the gear could rotate about the X axis and put a non-axial load on the actuating cylinder. Although both problems could be overcome, the test was redesigned to avoid any possibility of invalid or inaccurate test results.

Square Bracket Design

The test design illustrated in Fig. 5.13 resolved the problems of the previous design. The gear was no longer supported on a cantilevered beam and rested over the actuator so that no non-axial load was placed on it. The shaft was supported by two Unipac™ bearings and would still be rotated by the previously-selected motor. The loading would occur on two teeth simultaneously via a square bracket which would connect to the load cell through the shaft. The square bracket would continue to incorporate the V-block loading concept wherein the two halves of the square bracket would be drawn tight against the gear and secured with two bolts.

Final Design

There are two major alterations between the Square Bracket Design and the Final Design illustrated in Fig. 5.14. The first set of alterations stemmed from a concern with the dynamics of the previous design in a tension-compression experiment. To minimize possible instabilities such as machine error or system misalignment as the MTS passed
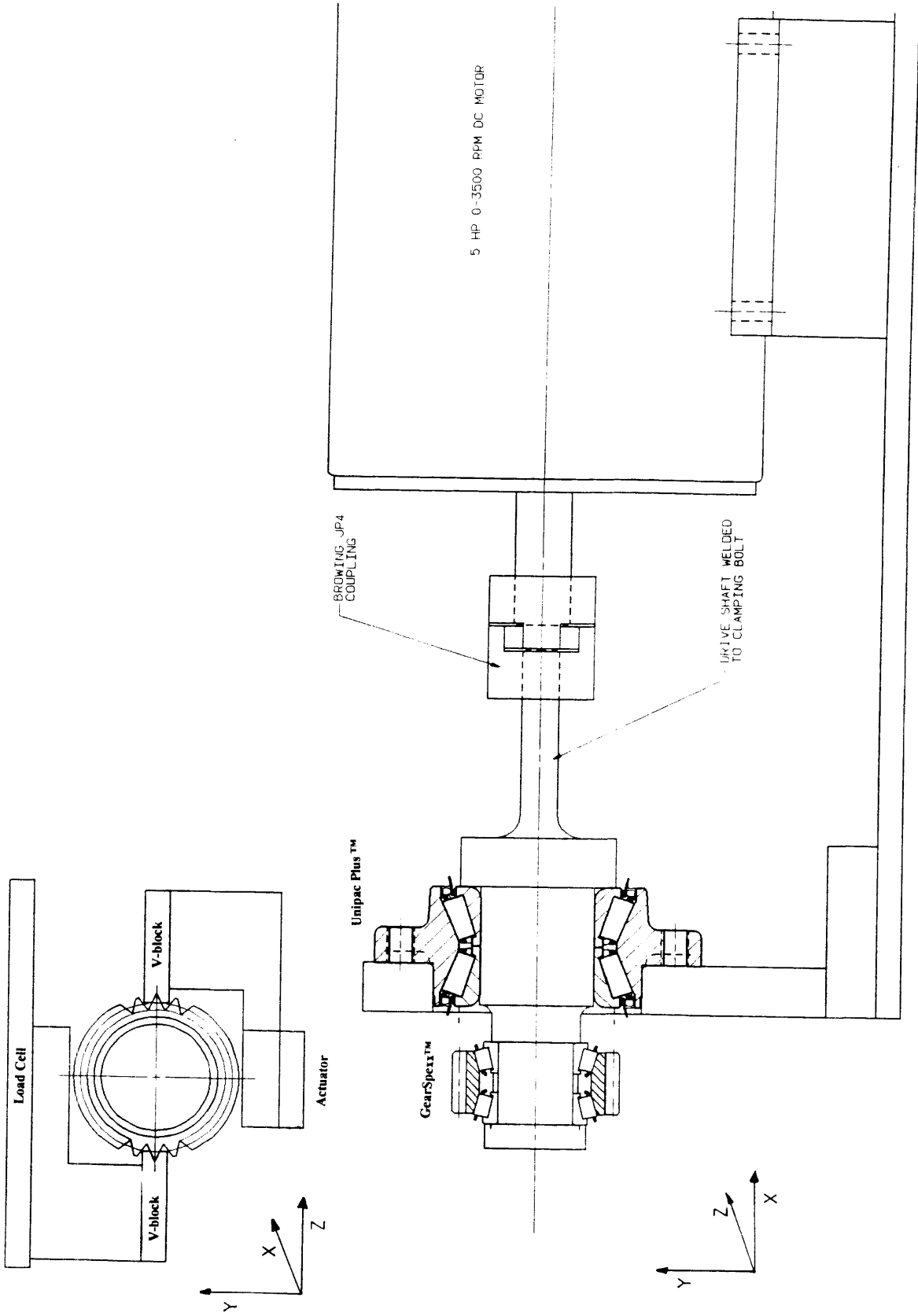
Figure 5.12: Cantilevered Design: initial test design proposed for the MTS.

Figure 5.13: Square Bracket Design: second iteration for designing an appropriate gear testing apparatus.
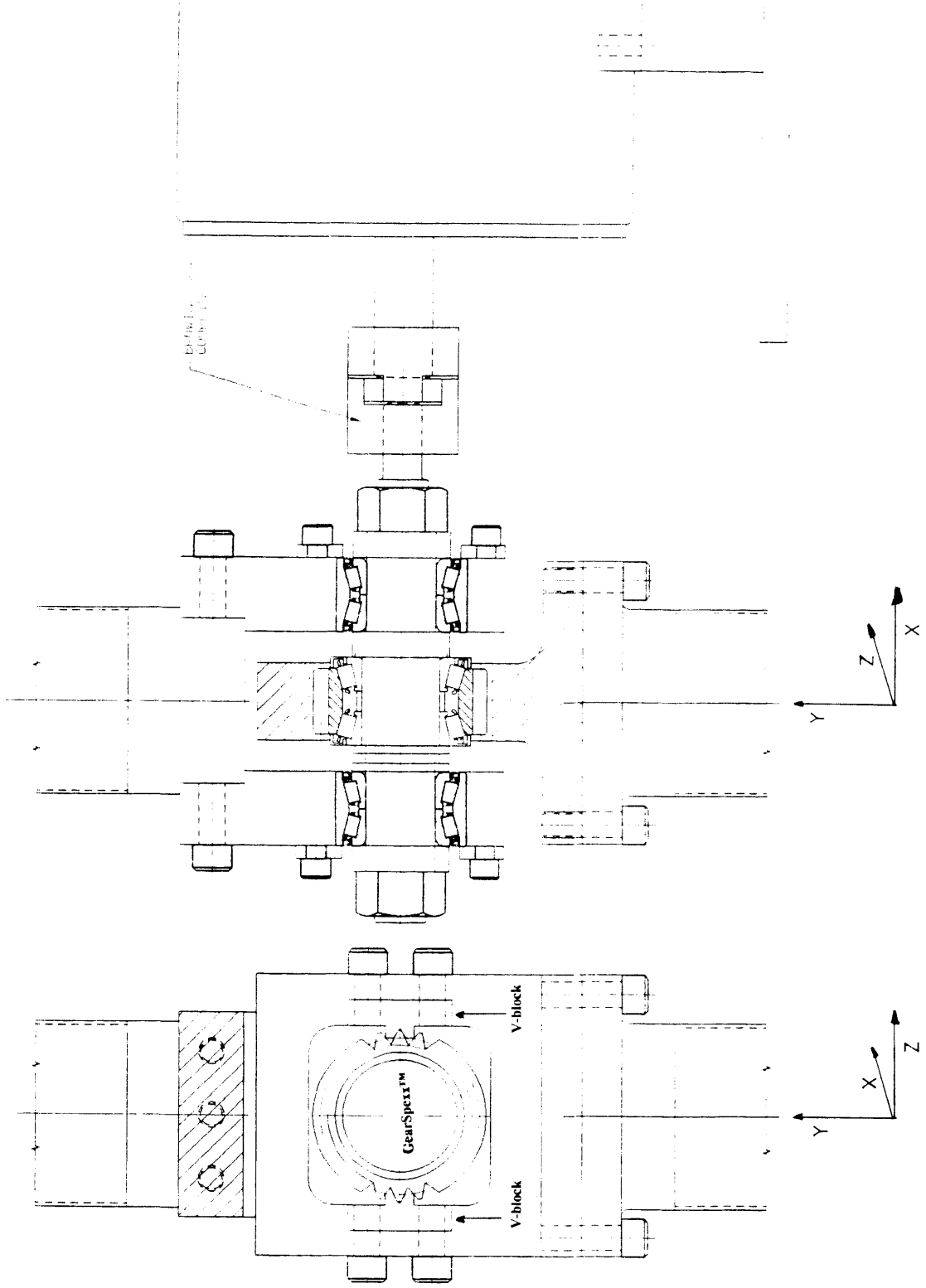
Figure 5.14: Final Design - ultimately used to test both tapered-bore and straight-bore gears.

through zero, several factors were examined and addressed to maximize the stiffness of the system. For example, the length of the shaft between the Unipac™ support bearing was made as short as possible to minimize the compliance. Another modification eliminated the pin connecting the actuator and square bracket, and redesigned the square bracket to mount directly to the actuator. This design not only eliminated any problems which might have been encountered as the loading cycle passed through zero, but also ensured that no detrimental loads would be applied to the actuating piston of the MTS.

The second major alteration was a decoupling of the square bracket from the V-blocks used for loading the gear teeth. The primary incentive for this change was the realization that if any portion of the test fixture would fail due to fatigue, it would most likely be the V-blocks. Since they had been decoupled from the square bracket, the entire square bracket would not need to be replaced if the V-blocks did fail. Also, since the angle of the V-blocks was so critical in proper gear tooth loading, it was possible to periodically regrind one set of V-blocks while another was used for testing. Decoupling the V-blocks from the square bracket also allowed different heat treating of the components. The square bracket could be given maximum hardness to withstand the high loads induced by the MTS. The V-blocks required a greater toughness because of the bending fatigue imposed on them during testing. With a decoupling of the two functions, all stipulations were easily satisfied.

The final design successfully fulfilled the requirements necessary to complete the goals of the testing. While remaining relatively inexpensive and uncomplicated, the test design simulated the loads on a planet gear at a given moment in time and represented full rotations of the gear via cyclic loading. Also, the variability in rim stiffness was

successfully simulated through the rotation of the bearings by way of a rotating shaft. The final design had additional benefits over more traditional designs.

Some of these benefits are listed below:

- lower cost

- fewer parts

- easier assembly and disassembly (1-2 hrs. for complete changeover)

- no gear lubrication necessary

- easier viewing of gear during testing

- successful decoupling of issues which are and are not affected by gear rim design

- single gear testing possible

- shorter fatigue-life test time

- lower weight

- smaller motor necessary (low torque needed because motor is rotating a shaft in 'air' rather than inputting torque to a set of gears)

- greater flexibility for test variables (magnitude of load, speed, method of loading, loading signal, location of load, number of teeth loaded at one time)

Thus it was demonstrated that a more simple gear experiment could be devised to test general gear design alterations. Appendix B is a collection of photographs illustrating the final experimental design as it was implemented.

Comparison of Test Design and Case Study

The primary goal of this test was to examine the fatigue in the rim of the gear. As mentioned before, the test designed for this research was not proposed as a replacement to a full-scale life test, but merely intended as a relatively simple tool to aid in creating successful gear designs. In an effort to keep the scope of the test simple and free of coupling with other variables, the test was designed to examine a planet gear independently of surrounding machinery, so there are some aspects of gear operation that were not addressed with the final design. For example, the test design did not attempt to investigate the interaction between two gear teeth or interactions of the gear with the housing. Instead, it examined the reactions of the planet gear under forces to which it is subjected during actual operation. The test design simulated rotation of a bearing inside the gear but was constrained to using a rotating cone and stationary 'cup' rather than a rotating 'cup' and stationary cone as is the situation in the case study. To aid in a comparison of the final test design to the case study application, Table 5.1 lists factors which could affect gear performance and the effects on performance. A comparison of these factors to expected test data follows.

Factor	Effect
I. Fully-reversed tooth loading	• Increased fatigue due to tension - compression stressing
II. Rotating gear vs. rotating bearing	• Rotating "cup" with a stationary "cone" • Constant load zone on one portion of the gear raceway
III. Low speed	• Little or no lubrication film created
IV. Lubrication: no seals on bearing, gear lubricated by oil bath	• Possible increase in heat generated, surface wear, etc.
V. Improper tooth mesh	• Tooth impact as the teeth mesh • Improper tooth loading along face - resulting in surface wear, tooth chipping or even tooth breakage
VI. Multiple tooth mesh	• Tooth is not fully loaded during a cycle because adjacent teeth also carry part of the load through some portion of the cycle • Tooth root does not experience sinusoidal loading
VII. Surface wear	• Noise • Shorter tooth or bearing life
VIII. Compliance in housing/pin	• Misalignment of the planet gear with respect to the sun and ring gears

Table 5.1: Factors which could have an effect on gear performance.

Test Design

I.   Fully-Reversed Tooth Loading

The effects of fully-reversed tooth loading will be addressed because of the care

taken in designing a test which would allow a the tension-compression experiment on the

MTS machine.

II.   Rotating Gear vs. Rotating Bearing

Though the gear will not be rotated, the shaft and bearing cone will be rotated, thus

maintaining the motion of the bearing rollers against the gear rim. The stiffness added and

detracted from the gear due to the rotating rollers, induced by the rotating shaft , will be

observed in this test. However, in the actual application, the tapered gear bore acting as a

cup raceway was subjected to relatively uniform wear as it rotated through the load zone

(which was constant). It was the inner raceway (cone raceway) which sustained a

constant load in one area because the pin did not rotate. The result was that the gear bore

experienced uniform wear whereas the bearing cone encountered non-uniform wear with

higher wear in the load zone. As discussed previously, in the final test design the reverse

will be true - the gear raceway will undergo non-uniform wear. Fortunately, differences

between rotating cup and rotating cone applications are so slight that the effects are not

calculated in most bearing applications, so this change should have little, if any, effect on

the results. The slight differences which may result will only submit the gear to harsher

testing conditions than it would experience in the case study application so the resulting

gear design will be more robust as an effect of any differences experienced.

III.   Low Speed

The final test design would allow for testing to be conducted at a variety of speeds

and loads ranging from extremely low to relatively high velocities (to examine the results

on gear operation such as a very thin film thickness). The only limiting factor would be

the tensile test machinery itself, capable of applying the load at a maximum frequency of

12 Hz. However, this limitation can be eliminated by selecting a different, more powerful

tensile testing machine. Although it was possible to alter the speeds of the test, time

limitations prevented examining the effects of either extremely low or extremely high

speeds.

IV. Lubrication

As was the case with surface wear on the gear teeth, the changes in gear design

were not expected to affect lubrication issues. Bearing lubrication was kept as close to the

case study lubricant as possible, as discussed earlier in the chapter (General Assumptions -

Lubrication).

V. Improper Tooth Mesh

This factor was not addressed in any way in the final test design . In fact, improper

loading (via the V-blocks) would be very undesirable because it would result in an

inaccurate representation of tooth loading under normal conditions. However, if an

improper tooth mesh were to occur, it would occur as a result of the shaft or pin

deflecting and skewing the gear or as a result of a deformation of the gear shape itself (egg

shaped or increased tooth compliance). Deflection of the housing could cause of pin

motion but modeling such a situation would be extremely difficult and better reserved for

the more complex gear and three dimensional finite element analysis. Moreover, in the

design process it was established that any non-axial load on the MTS actuator could have

disastrous results.

Although not exercised in this experiment, the test design is very conducive to

analysis of deformations of the gear itself. The gear is far more accessible during testing

than other test designs so the use of gauging devices or coatings (such as photoelastic

coatings) could be utilized to establish the amount of deformation a planet gear would

exhibit as a result of the loads applied.

VI.   Multiple Tooth Mesh

It is possible to conduct the test using a function generator to create the exact load

cycle which the tooth and adjacent roots undergo during operation, as a result of multiple

tooth meshing. Although the machine targeted for this test had limited capabilities with

regards to wave generation, machines with access to function generators would be able to

create a load cycle to model loads on the gear tooth during gear rotation exactly.

VII.   Surface Wear

Due to the limited scope of this test design, surface wear on the gear teeth was not

addressed. Because the outer geometry of the gear (in particular the gear teeth) were not

altered in any way, it was not expected that surface wear would be affected. The only way

that surface wear could be altered by a change in rim thickness would be as a by-product

of overall gear deformation as discussed in section *V - 'Improper Tooth Mesh'*.

Surface wear on the inner raceway was addressed in the initial prototype design of

the bearing raceways by designing a crown[33]. Any additional or unexpected wear would

result as a by-product of overall gear deformation as was discussed in section

V - 'Improper Tooth Mesh'.

VIII.   Compliance in Housing/Pin

See 'Improper Tooth Mesh' above.

---

[33] See Chapter 4 for details.

Fine-Tune of Test Design

Once the test was assembled and ready for operation, some debugging of the apparatus had to be conducted. The first gear tested in the apparatus had a fatigue life of only ~15,000 cycles an unexpectedly low life, indicative of plastic deformation of the gear. The finite element analysis indicated that uniform loads would create maximum stresses well below the yield strength of SAE 8620 steel, so it was concluded that the gear must have been loaded incorrectly.
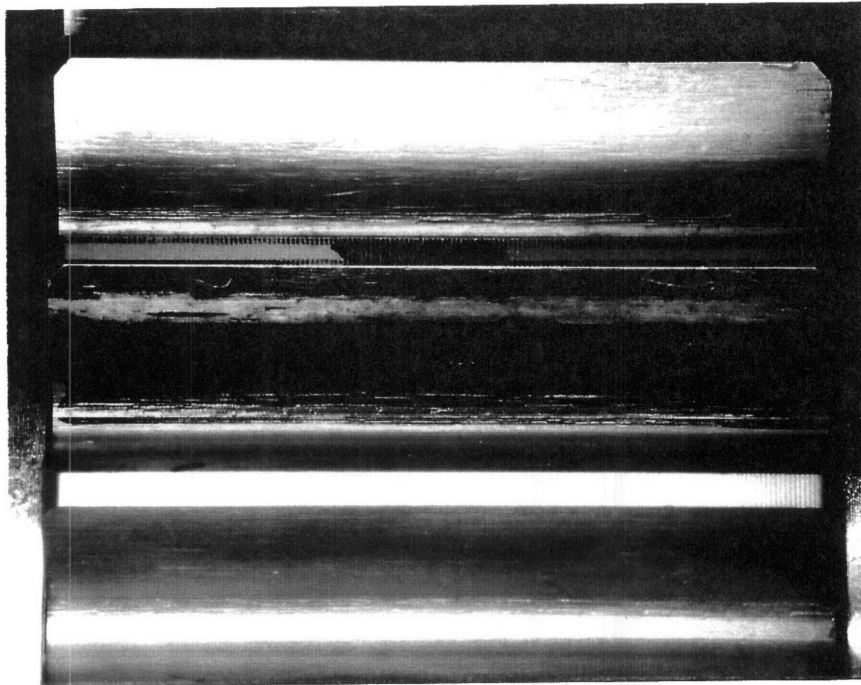
V-block Loading

The gear may have experienced loads which induced low cycle fatigue lives for any of several possible reasons. For example, the gear face or V-block face could have had a crown, or the V-block may not have loaded the gear at the radial location intended (at the HPSTC). If either the gear face or V-block face had a crown, the load would no longer be uniformly distributed along the length of the tooth but concentrated on the peak of the crown. Alternatively, the existence of a crown would have created an unstable situation which would ultimately cause the V-block to load the gear at the wrong radial location. However, upon measurement of the gear and V-block faces it was established that there were no such crowns.

Wear patterns created under varying conditions, as seen in Figures 5.15 and 5.16, proved that the V-blocks were indeed being loaded at the correct location on the gear tooth. Figure 5.15a is an illustration of the wear pattern created by inserting the gear without applying any load, Fig. 5.15b is the wear pattern created by inserting the gear and
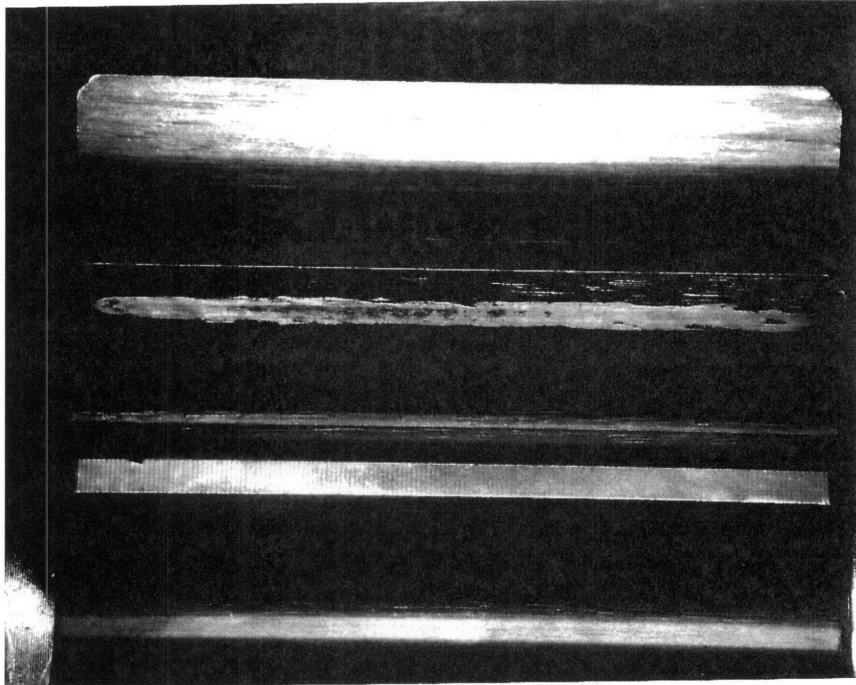
Figure 5.15a: Wear patterns created by the V-block when the gear was inserted in the testing apparatus.
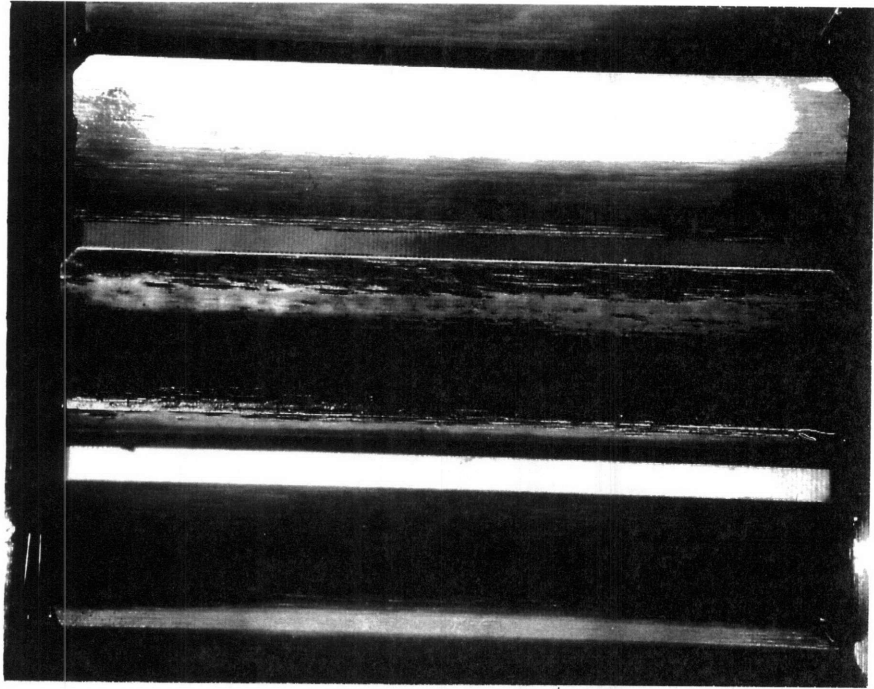

Figure 5.15b: Wear patterns created by the V-block during maximum loading of the prototype gear.

applying the maximum load. Fig. 5.16a is an illustration of the wear pattern created due to heat expansion of the gear. The heat was created by inserting the gear in the test assembly and running the shaft without applying any loads with the MTS. Lastly, the wear patterns in Fig. 5.16b illustrate the contact point of the V-block under a full scale fatigue test. In all the wear pattern experiments, it was established that the average V-block contact point was indeed at the HPSTC diameter (3.222 in, 81.839 mm) with an average contact thickness of 0.045 in. (1.143 mm). These results confirmed that the V-blocks were accurately loading the gear teeth at the HPSTC diameter.
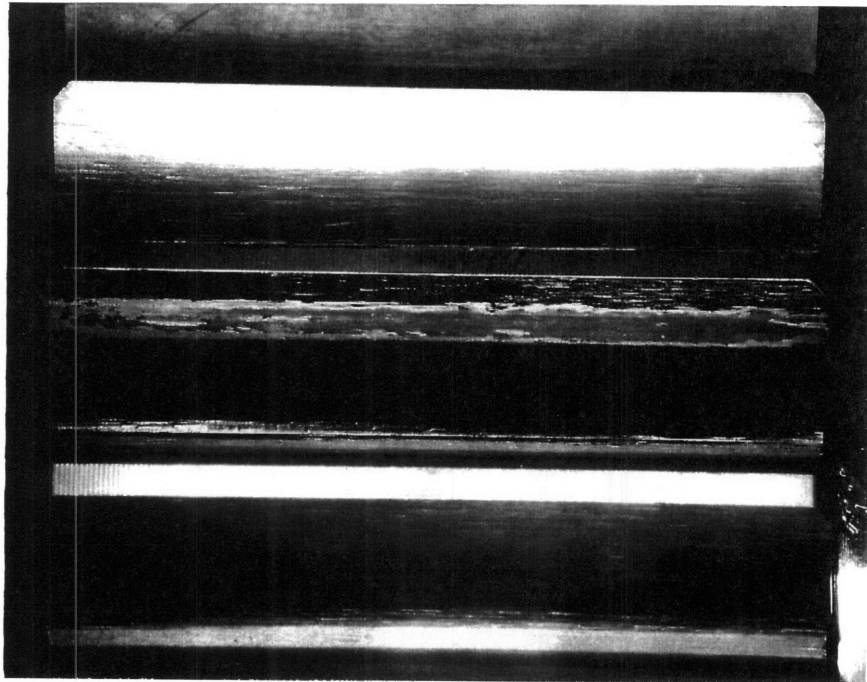
Strain -Gauged Gear

To examine the loads which the gear experienced during testing, a strain-gauged gear was prepared. Figure 5.17 illustrates three strain-gauges as they were mounted in the roots of the loaded teeth to give the most complete picture possible. Strain gauge number ten is located closest to the front face, number eleven is in the middle of the gear and number twelve is located closest to the back face of the gear. Figure 5.18 illustrates the location of each strain gauge used to asses loading of a gear prototype. Strain-gauges numbered one through three were mounted along the root of tooth **A** (A_{top}), while strain-gauges numbered four through six were mounted along the root on the opposite side of tooth **A** (A_{bottom}). The same situation existed with the strain-gauges seven through nine and ten through twelve which were situated on tooth **B** (B_{top} and B_{bottom}, respectively). Unfortunately, strain-gauge number ten was damaged, so it was not used in the test analyses.

Figure 5.16a: Wear patterns created by the V-block when the gear was brought to maximum operating temperature.

Figure 5.16b: Wear patterns created by the V-block during a full scale experiment.

Figure 5.17: Illustration of the strain gauged gear with strain gauges 10 through 12 visible.

Because measured stress is very sensitive to strain-gauge location[34], the

measurements of the strain-gauges could not be taken as absolute values but merely as

indicators of relative stresses. The results of the first examination were astonishing.

Figure 5.19 illustrates the results from the strain-gauged gear where each of the

twelve gauges mounted gave a reading of microinches per inch[35]. As seen in the figure, it

appeared that one side of the tooth experienced a stress five times higher than the other

side! For example strain gauge number seven registered a strain which is equivalent to a

stress of 40 ksi (280 MPa) for a load of 7000 lb (31,000 N), while strain gauge number

nine registered a strain which is equivalent to a stress of 200 ksi (1,400 MPa). Given the

loads and stresses the gear teeth would experience under *uniform* load, it was no longer

surprising that the first gear had exhibited a short fatigue life indicative of plastic

deformation when it was apparent that the applied load was so grossly misaligned.

[34] Recall the FEA results examined in Chapter 3.

[35] 1000 microinches/inch of strain equate a stress of approximately 33 ksi or 231 MPa.

B_top
Gauge #7 - front face
Gauge #8 - middle
Gauge #9 - back face

B_bottom
Gauge #10 - front face
Gauge #11 - middle
Gauge #12 - back face

A_top
Gauge #1 - front face
Gauge #2 - middle
Gauge #3 - back face

A_bottom
Gauge #4 - front face
Gauge #5 - middle
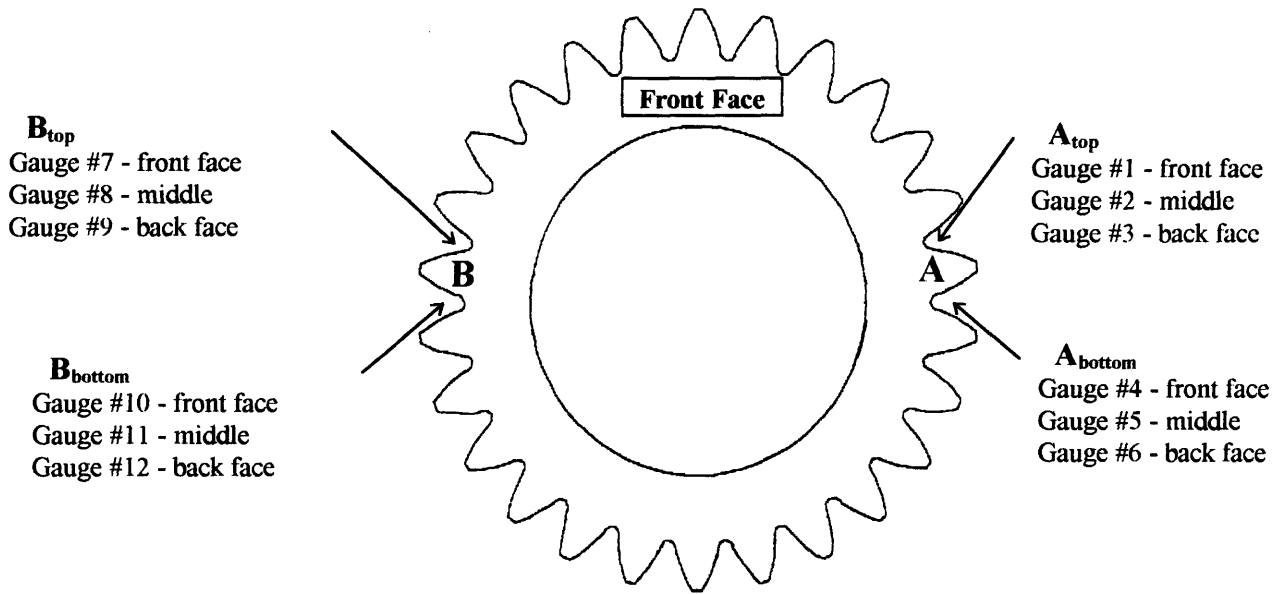Gauge #6 - back face

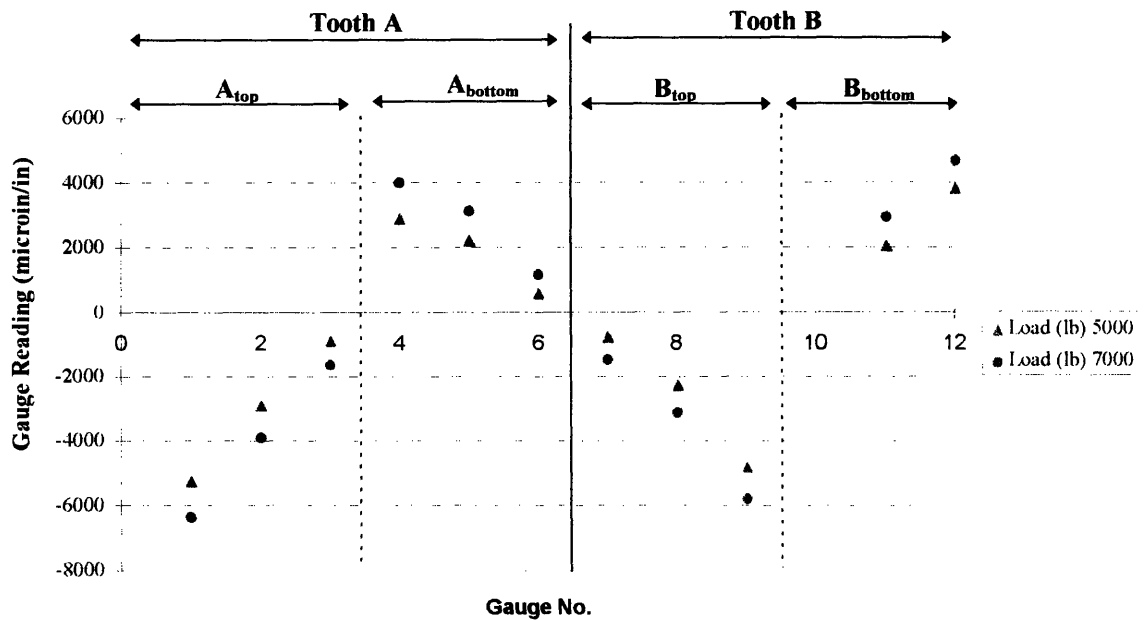**Figure 5.18:** Location of strain gauges along the roots on either side of teeth A and B.

Figure 5.19: Initial strain-gauge readings indicating severe misalignment of the gear.

Final Design Steps

Several steps were taken to eliminate the misalignment apparent during the strain-gauge test. For example, a detailed procedural checklist was developed (see Appendix C)

to ensure that the test was aligned throughout the entire assembly procedure. Also, all

mating surfaces were confirmed in location, straightness, and finishing. Although the

steps taken did eliminate a substantial amount of misalignment, it was not enough.

Moreover there was no apparent repeatability from assembly to assembly as is illustrated

in Fig. 5.20. The data sets marked by solid and hollow symbols represent two assemblies

of the test rig using identical set up procedures. As illustrated, the circular symbols

represent strains at a load of 7000 lb (31,000 N). From the figure it appears that from one

assembly to the next, the tooth represented by strain-gauges seven through twelve was

loaded in approximately the same way. However, the tooth represented by strain-gauges

one through six appears to be loaded in the opposite way from one assembly to the next!
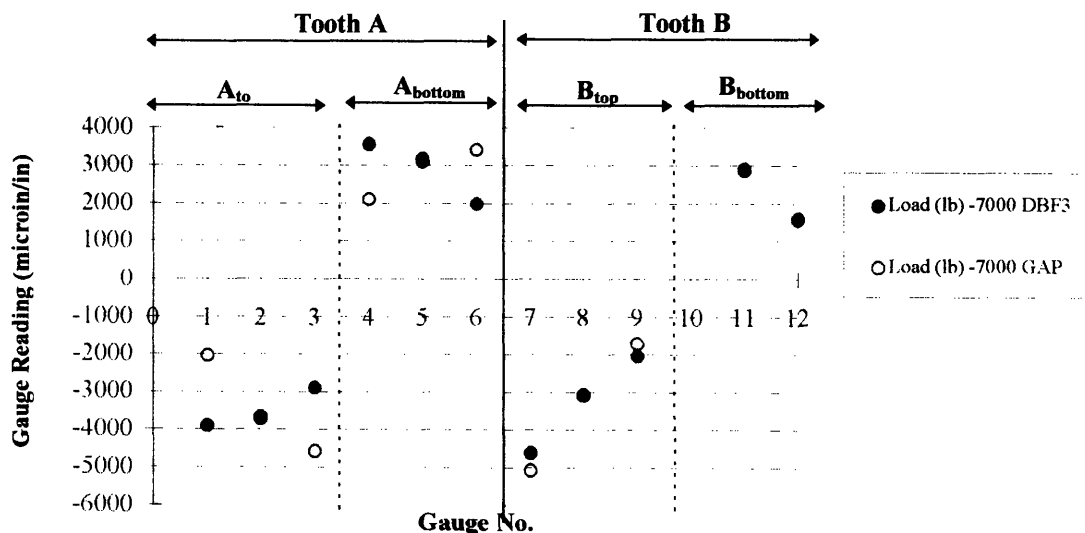
Figure 5.20: Illustration of strain-gauge results after preliminary changes. For simplicity, only the results of loading at 7000 lb are shown, all loads followed the same trend. Codes "DBF3" and "GAP" refer to two complete assembly and disassembly procedures.

Once the individual test pieces had been confirmed accurate, the only two points

where such misalignment from assembly to assembly could occur; was misalignment

caused by unwanted rotation of the MTS or V-block misalignment. Since the MTS was

designed to hold both axial and torsional positions, it was unlikely that the misalignment

was caused by the MTS machine. However, the V-block could theoretically misalign itself

in any of the degrees of freedom illustrated in Fig. 5.21.
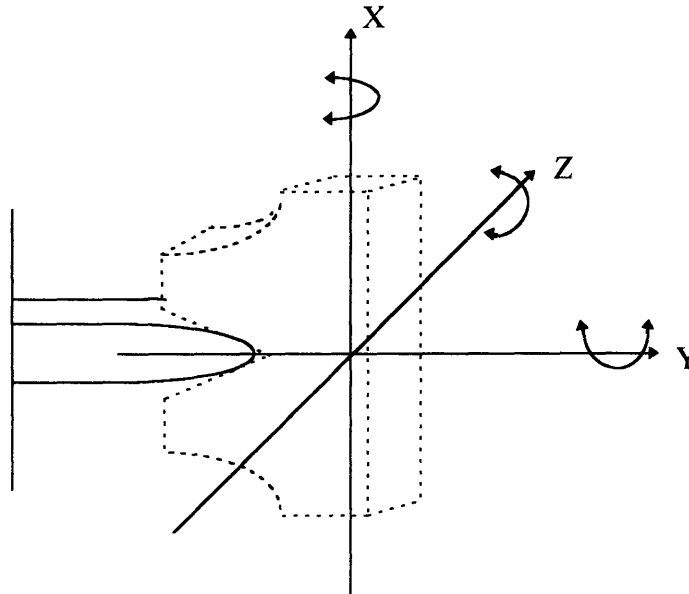
Figure 5.21: Theoretical misalignment of the V-block.

Since the block was designed to have an interference fit with the Square Bracketing,

motion in both the Z and Y directions would be negligible if at all existent. Therefore the

V-block only had freedom of motion only in the X direction.

Initially, the test design had not included any provisions for aligning the V-blocks

after assembly. To control the blocks, four set screw holes were added to the square

bracketing as shown in Fig. 5.22. Set screws on either side would be used to push against

the back of the V-block until it had been set securely against the gear tooth. Initially a

torque wrench was used to move the V-blocks against the gear tooth. However, it was

found that an oscilloscope could be employed to help establish when the V-block was

missalligned. The oscilloscope was used to display the torque measured by the load cell of

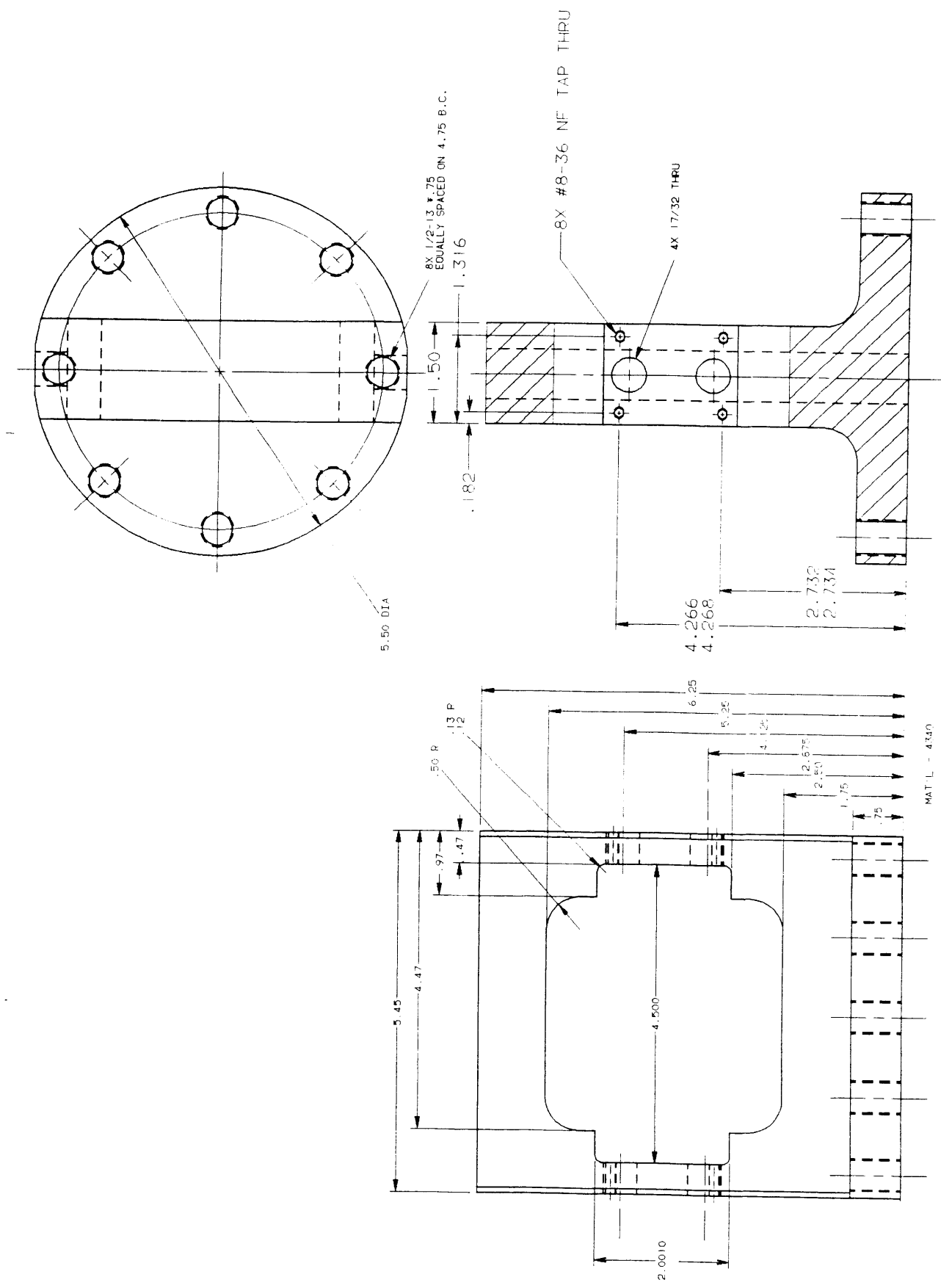the MTS machine (refer to Fig. 5.2). If the gear was not loaded uniformly across the face

Figure 5.22: Square bracketing illustrating four set screw holes for use in alignment of the *V*-blocks.

of the teeth, a small torque would occur about the vertical axis (the Y axis) and measured by the MTS torque cell. Using small loads, the tension-compression test was started. Misalignment of the gear resulted in a torque reading in the load cell which was also measured and displayed by the oscilloscope. Using this display, it was possible to adjust the set screws such that the gear was aligned and no torque was experienced by the MTS load cell. A double set of nuts would keep the screws in place throughout the test.

Conclusion

The strain-gauged gear confirmed that repeatable alignment had been achieved as a result of the combined efforts of the design changes. During multiple assemblies of the test the maximum variation which occurred was ~300 microinches/inch,(0.3 μm/mm) an example of which is illustrated in Fig. 5.23. Such variation was insignificant because it could be achieved purely by rotating the bearings and changing the properties of the gear rim or changing the temperature of the test assembly. A variation of ~1,000 μin/in (1 μm/mm)remained along the length of the gear tooth B, but this may simply have been a result of slight variation in gauge location inside the tooth root. As previously discussed, in an area as critical as the tooth root, a slight variation in gauge location would result in a substantial change in the strain recorded. Consequently, the strain-gauged gear should be used primarily as a relative measure to ensure repeatability in successive assemblies rather than as an absolute measure.
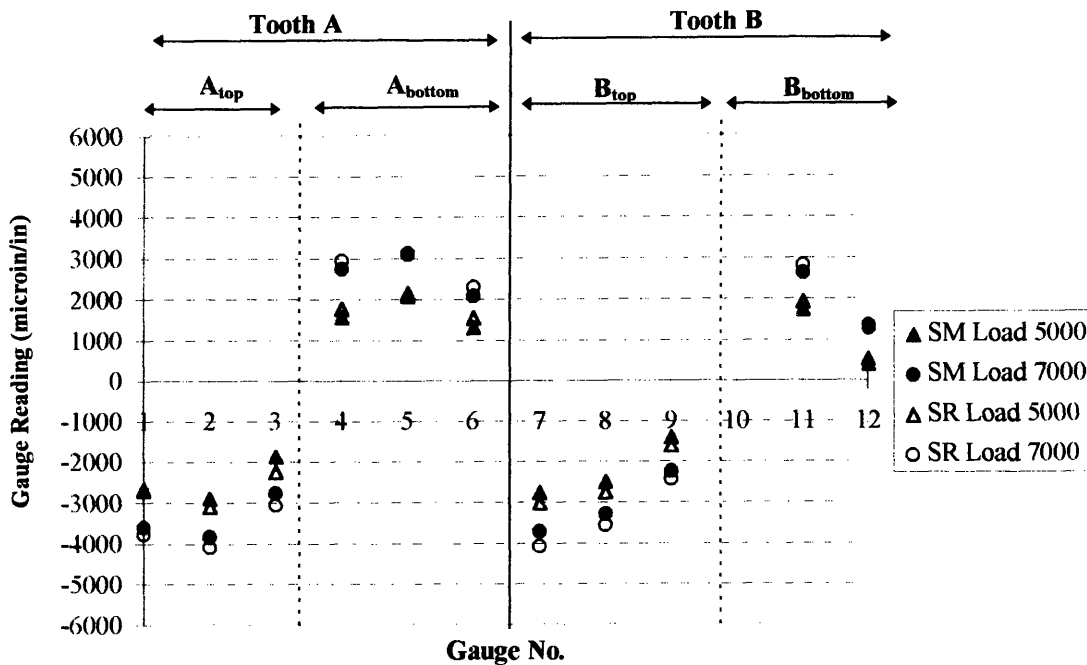
Figure 5.23: Two Tests Examining the repeatability using set screws

Test Results

Figure 5.24 is an illustration of the fatigue life data gained from the test. As illustrated, three sets of gears were tested: the Test category, the Control category and the Supplier category. As discussed in Chapter 4, the Test and Supplier category prototypes were manufactured by the same supplier. The Control category (indicated by squares) was supplied by the customer and employed a straight bore. The Test category (indicated by circles) prototypes employed the tapered bore while the Supplier category (indicated by triangles) used the straight bore. All three categories were tested at four loads between 8,000 lb (35,500 N) and 11, 000 lb (49,000 N) in 1,000 lb (5,000 N) increments.

10,000,000

Number of Cycles

1,000,000

■ Control Cat.
● Test Cat.
▲ Supplier Cat.

100,000

10,000

7,000   8,000   9,000   10,000   11,000

Load (lb)
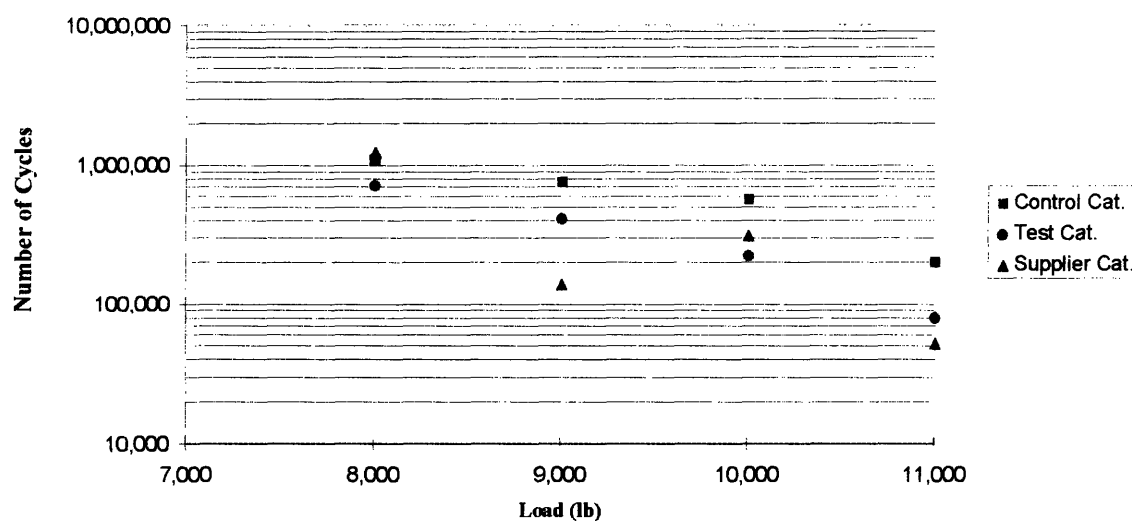
Figure 5.24: Test Results of (load vs. fatigue life) including the Test, Control and Supplier Categories.

It appears that the Control category consistently exhibited a longer fatigue life than the other prototypes. This was somewhat surprising because it was expected that the Supplier category would have exhibited a fatigue life which was equivalent the fatigue life exhibited by the Control category. Since there was no difference in design between the two sets, no substantial differences in fatigue life were expected. Even more surprising was the sporadic performance of the Supplier category. For example, in the 8,000 lb experiment, the Supplier category outperformed both of the other categories, however, in the 11,000 lb experiment, the Supplier category performed worse than any of the other categories.

This type of performance caused a re-evaluation of the prototypes in the Supplier category, as it was indicative of possible defects in the prototypes. The gears were double etched for grinding injury on the gear faces[36]. The results of the analysis, illustrated in Figures 5.25a and 5.25b, were staggering. The prototypes had been badly burnt during

---

[36] James C. Wingert, Internal Timken Research Report, 1996.

grinding of the gear faces by the supplier, resulting in pockets of low hardness[37] in the

case as well as hair-line cracks covering the entire face of the gear. The other prototype

categories which had been manufactured by the same supplier where also etched with

similar results. At that point, all further testing on these prototypes was suspended. The

combination of damaged case hardness and cracks would be very detrimental to fatigue

life tests.

---

[37] These pockets were a result of the re-tempering of the gear when it was subjected to the intense heat created in grind burning.
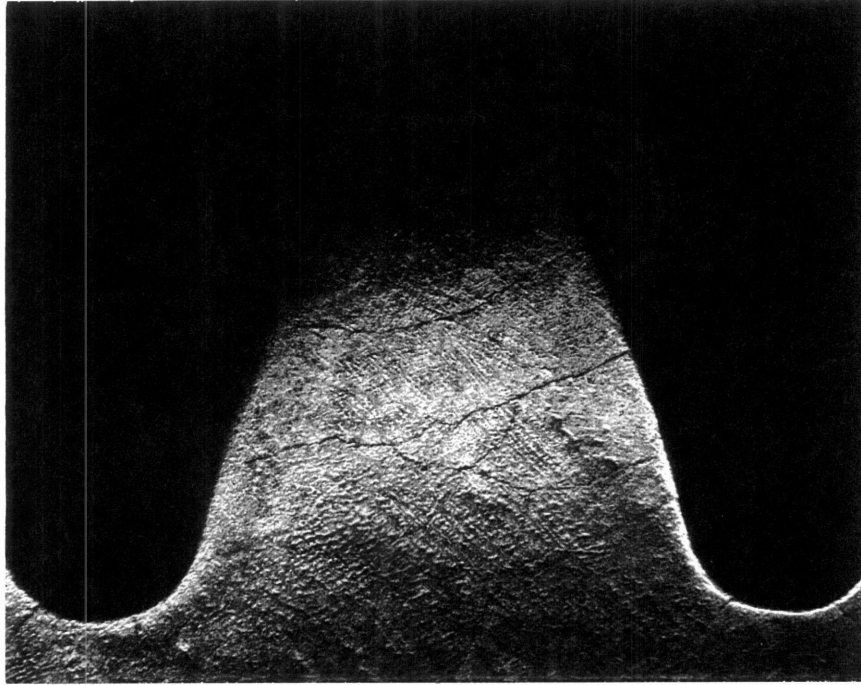
Figure 5.25a: Prototypes manufactured by supplier. Cracks in gear face seen before etching.
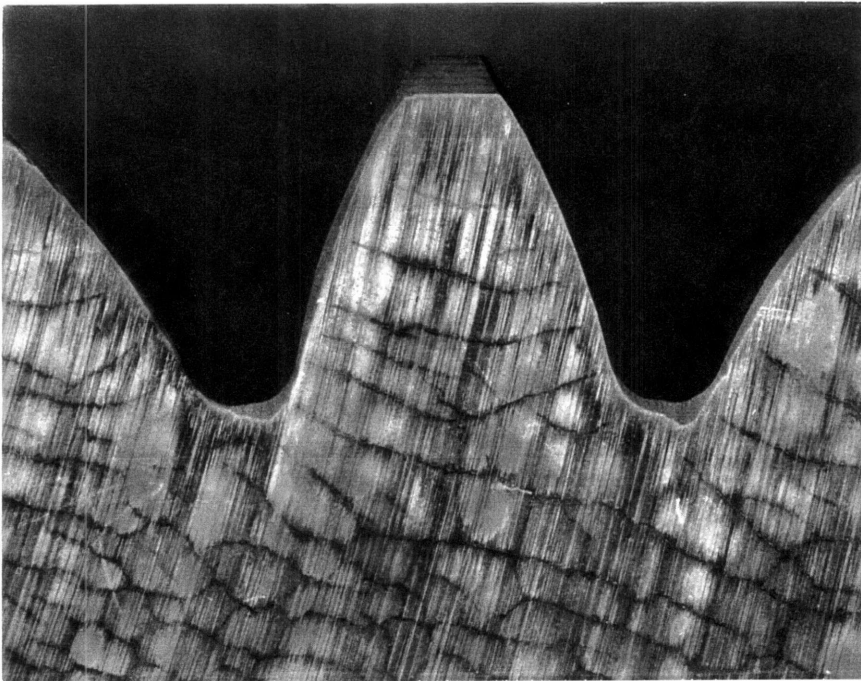
5b: Prototypes manufactured by supplier. Grind burn damage to gear face seen after etching.

CHAPTER 6

CONCLUSIONS AND RECOMENDATIONS

Conclusions

Despite the unfortunate event of supplier damage to the prototypes, both

objectives of this research were accomplished to a lesser or greater extent. The goal of

designing a test which would 'employ a simpler and more cost-effective scheme' was

achieved rather successfully as was illustrated in the stable trends observed in the fatigue

test. The second goal of establishing a correlation between the finite element results and

test results was partially accomplished, but could not be fully achieved because of the poor

quality of the prototypes.

Proof-of-Concept

The results illustrated in Fig. 6.1 serve as a proof-of-concept for the test designed.

The trends of life versus load are relatively stable for the prototype categories. Many of

the variables needed in other tests were successfully eliminated (such as meshing gears) so

trends can be correlated to testing factors more easily. Moreover, control over the test

variables is sufficient to allow for easy alterations (i.e. speeds or loads). Perhaps the most

valuable characteristic of the resulting test is that changeover time is extremely low - the

experiment can be disassembled and reassembled in just over an hour - a great

improvement over many other test designs. With such low changeover time requirements,

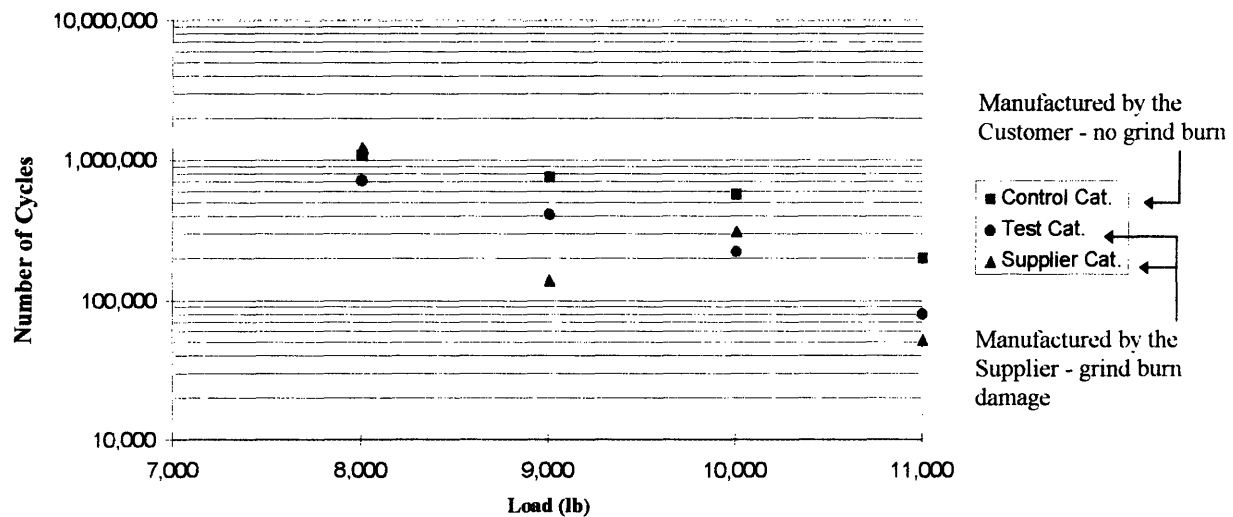gears can be tested almost non-stop.

Figure 6.1: Test Results including the Test. Control and Supplier Category.

Finite Element Analysis Correlation

Correlation between the finite element analysis and experimental results could only

be partially achieved because of the poor quality of all the gears which were not supplied

by the customer. As discussed in Chapter 5, *grind burn* on all gear faces resulted not only

in a re-tempering of the gear but also in a great number of small cracks over the entire

surface of the gear faces (recall Figures 5.25a & 5.25b). The customer-supplied gears in

Fig. 6.1 (Control category) clearly outperformed both the straight and tapered bore

prototypes manufactured by the supplier. The signature of grind burn in the Test and

Supplier categories is clear because the gears in these categories performed poorly

regardless of gear design. However, when comparing only the gears furnished by the

supplier, it is apparent that both designs fared equally well. The tapered bore gear (Test

category) outperformed the straight bore gear (Supplier category) fifty percent of the time. This result correlates rather well to the results of the finite element analysis which indicated similar peak Mises stresses in both designs. Recall that the peak stresses in the straight bore model were calculated to be 87.3 ksi (611.1 MPa) whereas the peak stresses in the tapered bore model were somewhat larger at 96.7 ksi (676.9 MPa). From the finite element analysis results, it was expected that the fatigue life performance of the gears would not vary greatly. This trend appears to be evident in the test results of the gears which were manufactured by the same supplier.

Graceful Failures

One surprising revelation of this experiment was that the tapered-bore gear failures were more graceful than the straight-bore gear failures. As had been predicted, all the tapered-bore gears failed through the rim, while the straight-bore gears failed through the tooth. Obviously, the weakest link in the tapered-bore gear was the rim and the weakest link in the straight-bore gear was the tooth. It is true that gears are created with a defect free design approach which implies that no failures of the gear should occur at all. However if the gear *should* fail, a failure through the rim is likely to be less damaging to the surrounding machinery than failure through the tooth. If the failure is through the tooth, the broken tooth is free to move through the rest of the planetary system (such as the one in the torque hub of the case study). Such a tooth fragment could cause further damage to adjacent planets, the sun and/or the ring gears. On the other hand, if the gear fails through the rim, no pieces of the failed gear are free to move through the planetary system. Though failure through the rim may result in more noise, there is a lower probability that the failed planet gear will damage the surrounding machinery. In this

sense, it would be preferable to design a gear which is likely to fail through the rim rather than through the tooth, so the tapered-bore gear may be the preferred design.

Recommendations

Because the prototype gears were all damaged in the manufacture, it was not possible to truly compare the tapered-bore prototypes to the actual customer prototypes which are targeted for replacement by GearSpexx™. Also, since the prototype gears were damaged, it was unreasonable to conduct a statistical analysis on fatigue life as had previously been intended. The surface cracks introduced by the grind burn could be the cause of extreme fatigue data scatter, making statistical data gathering impractical. Therefore, it is recommended that the testing be repeated with undamaged prototypes to establish a statistical correlation.

There is ample opportunity for further study with finite element analysis. For example, the analyses conducted only examined one of the many possible situations as a result of variable roller location, and resulting variable rim stiffness. In the analyses, a bearing roller was placed exactly under the loaded tooth (recall Chapter 3). It would be of interest to examine the finite element result if the rollers were placed at different locations along the gear raceway to investigate the resulting stresses of 'rotating' rollers via a number of finite element 'snapshot' analyses. Other opportunities for further investigation lie in the fact that the peak Mises stresses in the tapered-bore model did not differ greatly from those in the straight-bore model. This indicates that this design may not have been aggressive enough - for example, the maximum rim thickness of the tapered-bore model is not substantially smaller than the rim thickness of the straight-bore model. Finally, further

examination of the loads applied to the gear in the finite element model could be beneficial in creating a theoretical fatigue life curve.

The test designed also supplies several avenues for further research. It would be beneficial to devise a method which allowed for no misalignment or for self-alignment of the gear in the test apparatus. Also, it is possible to create a means by which misalignment might be better measured and corrected than was discussed in this document. For example, the test could be mounted in such a way as to make better use of the MTS load cell's capacity for torque readings. Finally, the test design could be optimized to benefit from a strict control of the operating variables such as lubrications and speeds.

GLOSSARY OF TERMS USED

Cage - A component of tapered roller bearings, the cage retains and separates the bearing rollers.

Case - The strong outer shell of material in a case carburized steel part. The case is very hard and fatigue resistant but is also quite brittle and thus can not resist crack propagation once a crack has begun.

Case Carburization - a certain type of heat treatment which ensures that the proper material properties are achieved by introducing carbon into the surface of the material. In steel gears and bearings, case carburization results in parts with a relatively soft but tough inner core with a very hard outer shell. The outer shell can resist higher loads but is brittle whereas the inner core is not as strong but resists crack propagation.

Cone - Also referred to as the 'inner ring', it is one of the components of a tapered roller bearing. The tapered rollers move along the outer raceway. The cone is usually mounted on a shaft or pin (see Fig. 2.2).

Cone Assembly - consists of a cone and a full complement of rollers with a retaining cage. The cone assembly is usually shipped in a pre-assembled, unseparable form.

Core - The softer steel inside the strong outer shell of a case carburized steel part. Though not as hard as the case, the core is more capable of resisting crack propagation.

Crown - The cross-sectional surface of tapered cup and cone raceways and rollers. The crown is the convex cross-sectional shape which ensures that there is an even distribution of stress concentration along the raceways. Appropriate crown geometry is extremely important to bearing life.

Cup - Also referred to as the 'outer ring', it is one of the components of a tapered roller bearing. The tapered rollers move along the inner raceway. The cup is often mounted in a housing (see Fig. 2.2).

Elements - the 'bricks' which compose the three dimensional structures on which finite element analysis will be conducted. The analysis will be conducted on each individual element in the model. Elements are numbered sequentially (1, 2, 3, . .).

Endplay - lateral clearance in a bearing between the cone assembly and the cup. Endplay is measured in positive inches.

Gear Blank - a disk of material with a circular hole in the center. Gear teeth are cut into the gear blank. Gear blanks can be created by cross-sectionally sawing tubing.

Gear Rim - the section of material which gives a gear its structural strength. The rim is measured as the radial distance between the root or dedendum circle and the gear bore. (see Fig. 2.3).

GearSpexx™ - a product of The Timken Company as illustrated in Fig. G.1. The integral gear has a double tapered bore which also acts as the outer raceway, or cup, for two cone assemblies. This product would be a package consisting of one gear with double integral raceways and two cone assemblies.
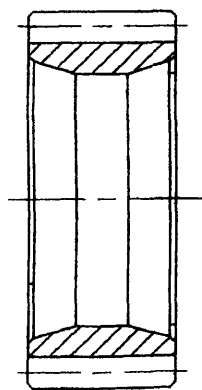
Figure G.1: Gear portion of Gearspexx™ illustrating a double tapered bore which also acts as a bearing raceway for two Timken Company tapered bearings.

Grind Burn - damage which often results in a re-tempering and creation of microscopic cracks in surfaces which are being ground. Grind burn occurs if the grinding is performed at speeds which are too high which causes the surface of the part being ground to heat up beyond acceptable levels.

Grinding - is a surface-finishing and fine-shaping technique wherein small amounts of material are removed at a time. Surfaces with tight tolerances and/or stringent surface finish requirements will be ground.

Heat Treatment - a process of creating specified material properties by heating and controlling the rate of cooling. Examples of heat treatment processes are: tempering, annealing and case carburizing.

Hobbing - the process by which gear teeth are cut. In hobbing both the tool and gear rotate about their own axes. The hobbing tool is a cylinder covered with cutting 'teeth' which moves perpendicular to the face of the gear blank.

Hone - a super-fine finishing process which produces a better surface finish than grinding but does not alter geometry. This technique, which removes almost no material, is used on those surfaces which are extremely sensitive to surface finishing. This process is primarily used to increase fatigue lives of steel parts.

HPSTC - the highest point of single tooth contact is the farthest radial distance on a gear, from the center, at which the gear tooth must support the entire load transmitted through the meshing gear.

Integral Gear - in this document, refers to a gear which employs tapered raceways in its bore. Thus the gear can also act as the cup for the tapered roller bearing which becomes an integral part of the gear.

Large End Diameter - in a cup the inner surface is conical. The large end diameter is the largest inner diameter of the cup(see Figure 2.2).

Load Zone - is the loaded arc of a bearing. The load zone refers to the number of rollers which support a load at one time and is measured in degrees of an arc. The greater the load zone, the less stress each individual roller must endure for a constantly applied load. For example, a load zone of 180° implies that half of the rollers in the bearing are loaded.

Ms - a method by which carbon concentration can be measured. The higher the carbon content of the steel, the harder the material. This method is used to ensure that the case thickness is acceptable (see Figure 4.7 for an example).

Node - points in three dimensional space which are used to create the three dimensional 'bricks' named elements in a finite element model. Nodes are numbered sequentially (1, 2, 3, . . .).

Pitch Diameter - the theoretical circle upon which most gear calculations are based (see Fig. 2.3).

Preload - theoretical lateral interference fit of the cone assembly and the cup. Preload is measured in negative inches.

Pressure Angle - represents the direction in which the resultant force acts between two gears and is the common tangent between two gear pitch circles.

Raceway - The surface along which the tapered rollers move. Both the cone and cup have raceways (see Fig. 2.2).

Rollers - The rollers move between the inner raceway of the cone and the outer raceway of the cup. The loads are transferred through the rollers which move in a 'true rolling motion', rather than sliding, thus reducing the amount of friction created.

The rollers are lubricated via oil or grease and are separated and retained by the cage (see Fig. 2.2).

Shave - a similar process to hobbing, but with more accurate results. Shaving is usually conducted after heat treatment is complete.

Small End Diameter - in a cup the inner surface is conical. The small end diameter is the smallest inner diameter of the cup(see Fig. 2.2).

Tapered Bore - refers to a conical inner diameter.

Tapered Roller Bearing - a bearing (anti-friction device) which employs tapered rollers rather than cylindrical rollers or balls. The primary advantage of a tapered roller bearing is that it can support combined radial and thrust loads whereas ball bearings can withstand only very limited thrust loads and cylindrical roller can only support radial loads. The primary components of a tapered roller bearing are the cup, the cone, the rollers and the cage (see Fig. 2.2).

Vibratory Finishing - an alternative method of creating a super-fine texture on steel parts. Vibratory finishing results are similar to Honing results.

Whole Tooth Depth - the radial distance between the outer diameter of the gear and the root or dedendum circle (see Fig. 2.4).

APPENDIX A

Example Of Abaqus Input Code For The Super Element And Main Models

```
*HEADING
Astrid Richter-Allen
Gearpack Model w/half web and involute tooth profile to be run week of
THIS MODEL IS TO BE RUN WITH THE MAIN MODEL NAMED:  INVOLUTEMM.INP
FAM Model: involutei     Date: 8-Nov-1995
*SUPER,ID=Z0001
*NODE,NSET=CUP
      1    0.00000   -1.23997   -1.11641
10799    0.63750    1.26648    1.08624
10800    0.63750    1.24889    1.10642
*NSET,NSET=ROLLT
 7677 7613 7578 7531
*NSET,NSET=ROLL
 8592 9310 9309 8571 7655 6708 5775 4819 3860 2818 1759 1053 1052 1757
 4837 5786 6723 8502 9142 9141 8484 7598 6701 5807 4886 3979 3020 2080
 2078 3040 3988 4899 5812 6719 8399 8997 8996 8381 7565 6702 5836 4947
 2391 1828 1826 2404 3252 4097 4975 5845 6720 8330 8835 8834 8304 7516
 5017 4206 3413 2657 2183 2182 2668 3424 4222 5037 5890 6722
*NSET, NSET=FIXED
      55,    56,    58,    59,    60,    80,    82,    85,    88,    94,
  10766, 10770, 10773, 10774, 10775, 10786, 10787, 10791, 10793, 10795,
  10797, 10798, 10799, 10800
*NSET, NSET=FORCEN
 1917 2014 2099 2227 2375 8952 9043 9184 9305 9492
*ELEMENT,ELSET=CUP,TYPE=C3D8R
      1 7766 7807 7818 7703 7677 7723 7734 7613
 7039 5125 5190 5199 5121 5189 5252 5250 5185
 7040 5190 5257 5274 5199 5252 5322 5328 5250
*SOLID SECTION,ELSET=CUP,MATERIAL=CUP
1.
*MATERIAL,NAME=CUP
*ELASTIC,TYPE=ISO
30E06, 0.30000
*RETAINED DOFS
ROLLT,1,3
ROLL,1,3
FORCEN,1,3
8032,1,3
2679,1,3
*SLOAD CASE, ID=BOUND
*BOUNDARY, OP=NEW
FIXED,1
*END SUPER
```

```
*HEADING
Astrid Richter-Allen
Gearpack Model w/half web and involute tooth profile to be run week of
THIS IS THE MAIN MODEL, TO BE USED WITH THE SUPERELEMENT MODEL: INVOLUT
FAM Model: involutei       Date: 8-Nov-1995
*NODE,NSET=CUP
      1    0.00000   -1.23997   -1.11641
  10799    0.63750    1.26648    1.08624
  10800    0.63750    1.24889    1.10642
*NODE,NSET=BEAM
  10801   -0.37232    0.00000    0.00000
  10802   -0.20234    0.00000    0.00000
  10803   -0.03236    0.00000    0.00000
  10804    0.13762    0.00000    0.00000
  10805    0.63750    0.00000    0.00000
  10806   -0.65850    0.00000    0.00000
*NSET, NSET=FORCEN
  1917 2014 2099 2227 2375 8952 9043 9184 9305 9492
*ELEMENT,TYPE=Z0001,ELSET=SUPER,FILE=involse96
      1 1052 1053 1452 1453 1757 1759 1826 1828 1917 2014 2078 2080 2099
   2227 2375 2391 2404 2657 2668 2679 2818 2830 3020 3040 3236 3252 3413
   3883 3979 3988 4079 4097 4206 4222 4819 4837 4886 4899 4947 4975 5017
   5786 5807 5812 5836 5845 5871 5890 6701 6702 6707 6708 6719 6720 6722
   7531 7565 7578 7598 7613 7655 7677 8032 8304 8330 8381 8399 8484 8502
   8834 8835 8952 8996 8997 9043 9141 9142 9184 9305 9309 9310 9492
*ELEMENT,ELSET=BEAM,TYPE=B31
   70411080110802
   70421080210803
   70431080310804
   70441080410805
   71301080610801
*ELEMENT,ELSET=ROLF1,TYPE=SPRINGA
   704510801 7677
   704610801 8592
   704710801 9310
   704810801 9309
   704910801 8571
   705010801 7655
   705110801 6708
   705210801 5775
   705310801 4819
   705410801 3860
   705510801 2818
   705610801 1759
   705710801 1053
   705810801 1052
   705910801 1757
   706010801 2830
   706110801 3883
   706210801 4837
   706310801 5786
   706410801 6723
```

```
*ELEMENT,ELSET=ROLF2,TYPE=SPRINGA
 706510802 7613
 706610802 8502
 706710802 9142
 706810802 9141
 706910802 8484
 707010802 7598
 707110802 6701
 707210802 5807
 707310802 4886
 707410802 3979
 707510802 3020
 707610802 2080
 707710802 1453
 707810802 1452
 707910802 2078
 708010802 3040
 708110802 3988
 708210802 4899
 708310802 5812
 708410802 6719
*ELEMENT,ELSET=ROLF3,TYPE=SPRINGA
 708510803 7578
 708610803 8399
 708710803 8997
 708810803 8996
 708910803 8381
 709010803 7565
 709110803 6702
 709210803 5836
 709310803 4947
 709410803 4079
 709510803 3236
 709610803 2391
 709710803 1828
 709810803 1826
 709910803 2404
 710010803 3252
 710110803 4097
 710210803 4975
 710310803 5845
 710410803 6720
*ELEMENT,ELSET=ROLF4,TYPE=SPRINGA
 710510804 7531
 710610804 8330
 710710804 8835
 710810804 8834
 710910804 8304
 711010804 7516
 711110804 6707
 711210804 5871
 711310804 5017
 711410804 4206
 711510804 3413
 711610804 2657
 711710804 2183
 711810804 2182
 711910804 2668
 712010804 3424
 712110804 4222
 712210804 5037
 712310804 5890
 712410804 6722
```

```
*ELEMENT,ELSET=EXTRA1,TYPE=SPRING1
8000,8032
8001,2679
*ELEMENT,ELSET=EXTRA2,TYPE=SPRING1
8002,8032
8003,2679
*ELEMENT,ELSET=EXTRA3,TYPE=SPRING1
8004,8032
8005,2679
*BEAM SECTION,ELSET=BEAM,SECTION=CIRC,MATERIAL=BEAM
    0.90140
0.0,0.0,-1.0
*MATERIAL,NAME=BEAM
*ELASTIC,TYPE=ISO
30E06, 0.30000
*SPRING,ELSET=ROLF1,NONLINEAR

 -5000.000-0.0277647
   -16.393-0.0005198
     0.000-0.0003867
*SPRING,ELSET=ROLF2,NONLINEAR

-10000.000-0.0275286
   -32.728-0.0002467
     0.000-0.0001136
*SPRING,ELSET=ROLF3,NONLINEAR

-10000.000-0.0276056
   -32.610-0.0002466
     0.000-0.0001136
*SPRING,ELSET=ROLF4,NONLINEAR

 -5000.000-0.0279167
   -16.275-0.0005196
     0.000-0.0003867
*SPRING,ELSET=EXTRA1
 1
 1000.000
*SPRING,ELSET=EXTRA2
 2
 1000.000
*SPRING,ELSET=EXTRA3
 3
 1000.000
*SUPER PROPERTY,ELSET=SUPER,POSITION TOL=0.0
*BOUNDARY,OP=NEW
BEAM,4
10805,1
10806,1,6
```

```
*STEP,INC=50
*STATIC
0.1,1.0,0.001,0.25
*FILE FORMAT, ASCII
*EL PRINT,ELSET=ROLF1,FREQ=50
S,E
*EL PRINT,ELSET=ROLF2,FREQ=50
S,E
*EL PRINT,ELSET=ROLF3,FREQ=50
S,E
*EL PRINT,ELSET=ROLF4,FREQ=50
S,E
*EL PRINT,ELSET=EXTRA1,FREQ=50
S,E
*EL PRINT,ELSET=EXTRA2,FREQ=50
S,E
*EL PRINT,ELSET=EXTRA3,FREQ=50
S,E
*NODE PRINT,NSET=BEAM,FREQ=50
U
*SUPER PATH,ENTER ELEMENT=1
*EL PRINT,ELSET=CUP,FREQ=50,POSITION=AVERAGED AT NODES
S,MISES
*EL FILE,ELSET=CUP,FREQ=50,POSITION=AVERAGED AT NODES
S,SINV,E,SJP
*NODE FILE,NSET=CUP,FREQ=50
U
*NODE PRINT, NSET=FORCEN
U
*NODE PRINT, NSET=FIXED
U
*SUPER PATH,LEAVE
*CLOAD,OP=NEW
 8952,2,-192.81
 8952,3,-331.29
 9043,2,-385.62
 9043,3,-662.58
 9184,2,-385.62
 9184,3,-662.58
 9305,2,-440.71
 9305,3,-757.23
 9492,2,-247.90
 9492,3,-425.94
 1917,2,192.81
 1917,3,-331.29
 2014,2,385.62
 2014,3,-662.58
 2099,2,385,62
 2099,3,-662.58
 2227,2,440.71
 2227,3,-757.23
 2375,2,247.90
 2375,3,-425.94
*END STEP
```
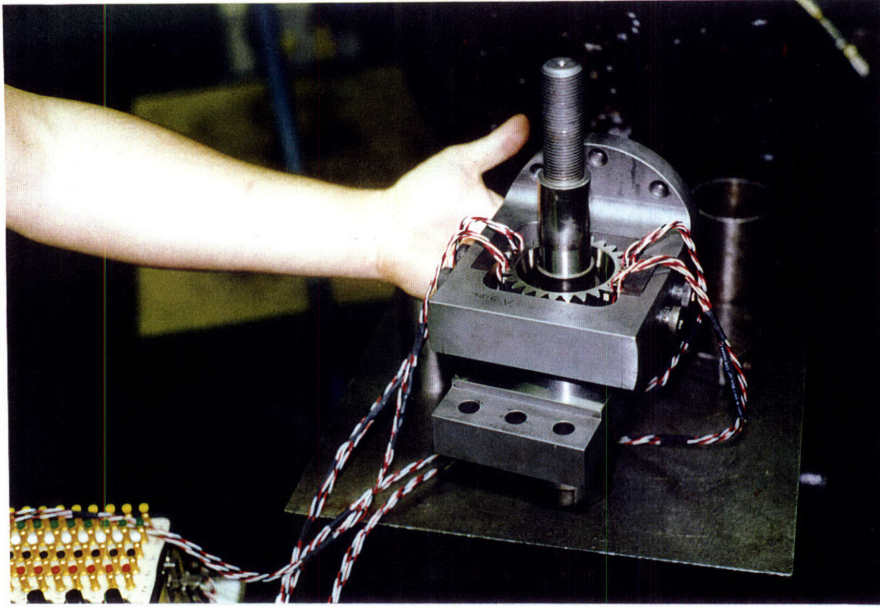
APPENDIX B

Testing Photographs
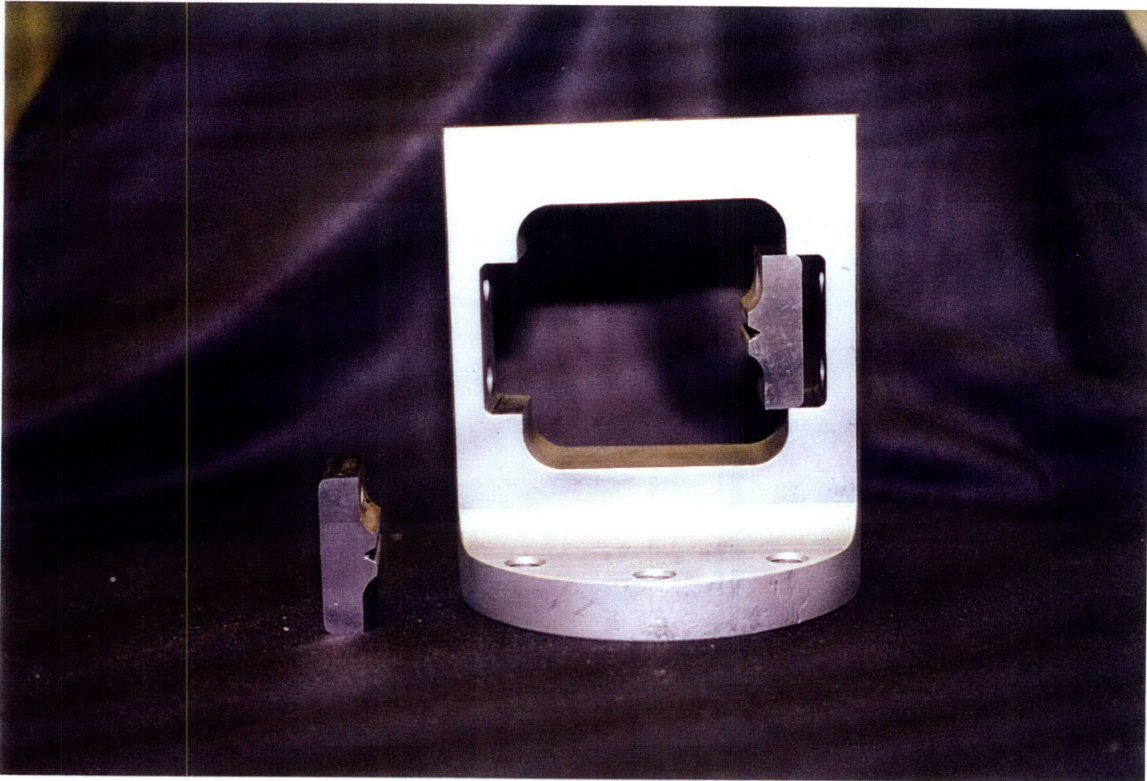
Figure B.1: The square bracket and V-blocks (see Fig. 5.14 for CAD drawing of final test design).
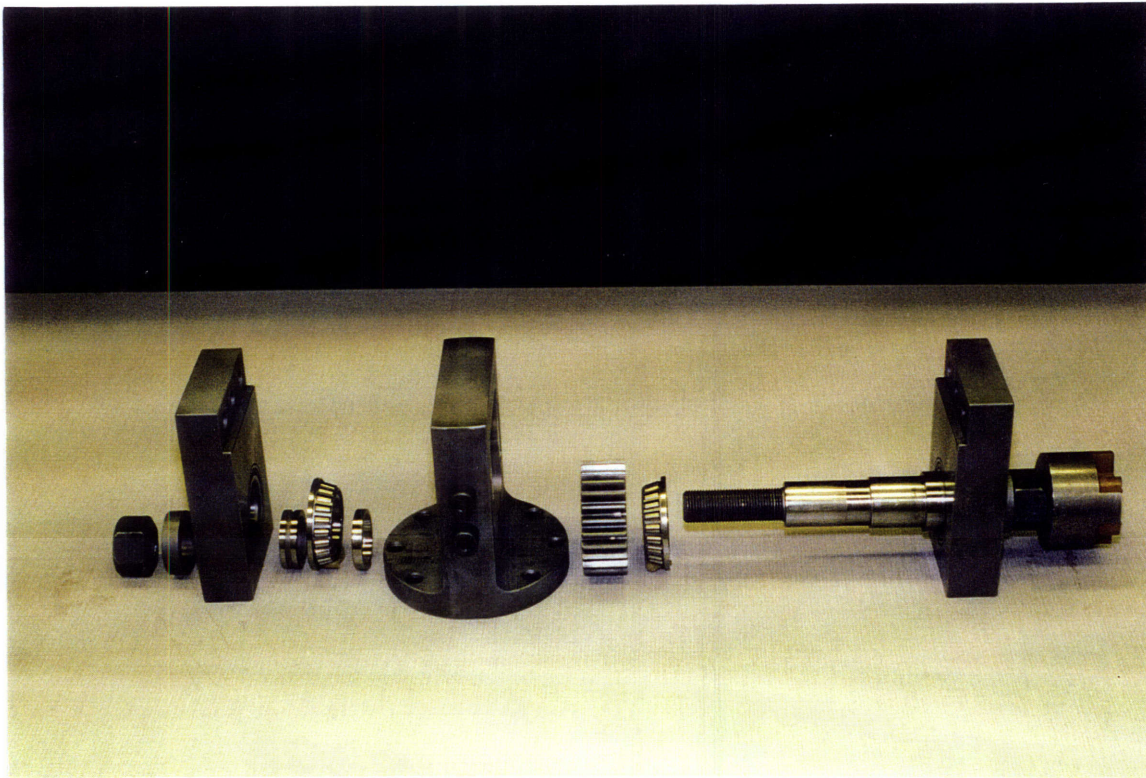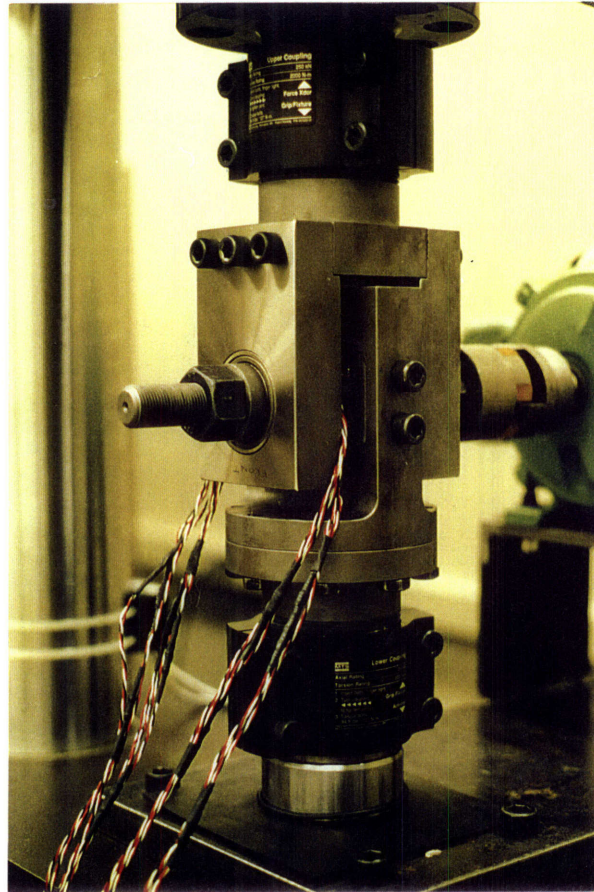

Figure B.2: Entire test assembly components. Components from left to right: nut, spacer, left slave bearing, spacer, left bearing, bearing spacer, square bracket, gear, right bearing, shaft, right slave bearing and motor coupling.

Figure B.3: Assembling strain-gauged gear for testing at a point when the left slave bearing had not yet been assembled.

Figure B.4: Completely assembled test - the strain gauged gear was included in the assembly here.

APPENDIX C

Procedural Checklist

Date:_____
Load: +/-_____
Cycles to Failure:_____

☐ **Assemble gear** assembly without any shims.

☐ **Bottom screws finger tight** ensuring that all screws do not have any resistance while being screwed in (resistance marks misalignment of the square bracket to the bottom adapter).

☐ **Actuator up** to where there is a small space to be seen between the slave bearings and the top adapter.

☐ **Insert appropriate shims between top adapter & slave bearings**: Measure space between the top adapter and the vertical section mating with the 'front' slave bearing for insertion of shims. Insert a shim with a thickness which is the average between the two sides. Screw the front slave bearing tightly to the top adapter. Measure the space and select the appropriate bearing for the back slave bearing. Release the screws in the front slave bearing so they hang loosely.
Front Shim: **Back Shim:**

☐ **Measure the Eric Factor** (alignment of slave bearing holders and top adapter) and make adjustments. Not critical at this stage but makes the future steps easier.

☐ **Apply a compressive load** of ~300 lb to ensure that all four corners of the slave bearings seat firmly against the horizontal section of the top adapter, this may require some light tapping or moving of the test rig. If absolutely necessary the load applied can be increased. Ensure proper seating by using a feeler gauge at the four corners.

☐ **Tighten top bolts** in the same pattern as a car wheel - alternating front to back and side to side. Tighten bolts as tight as possible.

☐ Bring both the **load and torque readings** of the machine to **zero** or near zero.

☐ **Tighten the bottom bolts** in the same pattern as a car wheel, keeping the torque approximately equal.

☐ **Begin Loading Cycle with very low load.**

☐ Using the Oscilloscope, adjust set screws until the torque reading has "flat lined".

☐ **Tighten** set screw bolts.

☐ **Measure the gaps** between the vertical surface of the v-block and the square bracket. **Insert a shim** which is the thickness of the smallest gap.
Left Front: **Right Front:**
Left Back: **Right Back:**
Left Shim: **Right Shim:**

☐ **Begin Motor Rotation. Confirm motor speed** to be the same speed as the MTS actuation.

☐ Locate **fans** so that the rig will gain maximum cooling